POSITIVE TIME-FREQUENCY DISTRIBUTION ANALYSIS OF THE HUMAN COLONIC ELECTRICAL ACTIVITY

POSITIVE TIME-FREQUENCY DISTRIBUTION ANALYSIS OF THE HUMAN COLONIC ELECTRICAL ACTIVITY

by

Miguel Barrientos, B. Sc.(National Autonomous University of Mexico)

A Thesis

Submitted to the School of Graduate Studies

in Partial Fulfillment of the Requirements

for the Degree

M. Eng. in Electrical and Computer Engineering

McMaster University

MASTER OF ENGINEERING (1994) McMASTER UNIVERSITY

(Electrical and Computer Engineering) Hamilton, Ontario

TITLE: Positive Time-Frequency Distribution Analysis of the Human Colonic Electrical Activity

AUTHOR: Miguel Angel Barrientos Martinez, B.Sc.
(National Autonomous University of Mexico)

SUPERVISOR: Dr. Jan D. Huizinga and
Dr. Hubert de Bruin

NUMBER OF PAGES: xvi, 152

Abstract

The electrical activity recorded from the human colon could play an important role in analyzing the pattern of contractions under different physiologic or experimental states. In general, the frequency of the electrical activity is extremely irregular and time-varying. Its analysis requires a technique that considers variations in both time and frequency domains. The research undertaken was to analyze time-frequency variations of the human colonic electrical activity, to implement positive time- frequency distribution techniques in a computer system and to analyze theoretical signals using this technique to characterize a kernel function. Our results show that the uncertainty coefficient together with the marginal conditions and the average of the conditional PTFD in time and also in frequency can be applied to determine which kernel function and c-value were appropriate for calculating the PTFD of a sinusoidal signal. The selected kernel function constituted a comparative template of signals with similar characteristics. We found that those results were useful in analyzing the time- frequency variations of the electrical activity recorded in the human colon. The comparison of relative contributions of frequency bands showed that the band with the highest values during the pre- and interprandial period was 30-40 cpm suggesting an important role in the generation of bursts of these signals. The numerical results suggested that a meal can induce changes in the relative importance of frequencies below 10 cpm and a significant change in the 30-40 cpm band. In addition, a computer program of the Chakravarti method was implemented to calculate the Fourier

transform of nonperiodical signals. This program was part of the computer program system developed to compute the PTFD of theoretical and experimental signals.

Acknowledgements

I would like to express my special thanks to Dr. Jan D. Huizinga, for giving me the opportunity to come to McMaster University, his helpful criticism and financial support during the great part of my Master's study.

I am grateful to Dr. Hubert de Bruin for his valuable comments and recommendations. I express my thanks to Dr. Berj L. Bardakjian for his suggestions about time-frequency analysis and Dr. Gervais Tougas for his financial support during the last part of my Master's study.

Financial assistance from Duphar Weesp is also recognized and appreciated.

My deepest thanks are dedicated to Dr. Carlos Barajas-Lopez and his lovely family for their friendship and enthusiastic support.

I would like to devote my heartfelt thanks to my family, specially to my parents Mrs. Angelina Martinez and Mr. Guillermo Barrientos. To my sisters and brothers for their continuous encouragement and support.

Finally, I wish to thank Laura Torres for her spiritual support.

Contents

1 Introduction 1

1.1 Human Colonic Electrical Activity 2

1.1.1 Brief anatomic and physiologic description of the human colon 2

1.1.2 Composition and main characteristics of the colonic electrical activity 4

1.1.3 In vivo techniques of studying electrical activities 5

1.1.4 Main problems in analysis of colonic electrical activity 6

1.2 Different approaches to analyze the colonic electrical activity 8

1.2.1 Fast Fourier Transform 9

1.2.2 Spectrogram or Running Analysis 10

1.2.3 Adaptive Spectral Analysis 10

1.3 Objectives 14

2 Time-Frequency Distribution Analysis 15

2.1 Introduction 15

2.2 General Method of Time-Frequency Distributions 17

2.3 The Spectrogram or Short-Time Fourier Transform 20

2.4 The Wigner Distribution 22
2.5 Positive Time-Frequency Distribution 23

3 Implementation of a numerical method for calculating the Fourier integral 25

3.1 Abstract 25
3.2 Introduction 26
3.3 Methods 28
3.4 Numerical Results and Discussion 31
3.5 Concluding remarks 36

4 A computer program for positive time-frequency analysis of human colonic electrical activity 39

4.1 Abstract 39
4.2 Introduction 40
4.3 Computational methods 41
4.4 System description 43
4.4.1 Data acquisition system 43
4.4.2 Analysis program system 44
4.5 Menu interface and control process 49
4.5.1 Control process 51
4.5.2 Data Analysis 51
4.6 Conclusions 52

5 Positive Time-Frequency Distribution of theoretical time-varying signals 55

5.1 Abstract 55
5.2 Introduction 56
5.3 Uncertainty coefficient and frequency- conditional and time-conditional PTFD 59
5.4 Discrete Representation of PTFD 62
5.5 Sinusoidal signals and Kernel functions 65
5.6 PTFD of sinusoidal signals. Numerical Results and Discussion 86
5.7 Conclusions 105

6 An analysis of the human colonic electrical activity using Positive Time-Frequency distribution techniques 112
6.1 Abstract 112
6.2 Introduction 113
6.3 Materials and Methods 115
6.3.1 Experimental method 115
6.3.2 Positive time-frequency distribution technique 116
6.4 Experimental results and discussion. 119
6.4.1 The main components for calculating the PTFD. 120
6.4.2 Kernel functions 124
6.4.3 PTFD analysis of experimental signals 126
6.5 Conclusions 136

7 Conclusions and future developments 140
7.1 Conclusions 140
7.2 Future developments 145

Bibliography **148**

List of Figures

1.1 Recordings of human colonic electrical activity. 7

1.2 Time-Frequency representation of CEA. 13

3.1 Power spectrum of $\sin(2\pi ft)$, with $f = 0.4766$Hz. 32

3.2 Power spectrum of s_2 for α_1 and α_2. 34

3.3 Power spectrum of colonic signal. 37

4.1 Interaction between main components for PTFD analysis. 53

5.1 The main components for calculating the PTFD of TS1. 72

5.2 Geometric figure of $\varphi_1(x,y)$ and $\varphi_3(x,y)$ for TS1. 73

5.3 Marginal representation of TS2. 76

5.4 Geometric figure of $\varphi_1(x,y)$ and $\varphi_3(x,y)$ for TS2. 77

5.5 Marginal representation of TS3. 78

5.6 Geometric figure of $\varphi_1(x,y)$ and $\varphi_3(x,y)$ for TS3. 79

5.7 Marginal representation of TS4. 81

5.8 Geometric figure of $\varphi_1(x,y)$ and $\varphi_3(x,y)$ for TS4. 82

5.9 Marginal representation of TS5. 84

5.10 Geometric figure of $\varphi_1(x,y)$ and $\varphi_3(x,y)$ for TS5. 85

5.11 Marginal representation of TS6. 87
5.12 Geometric figure of $\varphi_1(x,y)$ and $\varphi_3(x,y)$ for TS6. 88
5.13 PTFD of TS1. 90
5.14 Marginal distributions and average of conditional PTFD of TS2. . . . 92
5.15 PTFD of TS2 using φ_1. 93
5.16 $< f >_t$ and $< t >_f$ of TS2. 94
5.17 Marginal distributions and average of conditional PTFD of TS3. . . . 95
5.18 PTFD of TS3 using φ_1. 96
5.19 $< f >_t$ and $< t >_f$ of TS3. 97
5.20 Marginal distributions and average of conditional PTFD of TS4. . . . 99
5.21 PTFD of TS4 using φ_1. 100
5.22 $< f >_t$ and $< t >_f$ of TS4. 101
5.23 Marginal distributions and average of conditional PTFD of TS5. . . . 102
5.24 PTFD of TS5 using φ_1. 103
5.25 $< f >_t$ and $< t >_f$ of TS5. 104
5.26 Marginal distributions and average of conditional PTFD of TS6. . . . 106
5.27 PTFD of TS6 using φ_1. 107
5.28 $< f >_t$ and $< t >_f$ of TS6. 108

6.1 Short segments of experimental signals. 121
6.2 The main components for calculating the PTFD of ES1. 122
6.3 The main components for calculating the PTFD of ES2. 123
6.4 The main components for calculating the PTFD of ES3. 125
6.5 Contour level plot of φ_1 for ES1. 127
6.6 Contour level plot of φ_1 for ES2. 128

6.7 Contour level plot of φ_1 for ES3. 129
6.8 PTFD analysis of ES1. 130
6.9 PTFD analysis of ES2. 131
6.10 PTFD analysis of ES3. 133

List of Tables

3.1 $U_r(t_k)$ coefficients for cos and sin 30

3.2 $V_r(t_k)$ coefficients for cos and sin 30

3.3 *Power spectrum of* $s_1(t)$ *calculated by analytical method, trapezoidal sum and correction terms* δ^2 *and* δ^4 33

3.4 *Power spectrum of* $s_2(t)$ *calculated by trapezoidal sum and correction term* δ^4 35

3.5 *Power spectrum of the human colonic electrical activity calculated by trapezoidal sum and correction terms* δ^4 36

4.1 Format for an experiment trace file 46

4.2 Format for an analysis parameter file 47

4.3 Format for an analysis lattice file 48

4.4 Format for an analysis control file 49

5.1 *Time-frequency lattice representation.* 66

5.2 Range of values of each kernel function in sinusoidal signals 74

5.3 Entropy and uncertainty coefficients of each sinusoidal signal by marginal product and PTFD using a φ function. 89

6.1 Entropy and uncertainty coefficients of each experimental signal by marginal product and PTFD using a φ function. 124
6.2 *Comparison of relative contribution of bands of frequency for ES1 (percent).* 132
6.3 *Comparison of relative contribution of bands of frequency for ES2 (percent).* 134
6.4 *Comparison of relative contribution of bands of frequency for ES3 (percent).* 135
6.5 *Conditional PTFD given time of two bands of frequency (percent).* . 136

Nomenclature

ARMA	Autoregressive moving average
DWD	Discrete Wigner distribution
CEA	Colonic electrical activity
FFT	Fast Fourier transform
$\Gamma(t,f)$	Product of marginal distributions
H	Entropy
Hz	Cycle(s) per second
$\varphi(x,y)$	Kernel function
PTFD	Positive Time-Frequency distribution
$P(f\|t)$	Conditional distribution given time
$P(t\|f)$	Conditional distribution given frequency
STFT	Short-Time Fourier transform
TS	Trapezoidal sum
TFD	Time-Frequency distribution
U	Uncertainty coefficient
WD	Wigner distribution
c	Constant associated with kernel function
cpm	Cycle(s) per minute
$< f >_t$	Conditional average frequency

min	Minute(s)
s	Second(s)
$< t >_f$	Conditional mean duration
x(t)	Cumulative marginal distribution of time
y(f)	Cumulative marginal distribution of frequency

Chapter 1

Introduction

The human colon plays an important role in the gastrointestinal system. The colon receives semiliquid material, mixes it and extracts water and electrolytes, changing the material to a semi-solid state. The colon acts as a storage site, moves its contents and periodically, expels the faecal mass. Movements are such as to produce very slow flow, facilitating the extraction of water from the feces by diffusion [5]. The movements or contractions of the colon must occur in a well defined temporal and spatial order to accomplish its motor functions. The temporal characteristics include the frequency, amplitude, and duration of contraction. The propagation of contractions corresponds to spatial characteristics [29]. The patterns of contractions in the colon have been studied for a long time, which has resulted in defining the functional regions of the colon. Motility studies on human colon are usually carried out in order to monitor contractions or intraluminal pressure changes. The monitoring of contractions is useful in evaluating the effects of drugs and other stimulants such as meals, but it does not elucidate how colonic contractions are organized to accomplish the normal

patterns of flow in the colon. Several mechanisms control the temporal and spatial organization of contractions through the colon, one of them the myogenic control corresponds to the electrical activities generated in the colonic smooth muscle cells [29]. The analysis of temporal variations of colonic electrical activity is an important technique to study the functional and organizational characteristics of the human colon.

1.1 Human Colonic Electrical Activity

1.1.1 Brief anatomic and physiologic description of the human colon

The different functional regions of the human colon are (a) the proximal region, where antiperistaltic movements are the typical pattern of motor activity; (b) middle region, which is characterized by segmental contractions that can either be stationary or can progress over short distances in either direction; and (c) distal region, that is characterized by infrequent, powerful, caudad-moving contractions [33].

The motor activity of the colon is performed by two muscle layers with the long axis of their cells perpendicular to each other: the inner layer of circular muscle cells (circumferentially oriented) and the outer longitudinal muscle layer (continuous and concentrated into three bands called taeniae). The muscle of the colon generates electrical signals that constitute the elements of the electromyogram of the colon. The electrical activity recorded in the human colon is associated with the functions of initiation and integration of the colonic contractions. The former is achieved by a slow electrical transient called the electrical slow wave; the latter is accomplished by

a burst of much more rapid electrical transients, the spike burst. The slow wave is a mechanism to restrict a contraction of the muscular wall to a fixed place and time. The spike burst is a summation of action potentials. When the electromyogram is recorded from several points, slow waves can be seen to spread away from a source. The pattern of spread of the slow waves determines the pattern of spread of contractions. Therefore, slow waves coordinate contractions and they are also called pacesetter potentials or electrical control activity [5].

The myogenic factors play an important role in the initiation and control of colonic motility and they are

1. The electrical activities of both inner and outer muscle layers.
2. Communication between muscle cells.
3. Communication between muscle bundles.
4. Excitation-contraction coupling.

Myogenic electrical activities represent movement of charged ions across the muscle-cell membrane. Accurate recording of these events requires measurement of the potential difference between the outside and the inside of the smooth-muscle cell. Only some in vitro techniques can accurately measure this membrane potential. In vivo studies are needed to associate electrical activity with transit, and to study the integrated response of the organ to physiologic and other stimuli [5].

1.1.2 Composition and main characteristics of the colonic electrical activity

Two types of electrical activity are generated by the muscle cells of the human colon [19]:

i. Fast transient depolarization of a few milliseconds' duration (The spikes or action potentials).

ii. Much slower oscillations which last a few seconds and are distributed in bursts (slow waves or electrical oscillations).

The spiking activity of the colon appears to be organized in two classes of bursts (which do not have the same significance in regard to mechanical events) :

1. Long spike bursts lasting more than 6 s correspond to a large-amplitude phasic contraction.

2. Short spike bursts lasting less than 6 s correspond to small-amplitude contractions.

The slow waves occur in all regions of the colon and their configuration is variable, sometimes appearing as sinusoidal, biphasic, or polyphasic. Remarkable features of the electrical oscillations of the human colon are that their frequency is variable in time and their amplitude is low and also variable. In fact, the oscillations can be reduced to noise level, thus the electrical activity is not omnipresent. The amplitude of the slow wave potentials ranges from just detectable levels to approximately 1.5 mV. Some studies report peak to peak amplitudes around 0.5 mV or 0.6 mV using serosally sutured electrodes [6]. The frequency of slow waves in the human colon has

not been agreed on. Different studies indicate that the frequency ranges from 2 to 12 cpm. The spike activity occurs as short bursts at the frequency of the slow waves and as long bursts that do not seem to be related to ongoing slow wave activity. Spike activity is rapid oscillations ranging in frequency from 24 to 40 cpm [33].

The electrical activities of the circular and longitudinal muscle layers of the human colon have many common characteristics. One important difference is that only the circular muscle can generate oscillatory activity at frequencies lower than 12 cpm.

1.1.3 In vivo techniques of studying electrical activities

Electrical activity in vivo may be recorded either from the serosal or mucosal surface of the colon. In vivo recording techniques measure extracellular electrical current, rather than transmembrane potentials. In general, a recording procedure includes a bipolar electrode system with two electrodes sutured onto the serosal surface of the colon (at surgery), or electrodes mounted onto an intraluminal probe, or attached by suction or clipped to the mucosa. Intraluminal recording techniques suffer from a major disadvantage, namely no direct contact with the muscle layers. In addition , signals may be picked up from both the longitudinal and the circular muscle, which have different types of electrical activity. Furthermore, motion artifacts may complicate the picture. All in vivo techniques have to take into account that electrical activities from noncolonic sources are picked up to varying degrees [19].

In many investigations of the electrical activity of the human colon it has been seen that slow wave activity is not constant, but intermittent. This intermittency may be real, but it is also possible that it is artifactual, arising from an intermittency in

electrode contact with the signal source rather than an intermittency in the generation of the signal [5].

1.1.4 Main problems in analysis of colonic electrical activity

Both visual and computer-based methods are used to analyze electrical activity. Because of the complexity of colonic signals, usually selected portions of the recordings are analyzed (Figure 1.1). The outcomes of such analyses cannot be generalized and data from different subjects cannot be compared. Since the human colonic electrical activity is variable in time, different short segment analyses cannot simply be summed. Presentation of successive short section analyses is preferable and undoubtedly would indicate frequency changes in time [19]. A basic problem of in vivo recording is that one cannot be certain that all or most of the electrical activity generated by the muscle is actually recorded.

In general, the frequency of the colonic electrical activity is highly irregular and time-varying (the frequency can vary from cycle to cycle and from minute to minute at the same electrode). This gives rise to a power spectrum that has multiple fundamental frequency peaks, and the energy in each peak is not confined to a single frequency, but it is distributed over a band around the peak. Furthermore, these peaks shift in frequency from one block of data to the next and vary in amplitude.

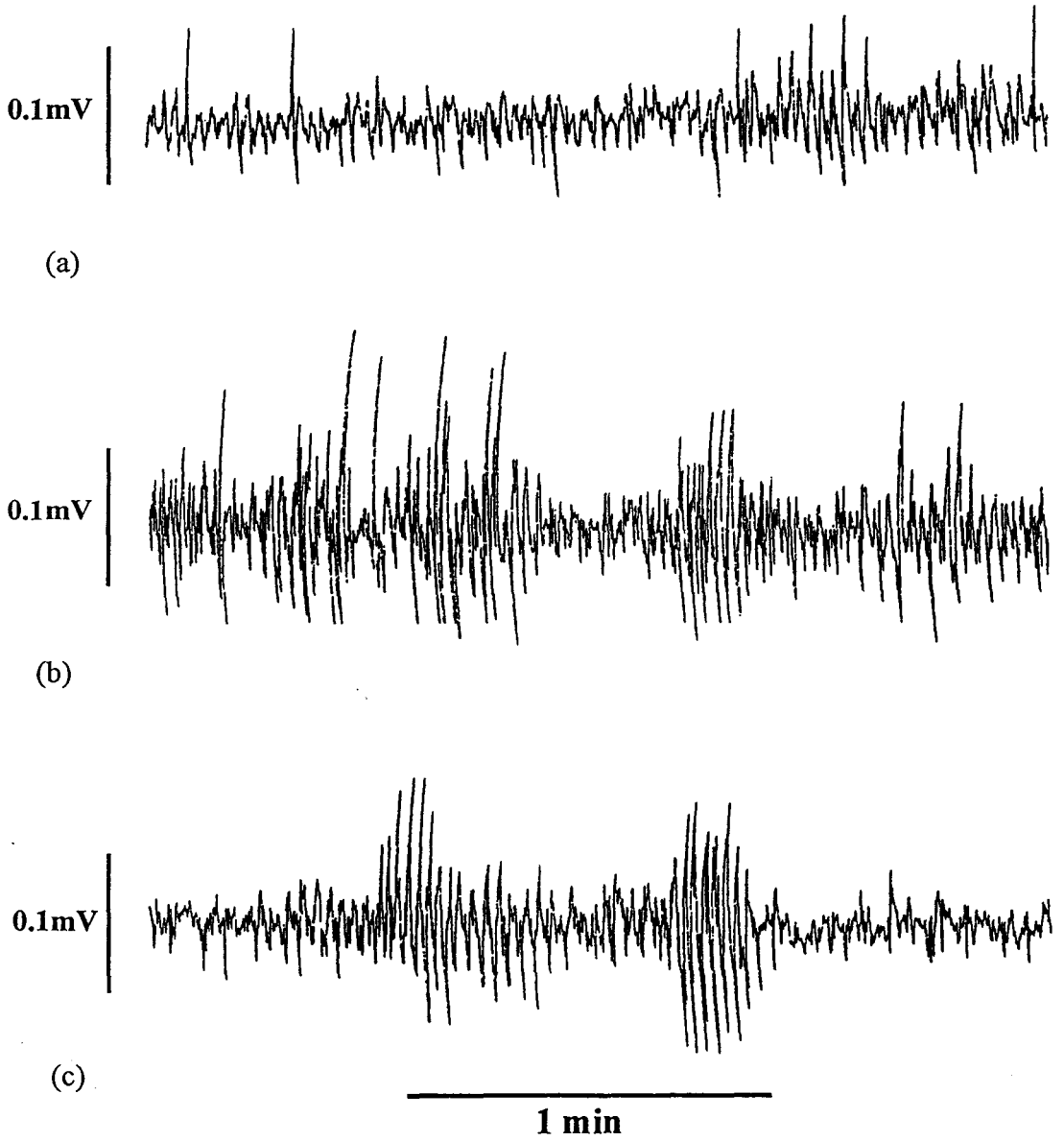

Figure 1.1: *Recordings of human colonic electrical activity during (a) preprandial, (b) interprandial and (c) postprandial period.*

Recordings were made using lower and upper cut-off frequencies of 0.16 and 30 Hz respectively. The plot shows frequency variations in the same recording under two different conditions. (Provided by Dr.W.E.Waterfall)

1.2 Different approaches to analyze the colonic electrical activity

In general, every physical event such as the human colonic electrical activity can be described in various ways for its analysis. One method is the description of the signal in time domain where the behaviour of the signal is characterized with measurements of some specific parameters in time, for example

- Amplitude of minimum and maximum values.
- Mean and standard deviation of the amplitude.
- Area under the curve.

These parameters depend on the peak detection. In general, a real peak is not clearly defined, therefore, its automatic identification is difficult to implement by a computer program. Some authors have proposed to approximate the gastrointestinal signals by using cubic B-spline functions with equally spaced knots and use the mathematical representation for estimating the peaks of the original signal and for data reduction [16].

The signal also can be analyzed in the frequency domain using the Fourier Transform which allows the decomposition of a signal into individual components and establishes the relative intensity of each component. The characteristics of a signal could be described in terms of its main frequency components. There are various parameters to analyze in the frequency domain, for example:

- Absolute value of each frequency component

- Relative importance of each frequency component
- Bands of frequency
- Signal intensity in individual or bands of frequency

Because for some events we need to know which frequency f was produced at time t, any of those descriptions is not complete by itself. Therefore, we need a method to describe an event taking into account information in time and frequency together. There are different techniques which can provide both time and frequency information in order to investigate frequency changes of the colonic electrical signal over time. The main objective of this thesis is to present one of those techniques and its application to the analysis of the colonic electrical signals (CEA).

1.2.1 Fast Fourier Transform

The spectral analysis of the CEA by utilizing the fast Fourier transform (FFT) is the most common method to calculate the power peak of a frequency range [15] or the power spectrum and to determine the importance of each frequency component. The signal recorded from any place of the human colon may have multiple frequency peaks present in its power spectrum. These peaks may or may not be related harmonically to each other. The frequency and intensity of these peaks vary in time and space [2]. The way to calculate the power spectrum is (i) applying the FFT to the complete segment or (ii) using window functions to shift and overlap sections of data according to a given percentage, calculating the FFT for each section of data and finally, averaging all section results.

1.2.2 Spectrogram or Running Analysis

The Spectrogram or FFT-based running spectral analysis is a technique which can provide both time and frequency information in order to investigate frequency changes of the colonic electrical signal over time. In this method Fourier Analysis is used to obtain a series of power spectra for periods that may overlap in time. A more accurate way to perform running spectral analysis is to calculate the power spectrum using the periodogram method: divide the complete signal into M overlapping frames with N samples in each one and then calculate the periodogram for each frame. For this case, N should be large and the overlapping could be about 75 percent of the size of the frame. This method is suitable for extracting information about slow waves due to the averaging effect created by the frame processing of the FFT. Van der Schee *et al.* [14] claimed that running spectral analysis offers a concise representation of electrogastrographical data in terms of frequency and its power over the course of time. However, the crucial part of this method is the selection of the window size and the percent of overlapping, both aspects being related to the signal characteristics.

1.2.3 Adaptive Spectral Analysis

The adaptive spectral analysis method using autoregressive moving average (ARMA) modelling is another technique which can provide time and frequency representation of the colonic electrical signal. This is a parametric approach to spectral estimation and it is based on the assumption that the measured data under investigation evolves from a process that can be approximately represented by a select model. The parametric approach is a three-step procedure:

1. Select a representative model set (AR, MA, ARMA and order).

2. Estimate the model parameters from the data.

3. Estimate the power spectrum using these parameters.

The major advantage of these model-based methods is that we can achieve higher frequency resolution since the data is not windowed [3]. In order to show how the frequency components evolve over time, a mathematical technique was implemented that identifies the parameters of the autoregressive moving average model (ARMA) and estimates the power spectrum of the signal at any time instant. This technique would be helpful to separate frequency bands based on functional significance and calculate their change over time.

The basic model representation of the colonic electrical signal y_t is

$$A(z^{-1})Y_t = C(z^{-1})\varepsilon_t, \tag{1.1}$$

or expressed as

$$y_t = -\sum_{k=1}^{n_a} a_k y_{t-k} + \sum_{k=1}^{n_c} c_k \varepsilon_{t-k} + \varepsilon_t, \tag{1.2}$$

where a_k $(1 \leq k \leq n_a)$ and c_k $(1 \leq k \leq n_c)$ are parameters of the ARMA model and ε_t is a white noise process.

Once the parameters of the ARMA model are identified the spectral estimation $S_{yy}(\omega)$ can be calculated as

$$S_{yy}(\omega) = \frac{\sigma^2 |1 + \sum_{k=1}^{n_c} c_k \exp(-i\omega k)|^2}{|1 + \sum_{k=1}^{n_a} \exp(-i\omega k)|^2}, \tag{1.3}$$

where σ^2 is the variance of the white noise and ω is the angular frequency [24].

Tracking of time-varying phenomena is an important problem in many areas of application [20]. A basic underlying technique for these problems is recursive identification [17]. A typical feature of a recursive identification algorithm is that the

current parameter estimate is updated using a transformation of the last observation, multiplied by a certain gain factor γ_t

$$\theta_t = \theta_{t-1} + \gamma_t \cdot f(\theta_{t-1}, y_t). \tag{1.4}$$

The recursive identification algorithm implemented was the recursive prediction error method [24] with the following scheme:

$$\hat{\varepsilon}_t = y_t - \hat{y}_t(\theta), \tag{1.5}$$

$$\hat{\theta}_t = \hat{\theta}_{t-1} + \gamma_t R_t^{-1} y_t \hat{\varepsilon}_t, \tag{1.6}$$

$$R_t = R_{t-1} + \gamma_t \cdot \{y_t y_t^T - R_{t-1}\}, \tag{1.7}$$

where $\hat{\varepsilon}_t$ is the prediction error one step ahead, and R_t is the discrete information matrix.

The gain was specified in terms of forgetting factor or θ value. A large gain means that considerable attention is paid to the most recent measurement y_t, and that information in old measurements is partially forgotten. The gain will determine how alert the algorithm will be to track changing properties of the system. A large gain means that it will quickly adapt to a new situation, but also that it will be sensitive to random errors in the signal y_t. The best choice of gain or forgetting is thus a trade-off between alertness and noise sensitivity, and will depend on how much the system changes compared to the noise level in the measurements. As the parameters are adaptively adjusted for each input sample, the power spectrum of the signal can be calculated at any time instant; but in practice it is better to calculate it once for a certain time interval or consider the averaged parameters over a small range of time (Figure 1.2).

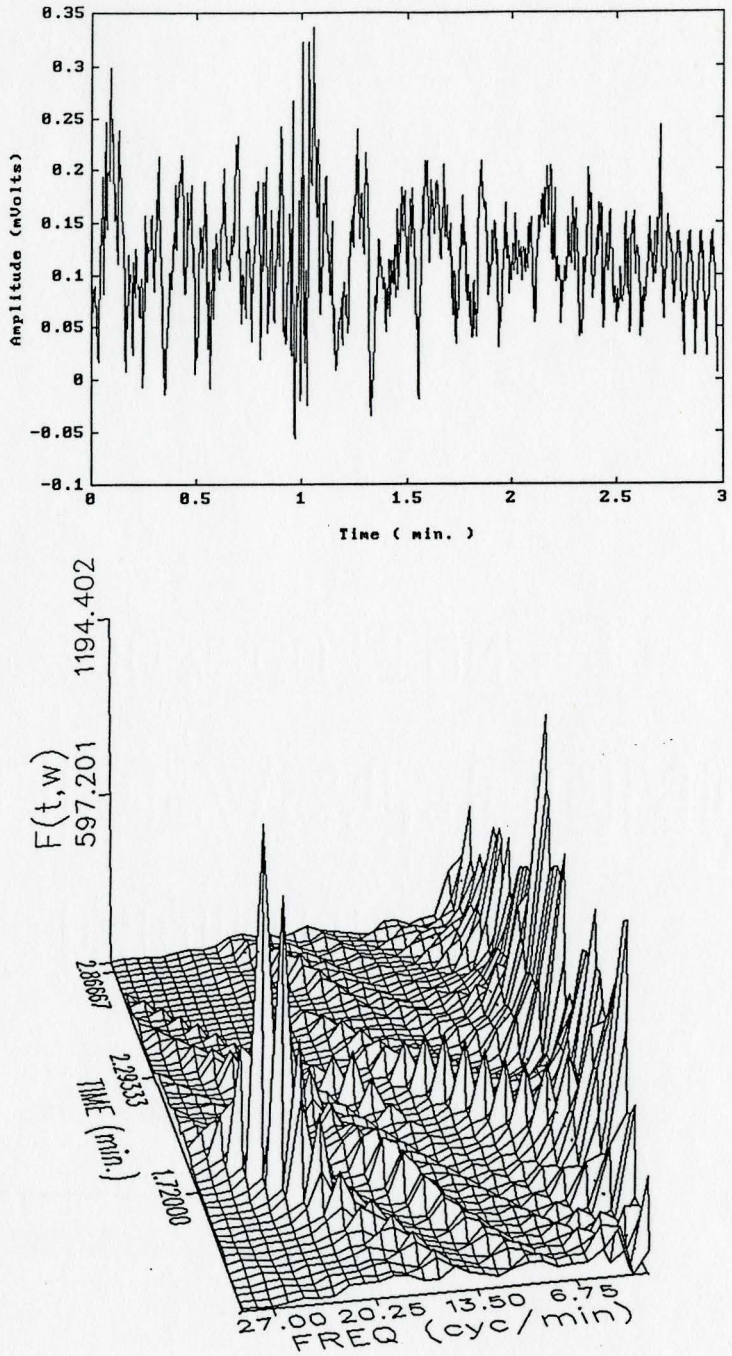

Figure 1.2: *Time-Frequency representation of colonic electrical signal using Adaptive Spectral Estimation.*

The distribution was calculated using an autoregressive model of order 30. The plot shows the frequency behaviour during a small interval of time.

1.3 Objectives

In this thesis, a methodology is presented whose main objective is to analyze time-frequency variations of the human colonic electrical activity. The methodology was developed by Cohen et.al. [23, 22] and it corresponds to positive time- frequency distribution (PTFD) techniques. The specific goals of this work are (a) to implement PTFD techniques in a computer program system, (b) to analyze theoretical signals using this technique to characterize a kernel function, and (c) to analyze a recording of the human colonic electrical activity using the same technique.

The remainder of this thesis is organized as follows: chapter 2 presents a review of time-frequency distribution techniques, chapter 3 describes an implementation of Chakravarti's method to calculate the Fourier integral, chapter 4 shows a computer program system to calculate, plot and print PTFD results, chapter 5 presents an application of PTFD analysis to theoretical signals, chapter 6 describes a practical application of PTFD to the human colonic electrical activity and finally, chapter 7 discusses the significance of the final work and gives conclusions.

Chapter 2

Time-Frequency Distribution Analysis

2.1 Introduction

The analysis of the frequency components of a biological signal has been the subject of a number of studies. The accurate determination of these components is important so that their value may convey information about the dynamics of the biological process or it might be necessary to discriminate among signal characteristics under different experimental conditions. For example, in the analysis of the colonic electrical activity, it is important to see if the frequency gradient is consistent with the main colonic motor function of temporary storage and mixing of contents. A frequency description is generally needed to obtain a better understanding of the phenomena which are involved. However, spectral analysis relies upon an implicit assumption of steady-state behaviour or stationarity (the spectral characteristics do not change over time).

Biological signals present multiple components, they are subject to noise, and on many occasions their frequency and amplitude continuously change over time. This characteristic motivates the need for descriptions which take into account frequency aspects together with a possible time dependence. The possibility of representing a signal in both time and frequency domains has opened new alternatives of analysis for time-varying nonstationary signals, in which the amplitude and frequency change in time. Since Wigner's original work [39] in quantum mechanics, there have been many joint time-frequency distributions (TFD) that have been proposed for the description of a signal in time and frequency. The general theory of TFD was developed by Cohen [7], who described the main properties of time- frequency distributions and showed the way to generate a complete class of distributions. Cohen also presented an interesting historical review of TFD [8].

The time representation or frequency representation, individually, cannot display the whole information conveyed by the signal; for example, a wide class of finite energy signals have the same power spectrum [8]. Therefore, the idea behind the TFD is putting together both domains that in implicit ways are interrelated and showing frequency variations during time. When the interrelationship maintains the same behaviour along time or when the signal spectral content does not change in time, we get a constant value in the TFD; then we can take a signal segment, analyze it and take it as the behaviour representative of the complete segment. Under such conditions, we can also analyze the general behaviour which will represent the local behaviour. However, several natural signals present variations in their frequency content during time and we need the description of these variations and, therefore, it is very important to obtain the mathematical model that describes this behaviour. The general TFD supports that description and, particularly, the positive time-frequency

distribution (PTFD) provides information in terms of true energy densities.

Intuitively, it is evident that the energy of a signal does have a distribution in time and frequency in some sense. Then the TFD will describe the energy density or intensity of a signal simultaneously in time and frequency. If we had such distribution we could ask what fraction of the energy is in a certain frequency and time range , we could calculate the distribution of the frequency at a particular time, we could calculate the mean frequency and its local spread.

This chapter is a topical review of time-frequency analysis techniques and it is organized as follows. In the first section the general properties and restrictions of TFD are described; the second and third sections are dedicated to two very important TFD techniques: the spectrogram and the Wigner distribution (WD) respectively; and the last section shows the main characteristics and advantages of positive TFD techniques.

2.2 General Method of Time-Frequency Distributions

The basic aim of Time-Frequency theory is to establish a function that will describe a time-varying spectrum. A joint TFD would give us the fraction of energy per unit time and per unit frequency. Using TFD we can ask what fraction of energy is in a certain frequency and time range; we can calculate the frequency distribution at any particular time and its global and local moments such as the mean frequency and local spread.

Let $F(t, f)$ be the joint function of time and frequency that represents the

energy distribution or intensity at time t and frequency f. Ideally the summing up of the energy distribution for all frequencies at a particular time would give the energy distribution at time or signal power, and the summing up over all times at a particular frequency would give the energy distribution at frequency or power spectrum. These are the marginal conditions that are specified by

$$\int_{-\infty}^{\infty} F(t,f)df = |s(t)|^2 \tag{2.1}$$

and

$$\int_{-\infty}^{\infty} F(t,f)dt = |S(f)|^2, \tag{2.2}$$

where $s(t)$ is the signal, $|s(t)|^2$ is the intensity per unit time at time t, and $|s(t)|^2dt$ is the fractional energy in time interval dt at time t. $S(f)$ is the Fourier Transform and is expressed by

$$S(f) = \int_{-\infty}^{\infty} s(t)e^{-j2\pi ft}dt. \tag{2.3}$$

$|S(f)|^2$ is the intensity per unit frequency at f or $|S(f)|^2df$ is the fractional energy in frequency interval df at frequency f.

The marginal or individual distributions satisfy the following condition

$$\int_{-\infty}^{\infty} |s(t)|^2dt = \int_{-\infty}^{\infty} |S(f)|^2df = 1. \tag{2.4}$$

The total energy E, expressed in terms of distributions is given by

$$E = \int_{-\infty}^{\infty} F(t,f)dtdf \tag{2.5}$$

and will be equal to the total energy of the signal if the marginal conditions are satisfied.

Cohen [7] proposed that an infinite number of TFD can be readily generated from

$$F(t,f) = \int\int\int e^{j2\pi\theta(u-t)}\phi(\theta,\tau)s^*(u-\frac{\tau}{2})s(u+\frac{\tau}{2})e^{-j2\pi f\tau}d\theta du d\tau, \qquad (2.6)$$

where τ and θ are the lag variables in time and frequency respectively, and $\phi(\theta,\tau)$ is an arbitrary function called the kernel. By choosing different kernels we obtain different distributions. For example, the Wigner distribution has the kernel $\phi(\theta,\tau) = 1$. In general, the properties of the TFD are related to the properties of the kernel. The TFD satisfies the marginal conditions (2.1 and 2.2) implies that the kernel must have the property: $\phi(0,\tau) = \phi(\theta,0) = 1$.

A time-frequency distribution can be considered to be the Fourier transform of the time-indexed autocorrelation function $C(t,\tau)$ which is estimated at a given time t. Therefore, we have the following expression

$$F(t,f) = \int e^{-j2\pi f\tau}C(t,\tau)d\tau, \qquad (2.7)$$

where

$$C(t,\tau) = \int\int e^{j2\pi\theta(u-t)}\phi(\theta,\tau)s^*(u-\frac{\tau}{2})s(u+\frac{\tau}{2})d\theta du. \qquad (2.8)$$

As can be seen in (2.8), the kernel function $\phi(\theta,\tau)$ plays an important role in determining the characteristics of the time-indexed autocorrelation function which can be estimated utilizing time averages.

2.3 The Spectrogram or Short-Time Fourier Transform

The spectrogram or Short-Time Fourier Transform(STFT) is the most familiar time-frequency distribution and it is based on the assumption that over a short time interval signals can be considered to be stationary. The spectrogram utilizes a short-time window whose length is chosen so that over the length of the window a signal can be considered to be stationary. Then the Fourier Transform of this windowed signal can be used to obtain the energy distribution of the signal along the frequency direction at a given time which corresponds to the centre of the window. To increase the frequency resolution, one must use a longer observation duration, which means that the nonstationarity components occurring during this interval will be smeared in time and frequency [18]. The STFT considers only specific time segments of the signal $s(t)$, which are obtained by applying a window function $w(t)$ to $s(t)$:

$$s_w(t_0, t) = s(t)w(t - t_0). \tag{2.9}$$

In general it is assumed that the window is real, has a finite duration D_w, and is centred at the instant t_0. The Fourier transform of a time segment of $s(t)$

$$S_w(t_0, f) = \int_t s(t)w(t - t_0)e^{-j2\pi ft}dt \tag{2.10}$$

represents this segment for all values of t:

$$s_w(t_0, t) = \int_f S_w(t_0, f)e^{j2\pi ft}df. \tag{2.11}$$

However, because of (2.9) it is additionally known that s_w is centred at t_0 and has duration D_w. Therefore, the STFT gives a time-frequency representation of $s(t)$ if it is evaluated for all values of t_0.

The squared modulus for the STFT, the spectrogram of $s(t)$,

$$F_s(t,f) = |S_w(t,f)|^2 \tag{2.12}$$

displays the signal energy density in time and in frequency. It can be expressed as

$$F_s(t,f) = \int_{t1}\int_{t2} s(t_1)s^*(t_2)w(t_1-t)w(t_2-t)\cdot e^{-j2\pi f(t_1-t_2)}dt_1dt_2, \tag{2.13}$$

where the window w is centered at the instant t for all values of t_1 and t_2. The time average of F_s

$$\int_t F_s(t,f)dt = \int_\nu |S(\nu)|^2|W(f-\nu)|^2d\nu, \tag{2.14}$$

where $W(f)$ is the Fourier transform of $w(t)$, gives an average of the spectral energy density $|S(f)|^2$. It coincides with $|S(f)|^2$ when $|W(f)|^2$ is an impulse function in frequency.

Likewise the frequency average of F_s

$$\int_f F_s(t,f)df = \int_t |s(\tau)|^2w^2(\tau-t)d\tau \tag{2.15}$$

gives an average of the power of $s(t)$. This average gives the instantaneous behaviour of $s(t)$ when $w^2(t)$ is an impulse function in time. While both averages (2.14) and (2.15) clearly show that a certain instantaneous energy distribution is approximated by the spectrogram, the conflicting conditions on the window function $w(t)$ also show that an ideal behaviour can never be obtained by the spectrogram. Integrating F_s over the whole (t,f) plane yields

$$\begin{aligned}\int_t\int_f F_s(t,f)dtdf &= \int_\tau |s(\tau)|^2\int_t w^2(\tau-t)dtd\tau \\ &= E_s\cdot E_w,\end{aligned} \tag{2.16}$$

i.e., if the window has unit energy,

$$E_w = \int_t w^2(t)dt = \int_f |W(f)|^2 df = 1, \tag{2.17}$$

then the average of the spectrogram is equal to the signal energy E_s [25]. In a strict way, the spectrogram is not an energy distribution in the sense of the marginal conditions (2.1 and 2.2).

2.4 The Wigner Distribution

The Wigner distribution (WD) has been applied to different aspects of signal analysis. There exist different texts that present the main properties of the WD in the continuous and discrete domain and describe the relationship with the general method of TFD techniques [34, 35, 36]. The WD has a kernel function equal to one and its spectrum is always real-valued, but it can very well take on negative values. Therefore, it does not give a true density. There exist interference effects between structures in the time frequency plane due to the bilinearity of the representation [37]. When the kernel is taken to be independent of the signal then the distributions generated are bilinear in the signal.

The WD is given by

$$W(t,f) = \int_{-\infty}^{\infty} e^{-j2\pi f\tau} s^*(t-\frac{\tau}{2}) s(t+\frac{\tau}{2}) d\tau, \tag{2.18}$$

where t and f are the time and frequency and $s(t)$ is the signal. The expression for the discrete Wigner distribution (DWD), as defined in ([35]), is

$$W(k,\theta) = 2 \sum_{m=-\infty}^{\infty} e^{-j2k\theta} s^*(k-m) s(k+m) \tag{2.19}$$

The DWD is a function of the discrete variable k and the continuous variable θ. The function, with respect to the latter variable, is periodic with period π rather than 2π. Hence the sampling frequency of the original signal would be two times the Nyquist rate [35].

The WD satisfies the marginal conditions (2.1) and (2.2), therefore it is an energy distribution. Furthermore, the WD is a real-valued distribution because the kernel satisfies the property

$$\phi_t(\theta,\tau) = \phi_t^*(-\theta,-\tau), \tag{2.20}$$

where ϕ_t^* is conjugate symmetric of the kernel. The WD for some signals gives a very good picture of the time- frequency structure. It also has the advantage that it is uniquely related to the original signal. The main shortcoming is that it can become negative in some regions without any possible interpretation. Beside it often indicates concentration of energy in places where one would not expect [12].

2.5 Positive Time-Frequency Distribution

A joint time-frequency distribution should be positive for all values of time and frequency to obtain the fraction of the energy per unit time and unit frequency. Cohen and Zaparovany [23] presented the properties that the kernel must have in order to obtain PTFD and developed the following model

$$F(t,f) = |s(t)|^2|S(f)|^2\{1 + c\cdot\varphi(x(t),y(f)\}, \tag{2.21}$$

where $\varphi(x,y)$ is any positive function of the variables x and y in the unit square $(0 \leq x,y \leq 1)$ and normalized to one such that

$$\varphi(x,y) = h(x,y) - h_1(x) - h_2(y) + 1, \tag{2.22}$$

and x and y are defined as

$$x(t) = \int_{-\infty}^{t} |s(t')|^2 dt', \tag{2.23}$$

$$y(f) = \int_{-\infty}^{f} |S(f')|^2 df'. \tag{2.24}$$

$h_1(x)$ and $h_2(y)$ are the marginals of any $h(x,y)$ function defined by

$$h_1(x) = \int_{0}^{1} h(x,y)dy, \tag{2.25}$$

$$h_2(y) = \int_{0}^{1} h(x,y)dx \tag{2.26}$$

and c is a numerical constant which must be in the range

$$\frac{-1}{l_2} \leq c \leq \frac{1}{l_1}, \tag{2.27}$$

where $-l_1$ and l_2 are the minimum and maximum value of $\varphi(x,y)$. The PTFD must satisfy the marginal conditions (2.1 and 2.2) such that the total energy of the distribution should be the total energy of the signal, that is expressed as

$$E = \int\int F(t,f)dtdf = 1. \tag{2.28}$$

The properties of a particular PTFD are determined by its kernel or $\varphi(x,y)$ function. x and y are the cumulative marginal distributions of time and frequency respectively. $\varphi(x,y)$ is then a function that represents the correlation between $|s(t)|^2$ and $|S(f)|^2$ for all values of time and frequency. To define a kernel function for any specific signal is a difficult issue. In the literature, several kernel functions have been proposed to define a PTFD ([9, 22, 26]). One of our objectives was to estimate the PTFD of sinusoidal signals using some of those kernel functions and characterize the relationship between signal and kernel function. These results were used to define practical criteria for selecting a kernel function. These criteria were useful for analyzing electrical activity recorded in the human colon.

Chapter 3

Implementation of a numerical method for calculating the Fourier integral

3.1 Abstract

An implementation of the Chakravarti method for improving the numerical approximation of the Fourier integral of nonperiodic signals is presented. It makes use of the generalized Euler-Maclaurin formula with forward and backward differences. The improvement in the numerical approximation is reached by using correction terms. Three non-periodic signals were considered as examples in the numerical implementation of the Chakravarti method. This method was implemented on a 386 IBM-PC compatible computer using Fortran language. The numerical results of the power spectrum using correction terms order 2 and 4 were compared with respect to the

analytical method (first case) and the trapezoidal sum (TS) evaluated by the FFT. The correction term results went toward zero when the frequency increased as well as the analytical results in the first non-periodic signal. The numerical error approximation was smaller using correction terms than the TS technique. The improved results were mainly in the fourth significant decimal figure. The power spectra of cases 2 and 3 decrease faster during high frequencies than TS results. The numerical difference between correction terms and TS results was small in case 2 (specially high frequencies) and case 3.

3.2 Introduction

During the past decades, Fourier analysis has been an indispensable instrument for the treatment of nearly every question in modern signal analysis. There exist different reasons for this development, some of them are : (a) Fourier analysis gives valuable insight into the structural properties of time series, (b) the theory is firmly established and well understood, and (c) powerful computer systems are generally available and even provide results in real time. In the field of gastrointestinal research, Fourier analysis has been a very important technique to understand the frequency content of the human colonic electrical activity [30, 31].

Fourier analysis is an analytic method that decomposes a complex periodic waveform into a sum of harmonically related sinusoids. The fundamental frequency is set by the length of the overall sequence. The spectral peak at the fundamental frequency depends on the segment length, the steepness of the segment, and the shape of the main time components. It is well known that the numerical approximation of the finite Fourier integral of periodic signals can be done by the Trapezoidal sum

with good results [27]. However, when the signal is not periodic or the truncation point does not match the complete period of the signal the approximation error using Trapezoidal sum could be large. Under almost every experimental condition, a signal may not satisfy the periodic restriction. In particular, the electrical activity recorded in the human colon presents not only a nonperiodicity problem, but also variability in amplitude and frequency. Time-frequency techniques are a viable option for analyzing this kind of signal [10]. Therefore, the positive time-frequency distribution technique (PTFD) by Cohen [23] was used as analysis method of the human colonic electrical activity. For this method, the numerical evaluation of the Fourier integral is a crucial part. Twenty years ago Chakravarti generalized the Euler-Maclaurin formulas for improving the numerical approximation to the Fourier integrals [4]. He developed his formulas in terms of derivatives and using forward and backward differences.

In this chapter, a computer implementation of Chakravarti's method for calculating Fourier integrals is presented. Its use is exhibited in three different types of signals which were considered as examples in the numerical development of the PTFD. We compared the results obtained by FFT and this implementation for two sinusoidal signals and one representing the human colonic electrical activity. We showed that this implementation with using only rectangular windows improves the numerical approximation of the power spectrum when the truncation point in the signal does not match with its fundamental period.

In section 3, we present a brief review of Chakravarti's method pointing out relevant aspects of its discrete representation (numerical implementation). Section 4 contains numerical results and discussion. Section 5 presents the concluding remarks and possible suggestions.

3.3 Methods

A complete description of Chakravarti's method may be found in [4]. For a given signal $s(t)$ the finite Fourier integral is represented as

$$A_n = A(n/N) = \int_{t_0}^{t_N} s(t)e^{-i2\pi nt/T}dt \quad for \quad n = 0, 1, ..., N \tag{3.1}$$

If we let the nodes t_k be given by $t_k = t_0 + k \cdot h$, $T = (t_0 - t_N)$ and $h = T/N$, then the trapezoidal sum for this integral is equal to

$$T_n = h\left\{\frac{1}{2}e^{p_n t_0}s(t_0) + \sum_{k=1}^{N-1} s(t_k)e^{p_n t_k} + \frac{1}{2}e^{p_n t_N}s(t_N)\right\} \tag{3.2}$$

where $p_n = -i2\pi n/T$.

The Trapezoidal formula with exponential weighting function and correction terms expressed in terms of forward (Δ^r) and backward (∇^r) differences may be written in the form

$$\begin{aligned} A_n \approx\ & T_n - h\chi_0(q)\{e^{p_n t_N}s(t_N) - e^{p_n t_0}s(t_0)\} + \\ & he^{p_n t_N}\sum_{r=1}^{m}(-1)^{(r+1)}\chi_r(-q_n)\nabla^r s(t_N) - \\ & he^{p_n t_0}\sum_{r=1}^{m}\chi_r(q_n)\Delta^r s(t_0) \end{aligned} \tag{3.3}$$

where $q_n = p_n h = -i2\pi n/N$ and

$$\chi_r(q_n) = \begin{cases} D_0(0, q_n) + 1/2 & r = 0 \\ \frac{1}{r!}\sum_{\nu=0}^{r} S_r^\nu D_\nu(0, q_n) & r \geq 1 \end{cases} \tag{3.4}$$

which express $\chi_r(q_n)$ in terms of the Stirling numbers of the first kind S_r^ν and the D-functions. $D_r(0, q_n)$ for $r \geq 1$ can be calculated from the following expression

$$D_r(0, q_n) = \frac{r!}{(-2\pi i)^{r+1}}\{(-1)^r\overline{J}_r(0) - J_r(0)\}. \tag{3.5}$$

The asymptotic formula for $J_r(0)$ when $r \geq 1$ is equal to

$$J_r(0) \sim \sum_{m=1}^{k-1} \frac{1}{(m - iq_n/2\pi)^{r+1}} + \frac{1}{2}\frac{1}{(k - iq_n/2\pi)^{(r+1)}} + \frac{1}{r(k - iq_n/2\pi)^r} + \sum_{\nu=1}^{\infty} \frac{B_{2\nu}}{(2\nu)!} \frac{(r+1)(r+2)\cdots(r+2\nu-1)}{(k - iq_n/2\pi)^{(r+2\nu)}}, \quad (3.6)$$

where the constants $B_{2\nu}$ are the Bernoulli numbers. The corresponding formula for $\overline{J}_r(0)$ may be obtained by writing $-q_n$ for q_n in (3.6), therefore, this formula is an asymptotic formula for $D_r(0, q_n)$ for $r \geq 1$.

The value of $\chi_0(q_n)$ may be computed using the formula

$$\chi_0(q_n) = \frac{1}{2}\left(\frac{e^{q_n}+1}{e^{q_n}-1}\right) - \frac{1}{q_n}. \quad (3.7)$$

The trapezoidal formula (TS) for the weighting functions $\cos(\beta t)$ and $\sin(\beta t)$ with the correction terms expressed in terms of the forward (Δ^r) and backward (∇^r) differences can be used for implementing the numerical method and it looks like

$$\int_{t_0}^{t_N} w(t)s(t)dt = \frac{h}{2}w(t_0)s(t_0) + h\sum_{k=1}^{N-1} w(t_k)s(t_k) + \frac{h}{2}w(t_N)s(t_N) - h\sum_{r=o}^{\infty}\{U_r(t_N)\Delta^r s(t_N) - V_r(t_0)\nabla^r s(t_0)\}, \quad (3.8)$$

where the coefficients $U_r(t_k)$ and $V_r(t_k)$ (k=0, N) for each weighting function $w(t)$ are presented in tables (3.1 and 3.2). The subindex r in the last sum of equation 3.8 indicates the order of the approximation. A maximum order of four was good enough to find a correct numerical approximation because of the finite precision arithmetic (double precision representation). Those tables use the following notation

$$\beta_n = \frac{-2\pi n}{T},$$

$$\chi_r^I(q_n) = \frac{1}{2}\{\chi_r(q_n) + \chi_r(-q_n)\},$$

$$\chi_r^{II}(q_n) = \frac{1}{2}\{\chi_r(q_n) - \chi_r(-q_n)\}.$$

Table 3.1: $U_r(t_k)$ coefficients for cos and sin

$w(t)$	$U_0(t_k)$	$U_r(t_k)$
$\cos(\beta_n t)$	$i\sin(\beta_n t_k)\chi_0(q_n)$	$(-1)^{r+1}\chi_r^I(q_n)\cos(\beta_n t_k) - i\chi_r^{II}(q_n)\sin(\beta_n t_k)$
$\sin(\beta_n t)$	$-i\cos(\beta_n t_k)\chi_0(q_n)$	$(-1)^{r+1}\chi_r^I(q_n)\sin(\beta_n t_k) + i\chi_r^{II}(q_n)\cos(\beta_n t_k)$

Table 3.2: $V_r(t_k)$ coefficients for cos and sin

$w(t)$	$V_0(t_k)$	$V_r(t_k)$
$\cos(\beta_n t)$	$i\sin(\beta_n t_k)\chi_0(q_n)$	$(-1)^{r+1}\chi_r^I(q_n)\cos(\beta_n t_k) - i\chi_r^{II}(q_n)\sin(\beta_n t_k)$
$\sin(\beta_n t)$	$-i\cos(\beta_n t_k)\chi_0(q_n)$	$(-1)^{r+1}\chi_r^I(q_n)\sin(\beta_n t_k) + i\chi_r^{II}(q_n)\cos(\beta_n t_k)$

The method was implemented using Fortran language on a 386 IBM-PC compatible with numerical coprocessor. Three cases are presented to show the main characteristics of the Chakravarti method. Two cases are taken from the set of sinusoidal signals whose PTFD analysis is presented in chapter five. The last case corresponds to a sample of the human colonic electrical activity whose PTFD analysis is also presented but in chapter six. For each case, a comparison of the power spectrum calculated by trapezoidal sum and Chakravarti method is presented. In particular, only the results using two correction terms (δ^2 and δ^4) are showed.

3.4 Numerical Results and Discussion

Case 1. Truncation interval not equal to period.

$$s_1(t) = \sin(2\pi f t), \quad f = 0.4766\text{Hz}$$

For this case the selected truncation interval ($T = 64$) was not equal to a multiple of the fundamental period, the zeros of the truncation function did not correspond to the sampling signal interval. The power spectrum results were exhibited using a frequency range between 0 and 32 Hz. The power spectrum calculated analytically tended to zero when the frequency increased (Figure 3.1). The results computed by correction terms δ^2 and δ^4 also went toward zero following the same behaviour as the analytical results. However, the trapezoidal sum results reached a tangential point far from zero. The correction term results using δ^2 and δ^4 showed a better approximation to the analytical results than those calculated by TS (Table 3.3). The difference between analytical results and TS was clear for high frequencies.

Case 2. Nonperiodic function.

$$s_2(t) = \sin(2\pi \cdot f(t) \cdot t), \quad f(t) = \alpha(1 - e^{-t})$$

In this signal, the sinusoidal frequency increased exponentially with an upper bound equals one. A truncation interval $T = 64$ was also selected with two different α values: $\alpha_1 = 0.5$Hz and $\alpha_2 = 0.4766$Hz. The power spectrum results using TS for α_1 and α_2 decreased until it reached a value above 0.0001 (Figure 3.2). However, the power spectrum using correction term δ^4 in both cases decreased reaching values below

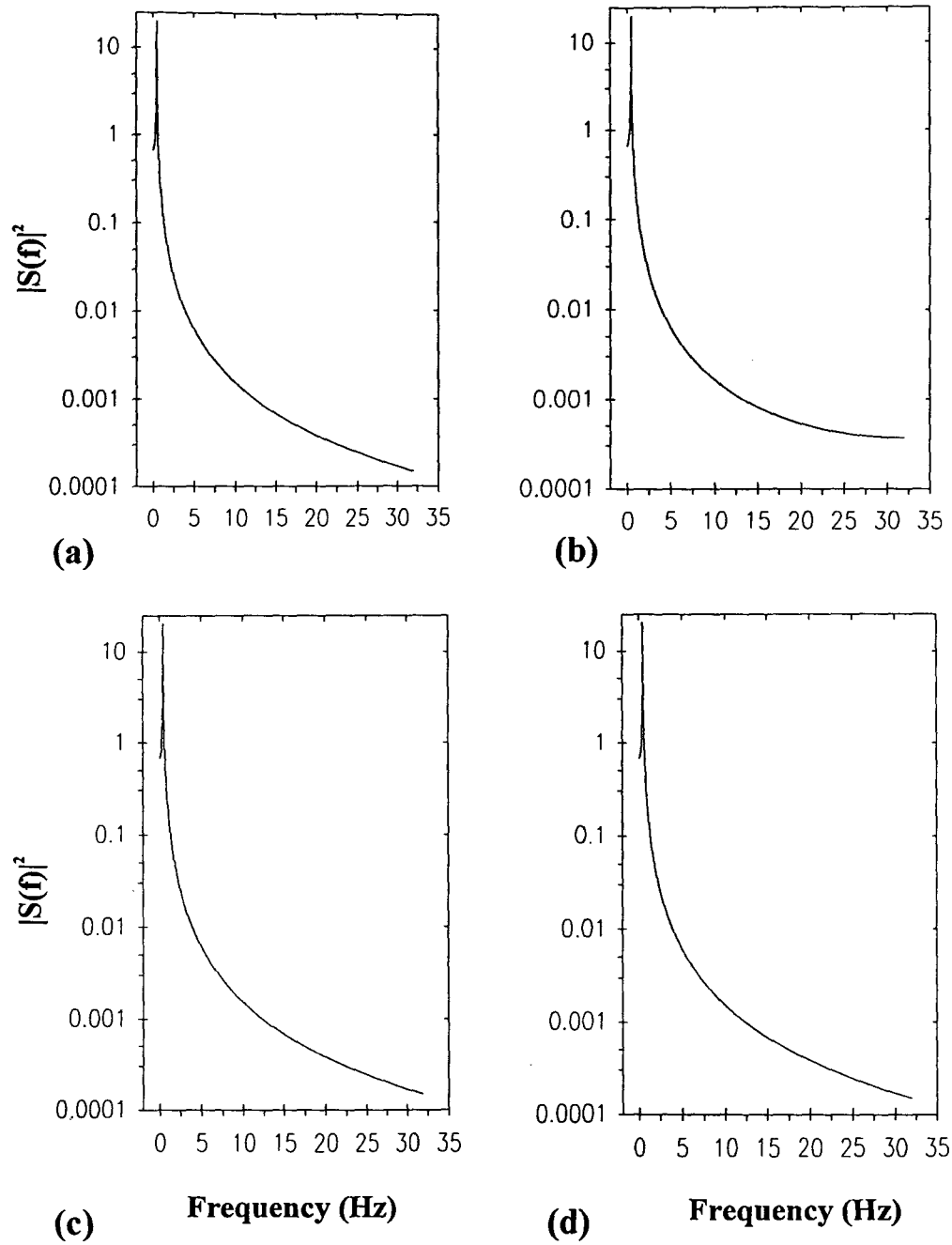

Figure 3.1: *Power spectrum of* $\sin(2\pi ft)$, *with* $f = 0.4766$Hz *calculated analytically and by TS and Chakravarti method.*

(a) Power spectrum calculated analytically; (b) using trapezoidal sum; and Chakravarti method with correction terms (c) δ^2 and (d) δ^4. The correction term results went toward zero when the frequency increased as did the analytical results. However, TS results reached a value far from zero.

Table 3.3: *Power spectrum of $s_1(t)$ calculated by analytical method, trapezoidal sum and correction terms δ^2 and δ^4.*

frequency (Hz)	Analytical	Trap Sum	δ^2	δ^4
5	0.00608	0.00621	0.00612	0.00612
10	0.00152	0.00164	0.00152	0.00152
15	0.00068	0.00081	0.00067	0.00067
20	0.00038	0.00053	0.00038	0.00038
25	0.00024	0.00041	0.00024	0.00024
30	0.00017	0.00037	0.00017	0.00017

0.0001. The power spectrum results for a set of frequencies using TS and correction term δ^4 showed differences in the fourth significant decimal figure (Table 3.4). TS results slowly decreased to zero, however, the correction term results showed improved behaviour for high frequencies.

Case 3. Biological signal: human colonic electrical activity

The original sampling rate was 200 cycles/s. To reduce the number of data points the signal was decimated (using a low pass filter with cutoff frequency 2.5 cycles/s before resampling) by a factor of 32, therefore, the sampling frequency was changed to 6.25 cycles/s. The number of data points to analyze was 2048 which corresponds in time to $T = 327.68$ s. The power spectrum was calculated using TS and the Chakravarti method with correction term δ^4 (Figure 3.3). After frequency 2.5 Hz, trapezoidal sum results went to zero faster than correction term results. The power spectrum results

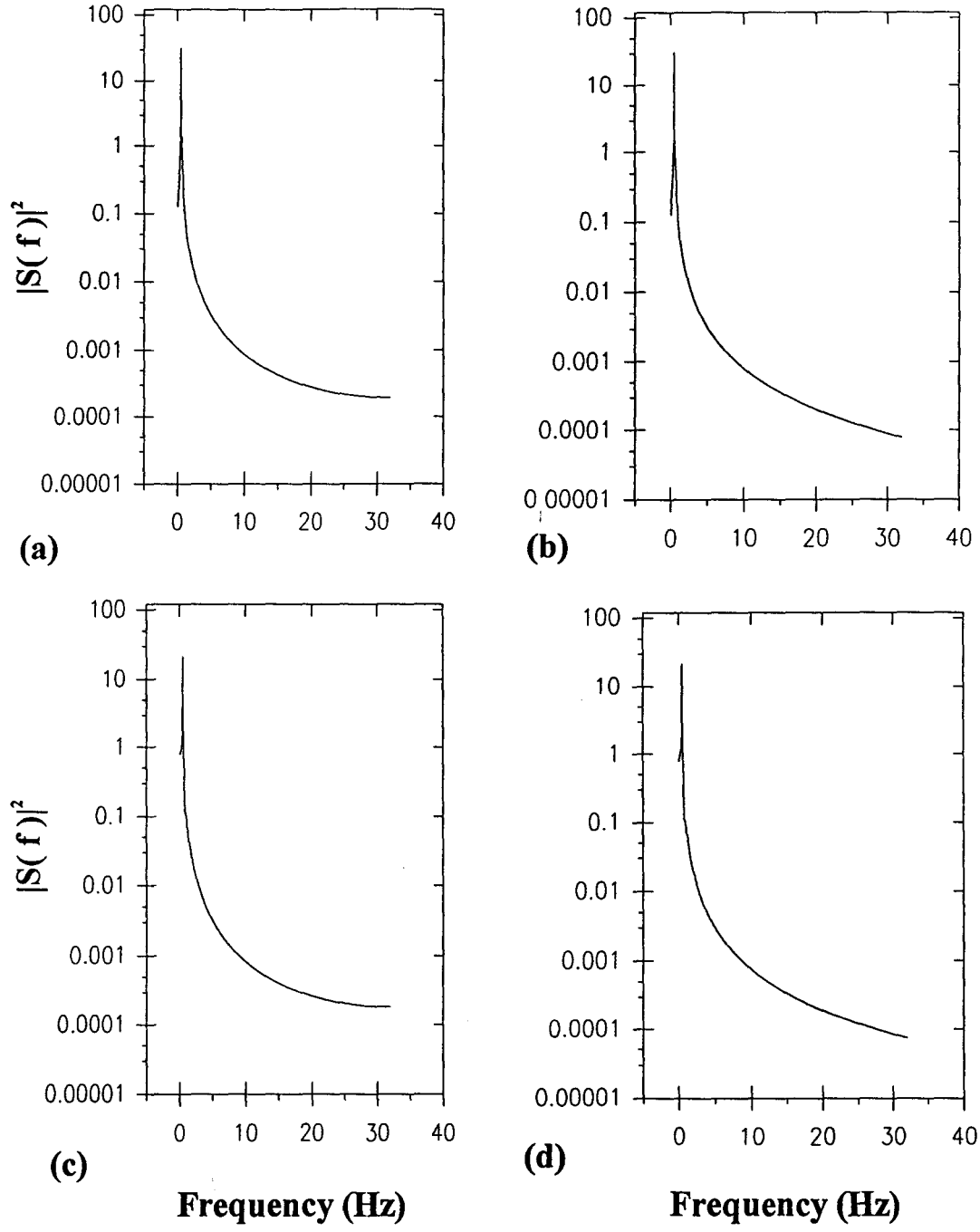

Figure 3.2: *Power spectrum of s_2 for α_1 and α_2 calculated by TS and Chakravarti method.*

Power spectrum of $s_2(t)$ using trapezoidal sum and δ^4 correction term for α_1 were shown in (a) and (b) respectively; for α_2 in (c) and (d). The Chakravarti method improved the numerical approximation especially for high frequencies.

Table 3.4: *Power spectrum of $s_2(t)$ calculated by trapezoidal sum and correction term δ^4.*

frequency	$\alpha_1 = 0.5$Hz		$\alpha_2 = 0.4766$Hz	
(Hz)	Trap sum	δ^4	Trap sum	δ^4
0.5	31.42549	31.42549	7.77458	7.77452
5	0.00328	0.00321	0.00314	0.00308
10	0.00086	0.00080	0.00083	0.00076
15	0.00043	0.00035	0.00041	0.00034
20	0.00028	0.00020	0.00026	0.00019
25	0.00022	0.00013	0.00021	0.00012
30	0.00019	0.00009	0.00018	0.00008

Table 3.5: *Power spectrum of the human colonic electrical activity calculated by trapezoidal sum and correction terms* δ^4.

frequency (Hz)	Trap Sum	δ^4
0.01831	1.608	1.636
0.0885	14.921	14.916
0.1831	4.399	4.426
0.5096	2.086	2.073
1.004	1.715	1.708
1.501	2.473	2.500
2.001	1.573	1.575
2.502	1.347	1.371

using correction terms were different in the second significative decimal figure from the TS results(Table 3.5).

3.5 Concluding remarks

The computation of the power spectrum by using FFT could result in large error approximations when the signal is not periodic or the truncation interval does not match the fundamental period of the signal. The use of "window" functions in time or frequency has been a method to deal with this kind of problem. The Chakravarti approach was an alternative method to improve the numerical approximation to the Fourier integral of nonperiodic signals. The improvement in the numerical approxi-

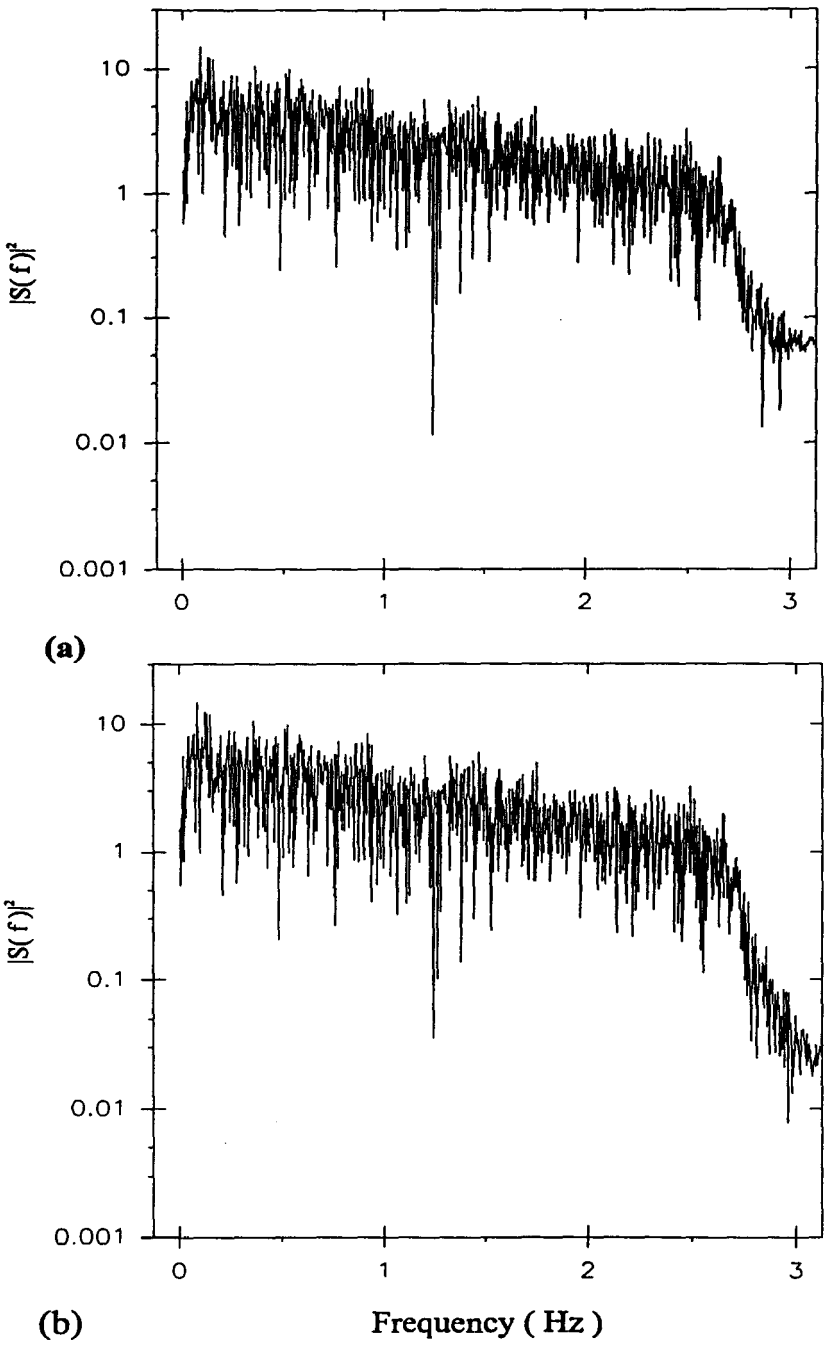

Figure 3.3: *Power spectrum of colonic signal calculated using TS and Chakravarti method.*

(a) Power spectrum calculated using trapezoidal sum; and Chakravarti's method with correction terms δ^4 (b). The difference between two methods after the frequency 5 Hz is clear.

mation was achieved by applying corrections to the TS. The correction terms were applied at the beginning and end of the time interval. The correction term results went toward zero when the frequency increased as well as the analytical results in case 1. The approximation error in this case was lower using correction terms than TS. The power spectrum of case 2 and 3 decreases faster during high frequencies than TS results. The numerical difference between correction terms and TS was small in case 2 (especially at high frequencies) and case 3. The Chakravarti method is an approach to calculating the Fourier integral while only using a rectangular window. The method can be used for non-smooth signals like the electrical activity recorded from the human colon. The implementation of this method was an important aspect for computing the PTFD of nonperiodic signals. An improved algorithmic implementation is being developed to reduce numeric computations.

Chapter 4

A computer program for positive time-frequency analysis of human colonic electrical activity

4.1 Abstract

The analysis of the human colonic electrical activity requires the use of time-frequency distribution techniques, since the amplitude and frequency of this activity change along time. To analyze these variations, a computerized data analysis system for the human colonic electrical activity is presented. The processing part of this system includes the computation of the positive time-frequency distribution (PTFD). An important part of the PTFD is the kernel function which is related to the signal to be analyzed. The system contains three known kernel functions to calculate the PTFD. A set of criteria is used to decide which kernel function can be selected for

any particular signal. The system includes a series of PC programs to prepare and process signals recorded from the human colon. The system shows by using tables and plots the analysis results in terms of relative and absolute values.

4.2 Introduction

The measurement of the electrical activity of the human colon plays an important role in clinical investigations. From the analysis point of view, this activity presents important characteristics: its amplitude and frequency change in time and vary depending on the recording area, preprandial and postprandial condition, daytime and night situations, healthy and diseased subjects. The electrical activity shows the action of different components which participate synchronously with other components or asynchronously if the activity is not related to the motility process. In general, the frequency content of the colonic electrical activity is highly irregular and time-varying. Its analysis is difficult, because its power spectrum presents multiple fundamental frequency peaks, and the energy in each peak is not confined to a single frequency, but it is distributed over a band around the peak. Furthermore, these peaks shift in frequency from one block of data to the next and vary in amplitude. Time-frequency analysis had its origins almost fifty years ago and during the last years, new developments and applications in signal processing have created new perspectives for analyzing a time-varying process [11]. A fundamental issue of time-frequency distribution techniques is to understand and to describe situations where the frequency content of a signal is changing in time [13]. With the power spectrum, the frequencies that exist for the whole duration of the signal are estimated, but with a combined time-frequency distribution the frequencies are determined at a certain time. Positive

time- frequency distributions (PTFD) developed by Cohen [23] are particular cases of the general distributions that have the property to be positive for the whole range in time and frequency. The kernel function is an important part of the PTFD and is related to the signal to be analyzed. It is useful to have a system where each kernel function can be tested for any particular signal. A numerical criterion is required to decide if a kernel function can be used to compute the PTFD of the electrical activity of the human colon.

The present chapter describes a set of computer programs for preprocessing and analyzing the time-varying electrical signals recorded from the human colon using positive time-frequency distribution techniques. In section 3, a brief description of the computational methods and numerical criteria are presented. In section 4, a set of characteristics of main components and a description of file formats are exhibited. Finally, in section 5 a graphic representation of interaction between system components is displayed.

4.3 Computational methods

For calculating the positive time-frequency distribution, from the computational point of view, there are two important concepts to mention: the numerical approximation of the Fourier integral and the discrete representation of PTFD. A complete description of the former is presented in chapter 3 and in this section a few aspects are developed. A detailed description of the latter is given in chapter 5 and some points are mentioned here.

Numerical Fourier integral

The computation of the numerical Fourier integral is an important aspect of the PTFD. A variable order method for the accurate computation of the Fourier transform was used. The increase in accuracy was achieved by applying high order correction terms to the trapezoidal sum approximations. The method is based on the generalized Euler-Maclaurin formulas of Chakravarti given in [4].

Positive time-frequency distribution

The electrical activity of the human colon requires simultaneous analyses in both time and frequency, because the signal changes its parameters in time and frequency. Time-Frequency distributions is an appropriate technique to analyze this kind of signal, particularly PTFD analysis gives us the possibility to consider the time-frequency description in terms of true energy densities. The method for obtaining PTFD consists in first, choosing a kernel function; second using any constant c from the range given by the kernel. These two steps assure that the proper PTFD is satisfied and makes the joint distribution positive [9]. A set of criteria was used to decide if a kernel function can be selected for calculating the PTFD of a signal. The criteria consisted of the uncertainty coefficient, the marginal conditions and conditional time-frequency distribution. The system includes three known kernel functions [22]; however, it allows us to also test a new set of kernel functions. Moreover, the system comprises a set of time-varying sinusoidal signals which can be used with the same purpose of developing new kernel functions.

4.4 System description

The system is running on a 386 PC-IBM compatible with numerical math-coprocessor under DOS operating system. The system is integrated by two important components:

1. Data acquisition system. Receiving and sampling the analog signal.
2. Analysis program system. Calculating and plotting the PTFD of the discrete signal.

4.4.1 Data acquisition system

Characteristics of the A/D system

The CODAS system (Dataq instruments Inc.) includes A/D converter and a real-time graphics display controller card that allows us to convert, save and display almost simultaneously the biological data. Moreover, it consists of the software to control the A/D process and playback the signal postacquisition with waveform export capability. The A/D converter (DATA TRANSLATION, serie DT2801-A) has a resolution of 12 bits, and can resolve differences on an analog input as small as 0.024% of the selected analog input range. It supports unipolar (0 to 10 volts) and bipolar (+/-10 volts) configurations. It can use 8 single-ended or 16 differential input channels. It has a programmable gain amplifier that can be set for 1,2,4, or 8 in unipolar and bipolar modes. Data collection approaches are easily implemented with the CODAS software as well as the manipulation of data for the analysis procedure.

Preprocessing data file

The data file created by the CODAS system must be translated to double precision format. After that, in some cases it is necessary to remove the linear trend and to reduce the sampling frequency. Finally, a data file is generated which can be analyzed by the PTFD option. A set of programs are used for these activities: (a) a program in C language to read data files with CODAS format; (b) a MATLAB (The Mathworks,Inc.) package to remove linear trend, decimate or reduce sampling frequency and filter a signal.

4.4.2 Analysis program system

A Time-Frequency distribution system was developed to receive data files, to calculate time and frequency components, to plot numerical results and to permit the change of the mathematical model parameters for the best approach to signal characterization. The computerized system is implemented by a set of programs in FORTRAN and C language for realizing the PTFD analysis method described in chapter 5. In this method, the time and frequency characterization of colonic electrical activity is modeled by a set of kernel parameters.

During the development of any experimental analysis using PTFD, four descriptive data files are produced: (a) a trace file containing some important information about the recording and event marks indicating the starting point of each experimental condition (meal, sleep, drug injection, ...); (b) an analysis parameter file indicating sampling frequency, number of data points, frequency resolution in samples/s, kernel function, ...; (c) a lattice file which describes the quantity and size of time and frequency intervals; and (d) an analysis request file that includes

instructions to execute specific tasks.

Experiment trace file

This file contains information for a complete description of the experimental signal which is used during the analysis procedure. The identification part includes a brief text or label associated with the experiment, an experiment date and the signal type. Information about the signal recording consists of time constant, upper cutoff frequency, recording speed of tape recorder and the number of channels that were used. Moreover, a brief label for each channel is included and the units in time for presenting numerical and graphical results. In the last option a label is associated with each experimental event indicated during the recording process (table 4.1).

Analysis parameter file

For each experimental trace, it is possible to have more than one analysis, in that case the analysis parameter file describes each separate procedure. This file includes an identification part which can be associated with the same experimental trace or various different experimental traces. It contains the number of data points and/or the sampling frequency (indicated in cycles per second), an indication of time interval to analyze in terms of the first and last point (units should be specified otherwise seconds is the default) and the maximum frequency in the experimental trace (table 4.2).

Analysis lattice file

The basic idea is to generate a matrix of PTFD or $P(t, f)$ values which shows absolute and relative energy values. The rows correspond to time intervals (t) and columns to

Table 4.1: Format for an experiment trace file

Command	Argument
Identification	[Text]
Type	[Human, Dog, Rabbit]
Date	[dd/mm/yy]
Time_constant(sec)	[sec]
Upper_cutoff(Hz)	[Hz]
Recording_speed(cm/sec)	[nnn]
Number_channels	[n]
Ch[i]	[Text]
Ch[j]	[Text]
...	...
Units	[sec/min/hour]
E[time]	[Text]
E[time]	[Text]
...	...
E[time]	[Text]

Table 4.2: Format for an analysis parameter file

Command	Argument
Identification	[Text]
Number_data_points	[nnn]
Sampling frequency(cyc/s)	[fff]
Units_time	[sec/min/hour]
Begining_time_interval	[fff]
End_time_interval	[fff]
Max_frequency(cyc/sec)	[fff]

frequency intervals (f). The basic units for time and frequency intervals are seconds and cycles per second respectively. It is possible to change the units to minutes and cycles per minute. The lattice in time or frequency is almost arbitrary, it is only necessary to define the total number of intervals and the values for each interval. The values indicate the start and end point of each interval. Each interval is opened on the left and closed on the right side (table 4.3).

Analysis control file

This file contains the description of the type of analysis to realize in all data files including the same identification. If some instructions are omitted the system will assume default values. The order of instructions is not important and the first character specifies the command (it is not sensitive to case). The same file may include

Table 4.3: Format for an analysis lattice file

Start point	End point
Time	[k]
t_1	t_2
t_2	t_3
⋮	⋮
t_{k-1}	t_k
Freq	[n]
f_1	f_2
f_2	f_3
⋮	⋮
f_{n-1}	f_n

Table 4.4: Format for an analysis control file

Command	Argument
Analyze	[ident]
Kernel_function	[nn]
Number_data_points	[nnn]
Units_time	[sec/min/hour]
Begining_time_interval	[fff]
End_time_interval	[fff]
Decimate_factor	[nn]
Cutoff_freq(cyc/sec)	[fff]
Time_intervals	[nnn]
Frequency_intervals	[nnn]
Lattice_filename	[Text]

different requests that always start with the instruction *Analyze*. Table 4.4 illustrates a file with a single request.

4.5 Menu interface and control process

A menu oriented interface was written in Microsoft (Microsoft Corporation, USA) command language to guide the user. Menu choices select the required programs and create command line options, switches and parameters. Throughout the session the interface verifies that the necessary file exists. Moreover, useful default values are

provided which are remembered in order to facilitate multiple analysis requests. The menu contains the following options

i. Create experiment protocol file

ii. Create analysis parameter file

iii. Create analysis control file

iv. Collect and save digitized data

v. Select signal segment to analyze

vi. Select kernel function and associated c-values

vii. Calculate the Positive Time-Frequency distribution

viii. Show three-dimensional plots of PTFD results

ix. Present curve level plots of PTFD results

x. Select a detailed analysis of specific time-frequency interval.

An option exists to analyze data without first having an analysis control file. This is advantageous for studying selected segments during periods when an experimental condition is applied, e.g., preprandial, meal, postprandial, drug injection, etc. and automatically creates a short analysis control file. Also, in a separate way it is possible to recreate the 3D or contour level plots under different specifications to extract information for different ranges of frequencies.

4.5.1 Control process

This part of the system implements and coordinates subprocesses for digitizing and storing data from the tape recorder or real-time experiment, extracting the portions of digitized data defined by the user's analysis request; performing PTFD analysis; plotting PTFD results; and formatting the results in an output file for subsequent statistical analysis (using commercial statistical packages, e.g., SAS and Minitab). The control process and some of the subprocesses for calculating the PTFD and plotting results are written in the C programming language. The Fourier numerical approximation routine was written in Fortran language. The software for data acquisition and playback correspond to the CODAS system.

4.5.2 Data Analysis

The data analysis section consists basically in the Positive Time-Frequency distribution technique and includes the following characteristics:

i. Calculate the Fourier integral.

ii. Select different h-functions and associated c-values.

iii. Calculate the PTFD and the uncertainty coefficient.

iv. Plotting main different components of the PTFD.

v. Calculate the instantaneous energy of a signal and intensity per unit frequency.

vi. Show three-dimensional plots of the PTFD.

An illustration of how the different components are interconnected is exhibited in figure 4.1. Phase zero indicates the starting point with different activities. The most important and crucial part is the data acquisition, all results depend on this step. Phase one is a preliminary step for the analysis procedure; it is a signal description in terms of individual components : time and frequency. During this phase, it is possible to recognise some signal characteristics in both domains. Phase two contains the model selection and global analysis by using the PTFD technique. In this phase, a selection of the lattice that covers the whole range in time and frequency is established. The selection model process corresponds to testing each kernel function by computing the uncertainty coefficient. This process finishes when a kernel function improves the uncertainty coefficient with respect to its upper bound. Phase 2 gives us global aspects of joint time-frequency behaviour. A detailed analysis of any specific range in time or frequency can be done during phase 3 and simultaneously the time or frequency resolution can be increased for computing the PTFD. A new lattice specification is generated and the program presents a table with numerical results and contour level or surface plots. Moreover, the program creates a data file with the numerical results for processing with any statistical package.

4.6 Conclusions

Time-frequency techniques are appropriate for analyzing time-varying frequency processes. The main parameters of the human colonic electrical activity change along time. A computerized data analysis system to analyze these variations represented a first approach to proceed with further developments. The computation of the PTFD was an important system component. The possibility to test kernel functions using

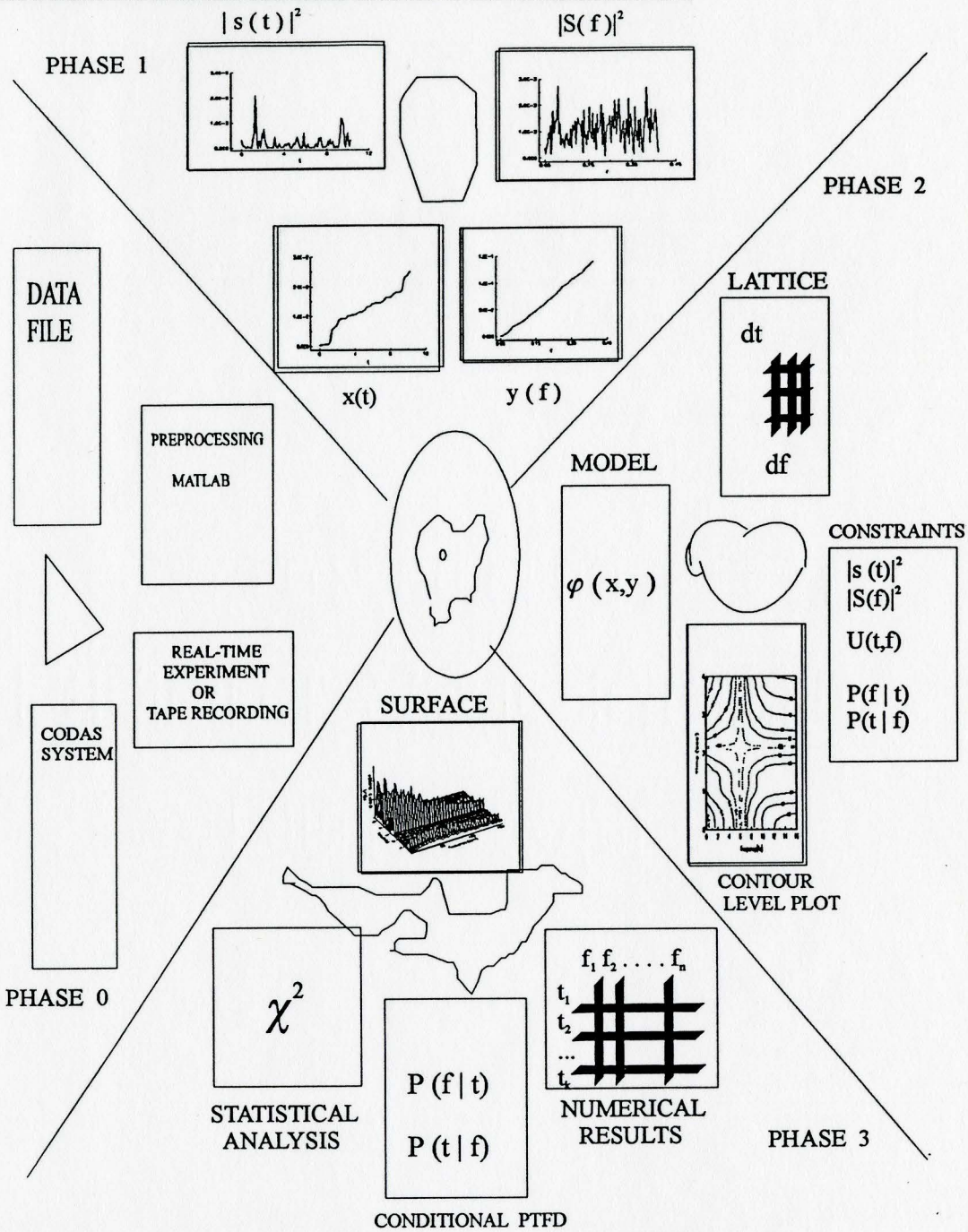

Figure 4.1: *Interaction between main components for PTFD analysis.*

The life of the analysis procedure starts in phase zero where the signal acquisition and discrete processes are realized, continues with its marginal representation in time and frequency, global analysis and finishes in a detailed analysis. In some cases, it starts again in phase 0 for a new analysis.

the uncertainty coefficient expedited the selection process and it was useful for determining appropriate criteria in the analysis of PTFD results. The system to analyze PTFD results can be used for different types of signals specially for those related with the electrical activity recorded in the human colon. The use of descriptive data files (experiment trace, analysis parameter, lattice and request file) facilitated the analysis of signals with similar characteristics, specially when identical setups were required. The control process was the most interactive part of the system, because the analysis activities (performing PTFD analysis, plotting results and formatting the results in an output file) can be done several times for the same experiment. The system was an important tool for going from theoretical signals to actual experimental signals. The computerized data analysis system presented in this chapter provides a ready-to-use software package for investigators who compare signal recordings under different experimental conditions. Some parts of the analysis system must be improved in terms of a computational viewpoint : numerical algorithm for calculating the Fourier transform, automatic selection of the kernel function and constant value.

Chapter 5

Positive Time-Frequency Distribution of theoretical time-varying signals

5.1 Abstract

The development of positive time frequency distributions (PTFD) is an important issue in the framework of time frequency analysis of nonperiodical signals. A PTFD can be interpreted as the signal energy localized in both time and frequency domains. A PTFD representation depends on a kernel function which is related with the signal to analyze. For any particular signal, it is difficult to know its PTFD by only using time and frequency marginal distributions. In this chapter, we show that the uncertainty coefficient based on the entropy principle and frequency-dependent PTFD (time-dependent PTFD) are good tools to decide which kernel function could be ap-

propriate for analyzing a set of sinusoidal signals. A discrete representation of PTFD using the numerical approximation to the Fourier integral described previously was also developed. Three known kernel functions were used to calculate the PTFD of six sinusoidal signals. These signals were considered as a simple approximation to oscillation changes in the electrical activity of the human colon. One of the kernel functions was found to be useful for analyzing almost all sinusoidal signals. Furthermore, a lower bound of the uncertainty coefficient was defined based on the marginal product (correlationless case of PTFD).

5.2 Introduction

The possibility of representing a signal in both time and frequency domains has opened new alternatives of analysis for time-varying nonstationary signals. These kinds of signals can be found in areas like biomedicine, acoustics, geophysics, and optics. Since Wigner's original work [39] in quantum mechanics, there have been many joint time-frequency distributions that have been proposed for the description of a signal in time and frequency. Most of them are members of the general class of time-frequency distributions developed by Cohen [7], where each member of this class is characterized for a specific kernel function. The properties of a distribution are reflected as constraints on the kernel. By examining the kernel, one can determine the general properties of the distribution. The Wigner Distribution is an example of a Cohen class whose kernel is signal independent and the distribution generated is bilinear in the signal (the signal appears twice in the distribution). It is known that the bilinear distributions cannot be positive except for some specific signals [8]. A joint time-frequency distribution should be positive for all values of time and frequency

to obtain the fraction of the energy per unit time and unit frequency. Cohen and Zaparovany [23] presented the properties that the kernel must have in order to obtain positive time-frequency distributions (PTFD) and developed the following model

$$P(t,f) = |s(t)|^2|S(f)|^2\{1 + c \cdot \varphi(x(t),y(f))\}. \tag{5.1}$$

$P(t,f)$ must satisfy a set of conditions such that the total energy of the distribution should be the total energy of the signal:

$$E = \int P(t,f)dtdf = 1.$$

This implies the marginal conditions

$$\begin{aligned} \int P(t,f)dt &= |S(f)|^2 \qquad \text{and} \\ \int P(t,f)df &= |s(t)|^2. \end{aligned} \tag{5.2}$$

In terms of the model 5.1, as well as the Cohen class (general time-frequency distributions) the properties of a particular PTFD are determined by its kernel or $\varphi(x,y)$ function, where x and y are the cumulative marginal distributions of time and frequency respectively, and their range of values is $0 \leq x,y \leq 1$. Then, $\varphi(x,y)$ is a function that represents the correlation between $|s(t)|^2$ and $|S(f)|^2$ for all values of time and frequency. The PTFD is positive for a certain range of values of c (constant delimited by the set of values of φ). In general, φ and c may be implicitly related to the signal and proper time-frequency distributions are nonlinear functionals of the marginals [22]. To define a kernel function for any specific signal is a difficult issue. In the literature, several kernel functions have been proposed to define a PTFD [9, 22]. One of our objectives was to estimate the PTFD of sinusoidal signals using some of

those kernel functions and to characterize the relationship between signal and kernel function.

It is still problematic to determine the main characteristics of the joint distribution by using the time and frequency marginal distributions by themselves. The uncertainty coefficient [32, 38] based on the entropy principle can be used to decide which kernel function is appropiate for analyzing a signal. We propose that given a kernel function a PTFD must satisfy both marginal conditions (5.2) and the uncertainty coefficient in a first approach. Since, it is often easier to visualize conditional distributions than joint distributions, we suggest that the conditional distribution must satisfy a simple restriction in time and frequency in order to determine that a kernel function is appropriate to estimate a PTFD for any particular signal [1]. We applied three known kernel functions [22] to a small set of sinusoidal signals. We decided which kernel function can be used for each sinusoidal signal using the uncertainty principle and the restriction in time and frequency of the conditional distribution. In addition, a numerical procedure for calculating the PTFD is presented.

The specific objectives of this chapter are to propose an additional criterion a PTFD has to fulfill to decide whether or not a kernel function is appropiate for a time- frequency varying signal and to determine which known kernel functions are useful in the analysis of time- frequency variations in a set of sinusoidal signals.

In section 3, a detailed explanation of the uncertainty coefficient and a criterion applied to the first conditional moment of the PTFD are presented. The numerical implementation of the PTFD is developed in section 4. The parameter estimation of the Cohen φ-functions for some sinusoidal signals are examined in section 5.

5.3 Uncertainty coefficient and frequency- conditional and time-conditional PTFD

The PTFD must satisfy the marginal conditions but in a practical situation for any signal we do not know the general characteristics of its PTFD. The description of any PTFD is determined both by the product of the marginal distributions and the kernel function with its c-value. When the PTFD represents a correlationless case the c-value is close to zero and the description only depends on the marginal product; otherwise, the kernel function plays an important role. The way to establish this role must be consistent with marginal constraints and we propose an additional condition in terms of the entropy principle.

The entropy of the marginal time and frequency distributions using a continuous domain are, respectively,

$$H(t) = -\int P(t,f)\ln P(t,f)df, \qquad H(f) = -\int P(t,f)\ln P(t,f)dt. \quad (5.3)$$

The entropy of the joint PTFD is given by

$$H(t,f) = -\int\int P(t,f)\ln P(t,f)dtdf. \quad (5.4)$$

A measure of the association between time and frequency is the uncertainty coefficient [32, 38] and it can be calculated in terms of the entropy as follows

$$U(t,f) = 2\left(\frac{H(t)+H(f)-H(t,f)}{H(t)+H(f)}\right). \quad (5.5)$$

U is zero if time and frequency are completely independent ($H(t,f) = H(t) + H(f)$). U equals unity if time and frequency are completely dependent ($H(t,f) = H(t) = H(f)$). We have a lower bound of the uncertainty coefficient calculated from

the marginal product ($\Gamma(t,f) = |S(f)|^2 \cdot |s(t)|^2$). We expect to improve this value and always satisfy the marginal conditions. We will select the kernel function and c-value that satisfy both conditions: improve lower bound of $U(t,f)$ and satisfy marginal conditions.

We can generate a conditional PTFD either in time or frequency from a PTFD. We do not know the characteristics of a PTFD, but we can decide which characteristics must satisfy a conditional PTFD, and use those characteristics to design a kernel function associated with a PTFD. The basic idea is to use simple characteristics that we can use for different types of signals. Another problem is to design a kernel function. Kernel functions and signals are implicitly related. A set of kernel functions could be infinite. One way to limit a set of kernel functions is to impose additional constraints to the PTFD.

We take a cross section of the function $P(t,f)$ in the plane given by $t = t_k$. An intersection is a curve lying in this plane, and having the equation $P(t_k, f)$. This curve normalized by the factor $1/|s(t_k)|^2$ represents the conditional PTFD given time (relative value of PTFD with respect to time) and its general expression for all values of t is given by

$$P(f|t) = \frac{P(t,f)}{|s(t)|^2}. \tag{5.6}$$

Now, we consider a cross section of the function $P(t,f)$ in the plane $f = f_n$ and the intersection is the curve $P(t, f_n)$. This curve divided by the factor $|S(f_n)|^2$ defines the conditional PTFD given frequency (relative value of PTFD with respect to frequency). Its general expression for all values of f can be represented as

$$P(t|f) = \frac{P(t,f)}{|S(f)|^2}. \tag{5.7}$$

We have that the conditional time-frequency distribution satisfies the following con-

dition

$$\int P(f|t)df = 1,$$

for the equation (5.6). We can see that for a range of values of t, for example $t_1 < t \leq t_2$ the expression $P(f|t_1 < t \leq t_2)df$ represents the mass in the rectangle $(t_2 - t_1) * df$ divided by the signal power in the interval $t_1 < t \leq t_2$. For the equation (5.7), we have the next condition

$$\int P(t|f)dt = 1,$$

and $P(t|f_1 < f \leq f_2)dt$ can be seen as the ratio of the mass in the differential rectangle $(f_2 - f_1) * dt$ over the mass given by the power sepctrum in the frequency strip $f_1 < f \leq f_2$.

The additional restriction in terms of the conditional time- frequency distribution that we propose is that the average value of $P(f|t)$ for all values of t should be proportional to the power spectrum $|S(f)|^2$ of the signal for each value of f. Also, the average value of $P(t|f)$ for all values of t should be proportional to the signal power $|s(t)|^2$. These restrictions are important in order to define if a kernel function can be used to estimate the PTFD of any particular signal. Beside, they can be used to determine the constant value associated with the kernel function.

Given a signal $s(t)$, we associate with it a positive distribution function $P(t, f)$ such that, the rth moment of such distribution for frequency is defined to be

$$< f^r >= \int f^r P(t, f)df, \tag{5.8}$$

the first moment $< f >$ is the average value of frequency under $P(t, f)$, which can be interpreted as the "center of gravity" of the area under the surface with respect

to frequency [40]. We have the same description in terms of time, whose rth moment is expressed as

$$< t^r >= \int t^r P(t,f)dt, \tag{5.9}$$

the first moment $< t >$ is the average value of time under $P(t,f)$.

In particular we are interested to know the average value of frequency for a given time. This is called the conditional average and is given by

$$< f >_t = \frac{1}{|s(t)|^2} \int f P(t,f)df. \tag{5.10}$$

The conditional average of time for a given frequency is expressed as

$$< t >_f = \frac{1}{|S(f)|^2} \int t P(t,f)dt. \tag{5.11}$$

5.4 Discrete Representation of PTFD

The definition of the PTFD for discrete time signals can be given as follows:

Let $t = t_k = k \cdot h_t$, where h_t is the sample interval in time, then

$$s(t) \approx s(t_k) = s(k \cdot h_t) = s_k \tag{5.12}$$

and

$$x(t) \approx x(t_k) = x_k = h_t \sum_{\tau=0}^{k} |s(t_\tau)|^2. \tag{5.13}$$

Let $f = f_n = n \cdot h_f$, where h_f is the resolution in frequency then

$$S(f) \approx S(f_n) = S(n \cdot h_f) = S_n \tag{5.14}$$

and

$$y(f) \approx y(f_n) = y_n = h_f \sum_{\nu=0}^{n} |S(f_\nu)|^2. \tag{5.15}$$

Therefore, the discrete representation of PTFD may be given by the following expresion

$$P(t_k, f_n) \approx |s_k|^2 \cdot |S_n|^2\{1 + c \cdot \varphi(x_k, y_n)\}, \tag{5.16}$$

where s_k and x_k are discrete variables in time, as are S_n and y_n in frequency.

The discrete version is mainly affected by the numerical method used to calculate the Fourier integral $S(f)$. The Fourier integral was calculated using the trapezoidal form of the generalized Euler-Maclaurin formula corresponding to the weighting function e^{pt} developed by Chakravarti [4]. In particular, as is explained in chapter 3, we used the formula with correction terms expressed in terms of forward differences at t_0 and backward differences at t_n. Therefore, the formula for the Fourier integral can be stated as

$$\begin{aligned}\int_{t_0}^{t_n} e^{pt}s(t)dt \approx h\{&\frac{1}{2}e^{pt_0}s(t_0) + \sum_{r=1}^{n-1} e^{pt_r}s(t_r) + \frac{1}{2}e^{pt_n}s(t_n)\} \\ &- h\chi_0(q)\{e^{pt_n}s(t_n) - e^{pt_0}s(t_0)\} - he^{pt_n}\sum_{r=1}^{m}(-1)^{r+1}\chi_r(-q)\nabla^r s(t_n) \\ &+ he^{pt_0}\sum_{r=1}^{m}\chi_r(q)\Delta^r s(t_0),\end{aligned} \tag{5.17}$$

where $p = \frac{-2\pi ik}{(t_n - t_0)}$, $h = \frac{(t_n - t_0)}{n}$ and $q = ph$,

$$\begin{aligned}\chi_0(q) &= D_0(0,q) + \frac{1}{2}, \\ \chi_r(q) &= \frac{1}{r!}\sum_{\nu=1}^{r} S_r^\nu D_\nu(0,q) \quad (r \geq 1), \\ \chi_r(-q) &= \frac{1}{r!}\sum_{\nu=1}^{r} S_r^\nu D_\nu(0,-q) \\ &= \frac{1}{r!}\sum_{\nu=1}^{r}(-1)^{\nu+1} S_r^\nu D_\nu(0,q) \quad (r \geq 1).\end{aligned} \tag{5.18}$$

See chapter 3 for more details.

This formula gives good results for calculating the Fourier integral of non-periodic functions or when the truncation point does not coincide with the fundamental period of the signal.

For a finite discrete set of values in time and frequency and using $P_{kn} = P(t_k, f_n)$ for all values of k and n, we derived a lattice representation organized in a set of cells of equal size. The size of the cell is specified by the interval in time and frequency, for example

$$\begin{aligned} \tau_k &= \{t_{k-1} < t \leq t_k\}, \\ \gamma_n &= \{f_{n-1} < f \leq f_n\}. \end{aligned}$$

For each cell we calculate three components:

i. A fraction of the PTFD, $P(\tau_k, \gamma_n)$.

ii. A fraction of the conditional distribution given time, $P(\gamma_n|\tau_k)$.

iii. A fraction of the conditional distribution given frequency, $P(\tau_k|\gamma_n)$.

The rows in the lattice representation correspond to time intervals and columns to frequency intervals. A description of the lattice representation is showed in table 5.1.

Two obvious constraints that we must require are

$$\sum_{n}^{N} P(\gamma_n|\tau_k) = 1, \quad \forall k, \tag{5.19}$$

and

$$\sum_{k}^{K} P(\tau_k|\gamma_n) = 1, \quad \forall n. \tag{5.20}$$

The final constraints to decide about the φ function and c value are specified by

$$\frac{1}{K}\sum_{k}^{K} P(\gamma_n|\tau_k) = |S(\gamma_n)|^2, \quad \forall n, \tag{5.21}$$

and

$$\frac{1}{N}\sum_{n}^{N} P(\tau_k|\gamma_n) = |s(\tau_k)|^2, \quad \forall k. \tag{5.22}$$

The entropy of the marginal time and frequency distributions in a discrete domain are, respectively,

$$H(t_k) = -\sum_{n}^{N} P(t_k, f_n) \ln P(t_k, f_n) \qquad H(f_n) = -\sum_{k}^{K} P(t_k, f_n) \ln P(t_k, f_n). \tag{5.23}$$

The entropy of the joint PTFD is given by

$$H(t_k, f_n) = -\sum_{k,n} P(t_k, f_n) \ln P(t_k, f_n). \tag{5.24}$$

The discrete definition of the uncertainty coefficient (variation measure for contingency tables [38]) can be expressed as follows

$$U(t_k, f_n) = 2\left(\frac{H(t_k) + H(f_n) - H(t_k, f_n)}{H(t_k) + H(f_n)}\right) \quad \forall k, n. \tag{5.25}$$

5.5 Sinusoidal signals and Kernel functions

A set of sinusoidal signals whose frequency varies in time were used to characterize how a kernel function is related with a signal. These signals are simplifications of the time-frequency variation of the electrical activity recorded in the human colon (CEA). The class of signals that we used are generated by the following model

$$s(t) = A\sin(2\pi t \cdot f(t)) \tag{5.26}$$

Table 5.1: *Time-frequency lattice representation.*

Time	*Frequency*					*Total*
	γ_1		γ_n		γ_N	
τ_1	$P(\tau_1,\gamma_1)$	$\cdots$	$P(\tau_1,\gamma_n)$	$\cdots$	$P(\tau_1,\gamma_N)$	$\lvert s(\tau_1)\rvert^2$
	$P(\gamma_1\lvert\tau_1)$	$\cdots$	$P(\gamma_n\lvert\tau_1)$	$\cdots$	$P(\gamma_N\lvert\tau_1)$	
	$P(\tau_1\lvert\gamma_1)$	$\cdots$	$P(\tau_1\lvert\gamma_n)$	$\cdots$	$P(\tau_1\lvert\gamma_N)$	1
	$\vdots$	$\vdots$	$\vdots$	$\vdots$	$\vdots$	$\vdots$
τ_k	$P(\tau_k,\gamma_1)$	$\cdots$	$P(\tau_k,\gamma_n)$	$\cdots$	$P(\tau_k,\gamma_N)$	$\lvert s(\tau_k)\rvert^2$
	$P(\gamma_1\lvert\tau_k)$	$\cdots$	$P(\gamma_n\lvert\tau_k)$	$\cdots$	$P(\gamma_N\lvert\tau_k)$	
	$P(\tau_k\lvert\gamma_1)$	$\cdots$	$P(\tau_k\lvert\gamma_n)$	$\cdots$	$P(\tau_k\lvert\gamma_N)$	1
	$\vdots$	$\vdots$	$\vdots$	$\vdots$	$\vdots$	$\vdots$
τ_K	$P(\tau_K,\gamma_1)$	$\cdots$	$P(\tau_K,\gamma_n)$	$\cdots$	$P(\tau_K,\gamma_N)$	$\lvert s(\tau_K)\rvert^2$
	$P(\gamma_1\lvert\tau_K)$	$\cdots$	$P(\gamma_n\lvert\tau_K)$	$\cdots$	$P(\gamma_N\lvert\tau_K)$	
	$P(\tau_K\lvert\gamma_1)$	$\cdots$	$P(\tau_K\lvert\gamma_n)$	$\cdots$	$P(\tau_K\lvert\gamma_N)$	1
Total	$\lvert S(\gamma_1)\rvert^2$	$\cdots$	$\lvert S(\gamma_n)\rvert^2$	$\cdots$	$\lvert S(\gamma_N)\rvert^2$	1
	1		1		1	

where $f(t)$ describes frequency range and complexity of the signal and goes from constant to modulated frequency by exponential and cosine functions, for example:

$$\text{TS1:} \quad f(t) = f_0, \tag{5.27}$$

$$\text{TS2:} \quad f(t) = f_0 \cdot e^{\frac{-t}{\tau}}, \tag{5.28}$$

$$\text{TS3:} \quad f(t) = f_0 \cdot (1 - e^{\frac{-t}{\tau}}), \tag{5.29}$$

$$\text{TS4:} \quad f(t) = f_0 \cdot \sin(t\tau), \tag{5.30}$$

$$\text{TS5:} \quad f(t) = f_0 \cdot (1 + \cos(t\tau)) \quad \text{and} \tag{5.31}$$

$$\text{TS6:} \quad f(t) = f_0 \cdot t(1 + \cos(t\tau)). \tag{5.32}$$

We considered $A = 1$ and $f_0 = 0.5$ Hz for all signals (an important range of frequencies of the human colonic electrical activity is around 0.5 Hz). This set was selected to understand the relationship between a signal and a kernel function. The characteristics of that relation were used thereafter to analyze the electrical activity recorded in the human colon. We applied three known kernel functions to these sinusoidal signals. We investigated what kind of relation exists between kernel function and these sinusoidal signals. Also, which kernel functions satisfied the constraints of the PTFD and what range of values corresponded to the c-constant of each kernel function. The kernel function describes the interaction between time and frequency cumulative marginal distributions. The range of values for a kernel function varies (Table 5.2). The cumulative marginal distribution is always an increasing function. Its shape is determined by the marginal distribution itself.

The kernel function plays an important role in the description of the time-frequency behaviour, therefore, for each test signal we applied three different φ– functions described in chapter 2 and checked various values of c. The mathematical ex-

pression of each $\varphi-$ functions is as follows

$$\varphi_1(x,y) = (2\cdot x-1)(2\cdot y-1), \qquad -1 \leq c \leq 1 \tag{5.33}$$

$$\varphi_2(x,y) = \frac{6}{7}(2xy-x-y+\frac{1}{2}), \qquad \frac{-7}{2} \leq c \leq \frac{7}{4} \tag{5.34}$$

$$\varphi_3(x,y) = \frac{2}{\pi}\cdot(1-\sqrt{1-x^2}-\sqrt{1-y^2}) \qquad \frac{-\pi}{2} \leq c \leq \frac{\pi}{2}, \tag{5.35}$$

where x is a function of time and it represents the cumulative distribution of the signal power and y is a function of frequency and it corresponds to the cumulative distribution of the power spectrum. x and y are defined in the unit square ($0 \leq x, y \leq 1$). The range of the constant value associated with each kernel function is selected to satisfy the positivity condition of PTFD. The above kernel functions were presented by Cohen et. al. ([9, 22]) as examples of how PTFD can be generated for analyzing particular signals. Here we took them as a starting point to decide which kernel function can be used for any of the predefined sinusoidal signals. The conditional PTFD should satisfy the previous restrictions specified in section 3 to select the kernel function and the associated constant value. Before presentation of the PTFD results for the sinusoidal signals, we show in each case how the kernel function is related to the original signal. The kernel is a function of both cumulative signal power and cumulative power spectrum. In terms of the PTFD, the mathematical expression of $\varphi(x,y)$ represents a weight function of the marginal product $\Gamma(t,f)$. A plot of the time and frequency marginal distribution of each sinusoidal signal with a contour plot of φ_1 and φ_3 are presented. A description of the contour plot of φ_2 was not included because it can be obtained from the geometric figure of φ_1. A contour plot was selected to present a geometric description of the kernel function, where each line or contour describes a level whose value increases (+ve) or decreases (-ve) the importance of the $\Gamma(t,f)$.

The direction of increasing or decreasing levels is useful to describe the influence of the kernel function in certain sections of the time-frequency plane. When we compare two levels with different values and varying distance between them, the rate of change can be used to compare this section with another of similar characteristics. The contour plot of a kernel function divides the plane defined by time and frequency into sections whose importance is given by the values of each line.

In general, a contour line parallel to the time axis corresponds to zero amplitude in the signal power. Similarly, a contour line parallel to the frequency axis corresponds to zero amplitude in the power spectrum. When the kernel function is equal at two different points in time and over the same frequency, the contribution of the signal power to the total signal power at the second point is practically zero or with small amplitude. For one unit of change in time, the kernel function does not change its value (same contour line); therefore, the rate of change over time at a specific frequency is zero. Furthermore, when the rate of change between two different contour lines at time t_i and t_{i+1} is equivalent to the rate of change between contours at time t_{i+1} and t_{i+2}. The signal power, then presents a homogenous change in amplitude or a steady step variation in amplitude for that particular interval of time. When the kernel function is equal at two different frequencies and the same time, the contribution of the power spectrum in the second frequency to the total power spectrum is practically null or with small amplitude. For one unit of change in frequency, the kernel function does not change its value at all (same contour line); therefore, the rate of change over frequency is zero in a specific time. Moreover, when the rate of change between two different contour lines at frequency f_j and f_{j+1} is equivalent to the rate of change between contours at frequency f_{j+1} and f_{j+2}. The power spectrum, then presents a homogenous change in amplitude or a steady step

variation in amplitude for that particular interval of frequency.

Test signal 1 (TS1).

For the test signal whose $f(t)$ is given by (5.27), we have a pure sinusoidal signal with constant frequency ($f(t) = 0.5$ Hz). The main components for calculating the PTFD of TS1 show separately its characteristics in time and frequency (Figure 5.1). The kernel function puts together both time and frequency domains using the cumulative distributions $x(t)$ and $y(f)$. The range of values of φ_1 for TS1 is between -1.0 and 1.0 with a mean value near zero and a large variance (see Table 5.2). The contour plot of φ_1 shows values around the frequency 0.5 Hz that are constant for different segments of time (Figure 5.2). The contour levels define a surface divided in four sectors. Positive values correspond to the lower left (between 0 - 0.5 Hz and 0 - 16 s) and upper right (0.5 - 2 Hz and 16 - 32 s) sectors, the other sectors correspond to the negative values. All levels are concentrated around the main frequency (0.5 Hz). The contour levels in lower left and upper right sectors are in a decreasing and increasing order respectively. The contour level variations are in a linear pattern parallel to frequency and time axes. The range of values of φ_3 for TS1 is between -0.9999 and 0.6333. Its mean value is also close to zero but with small variance. This contour plot is dominated by the main variations around the frequency 0.5 Hz (figure 5.2). The contour level with negative values moves from low to high values of time and from zero to the range of values around 0.5 Hz. However, positive values move in the opposite direction with a main concentration around 0.5 Hz. The geometric figure of both kernel functions φ_1 and φ_3 shows lines almost parallel to the time axis where the rate of change of φ along time is practically zero. Almost all contour lines in φ_1 and

φ_3 were concentrated around frequency 0.5 Hz where $\Gamma(t,f)$ mainly exists. Contour lines parallel to the frequency axis were presented in regions where $\Gamma(t,f)$ was zero.

Test signal 2 (TS2).

For the test signal whose $f(t)$ is given by (5.28), the frequency decreases exponentially with the rate controlled by τ ($\tau = 2$). The main components of TS2 in time and frequency show variations in amplitude with a small oscillation during the first part. These components decrease slowly to zero at end of time. The power spectrum has a frequency content close to zero (Figure 5.3). The kernel function combines both the cumulative time $x(t)$ and frequency distribution $y(f)$. The main variations in signal power occur before time 8 s and frequency changes below 0.6 Hz. The signal power reaches 50% of its total value at 4s and the power spectrum at 0.2 Hz. The contour level plot of φ_1 shows negative and small positive values in that section (Figure 5.4). The contour levels, outside the main variation range, move downward and upward for negative and positive values respectively. The values of φ_1 for TS2 are between -0.8956 and 0.9085 with a mean value of 0.363 indicating a preference for positive values (levels outside the main range of variation). The range for φ_3 is between -0.9342 and 0.4458 with a mean value close to zero. The contour levels of φ_3 have negative values during the main range of variation. Also, negative levels are below the range delimited by 10 s. Above that range, there are positive levels with changes in upward direction. TS2 is a signal concentrated in a small interval of time and frequency (finite energy). φ_1 showed the main range of time-frequency variation of TS2. It corresponded to a very short section where the signal is defined. $x(t)$ reached 50% at t=4s and $y(f)$ at f below 0.1Hz. This center point delimited four sections: two

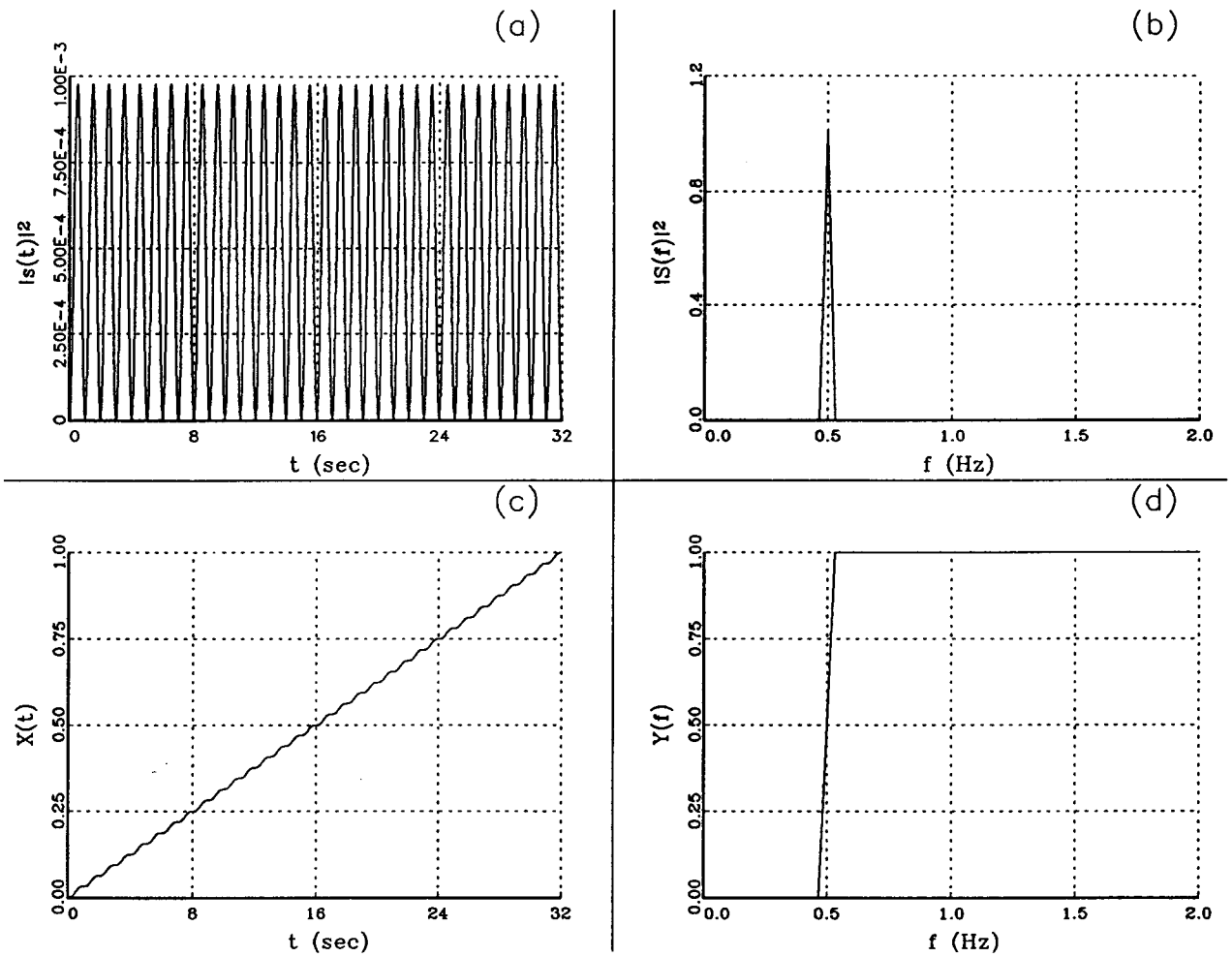

Figure 5.1: *The main components for calculating the PTFD of TS1.*

This graph displays the main components for calculating the PTFD of TS1. It is a correlationless case, the frequency is constant over time. (a) represents the signal power; (b) the spectral energy density with main frequency in $0.5Hz$; (c) the cumulative distribution of the signal power with respect to time; and (d) the cumulative distribution of the spectral energy with respect to frequency.

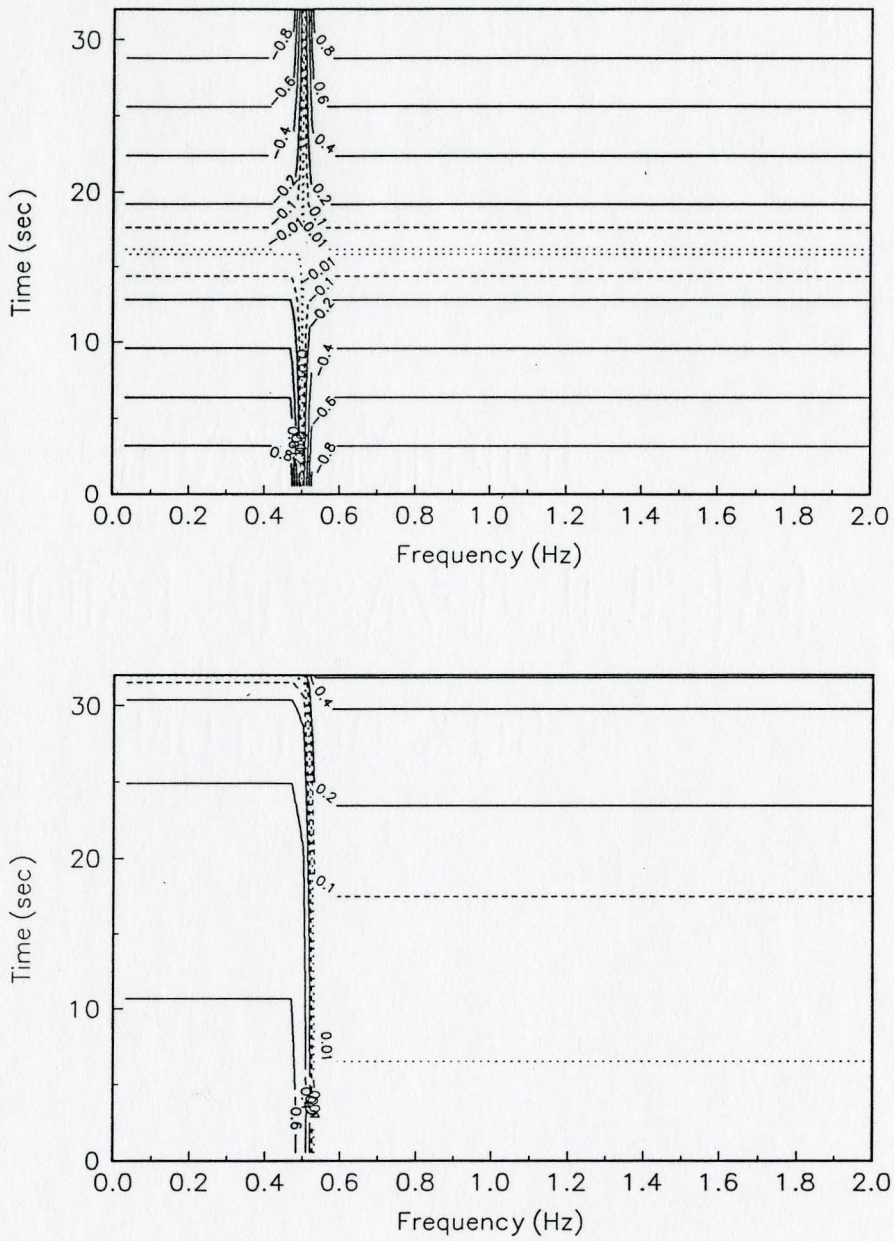

Figure 5.2: *Geometric figure of $\varphi_1(x, y)$ and $\varphi_3(x, y)$ for TS1.*

(a) Contour level plot of φ_1-function shows that around 0.5 Hz the rate of change along time direction stays almost constant in short segments of time; however, along the frequency direction the rate of change exhibits different values. (b) Contour plot of φ_3 presents clearly parallel lines to time axis that correspond to frequencies around 0.5 Hz.

Table 5.2: Range of values of each kernel function in sinusoidal signals

	TS1			
φ-function	Minimum	Maximum	Mean	Variance
φ_1	-1.0	1.0	0.0086	0.3385
φ_2	-0.4286	0.4286	0.0037	0.0622
φ_3	-0.9999	0.6333	-0.077	0.0306
	TS2			
φ_1	-0.8956	0.9085	0.3638	0.2312
φ_2	-0.3838	0.3893	0.1559	0.0425
φ_3	-0.9342	0.4458	-0.0114	0.0969
	TS3			
φ_1	-0.9639	0.9639	-0.0072	0.2344
φ_2	-0.4131	0.4131	-0.0031	0.0431
φ_3	-0.9998	0.4615	-0.3509	0.0423
	TS4			
φ_1	-0.9604	0.9618	0.0132	0.1647
φ_2	-0.4116	0.4122	-0.0057	0.0303
φ_3	-0.998	0.4902	-0.3958	0.0408
	TS5			
φ_1	-0.9546	0.9673	0.027	0.1630
φ_2	-0.4091	0.4145	0.0116	0.0299
φ_3	-0.9979	0.5041	-0.3604	0.0394
	TS6			
φ_1	-0.8707	0.8698	-0.0062	0.1335
φ_2	-0.3731	0.3728	-0.0027	0.0245
φ_3	-0.9979	0.3766	-0.5083	0.0457

of them corresponded to levels with positive values and elsewhere to negative values. The levels around the center point had small values indicating a low influence of the kernel function in the PTFD. φ_3 did not show a center point instead it presented levels that went from the origin in time and frequency toward the maximum point in time and frequency from negative to positive values.

Test signal 3 (TS3).

For the test signal whose $f(t)$ is given by (5.29), the frequency increases exponentially the rate being controlled by τ (for simplicity, $\tau = 1$). The main components in time and frequency for calculating the PTFD present oscillations with an increasing frequency that is dominated by 0.5 Hz (Figure 5.5). The power signal reachs its 50% at 4.2s ($x(t) = 0.5$)and the power spectrum reaches 50% at 0.5Hz ($y(f) = 0.5$). The range of φ_1 for this signal is between -0.9639 and 0.9639 with a negative mean value close to zero. φ_3 values are between -0.9998 and 0.4615 with also a negative mean value but away from zero indicating a preference for negative levels (Table 5.2). The importance of interaction between time and frequency can be expressed through a kernel function. There is a section in φ_1 where interaction between time and frequency is very small (section around 0.5Hz and 4.2s in Figure 5.6). This is partially consistent with frequencies that do not change over time. Contour lines with large values (positive and negative) are represented in the four corners of the time-frequency plane. The power spectrum in frequencies above 1Hz are practically zero; therefore, the contour lines are parallel to the frequency axis. The section of small variation of φ_3 covers all frequencies after t=5.5s. The contour lines during frequencies below 0.6 Hz represent large negative values.

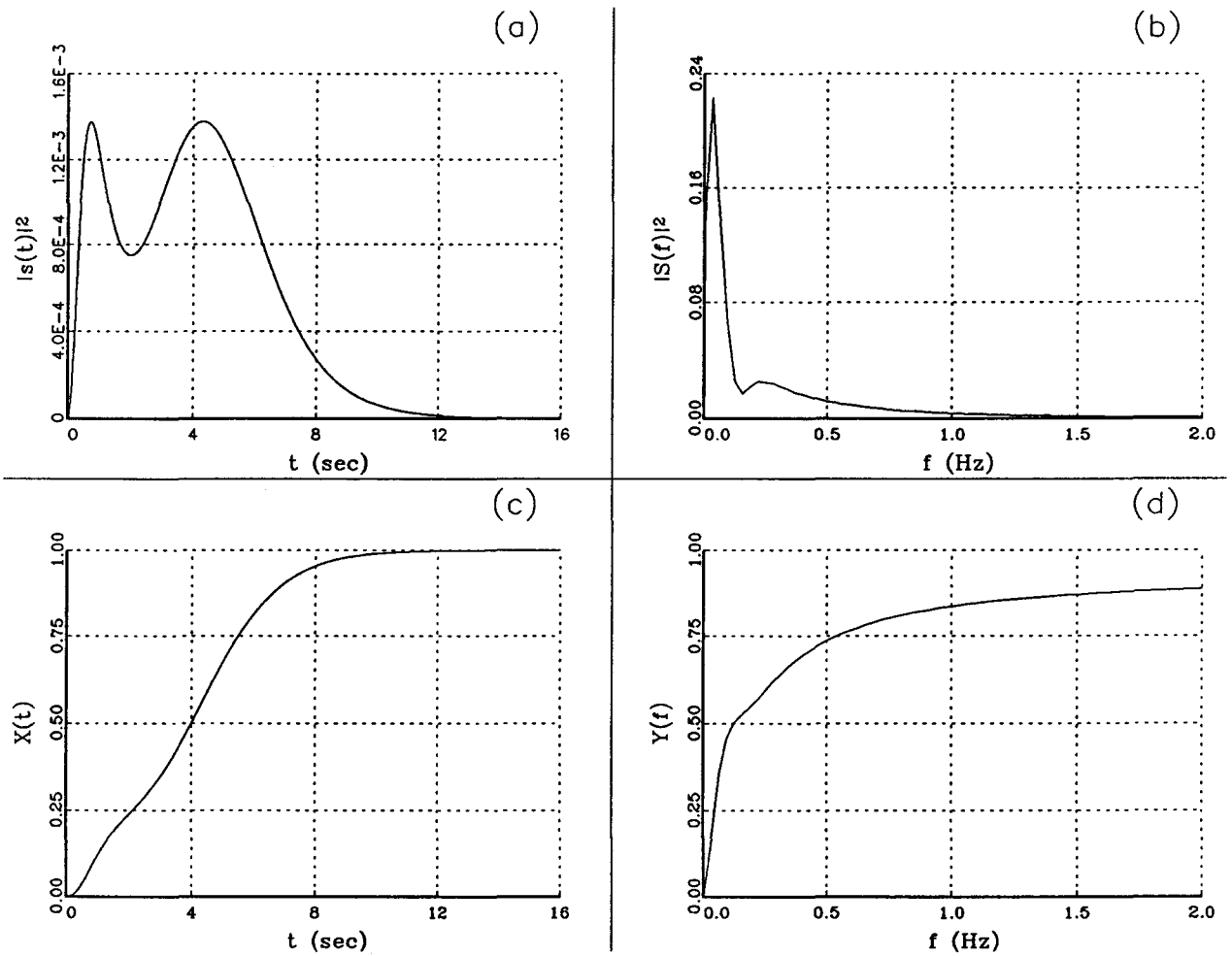

Figure 5.3: *The main components for calculating the PTFD of TS2*

(a) represents the signal power; (b) the spectral energy density with frequencies centre around zero; (c) the cumulative distribution of the signal power with respect to time, at time t=4s it reaches 50% of its power and 98% at t=8s; and (d) the cumulative distribution of the spectral energy with respect to frequency.

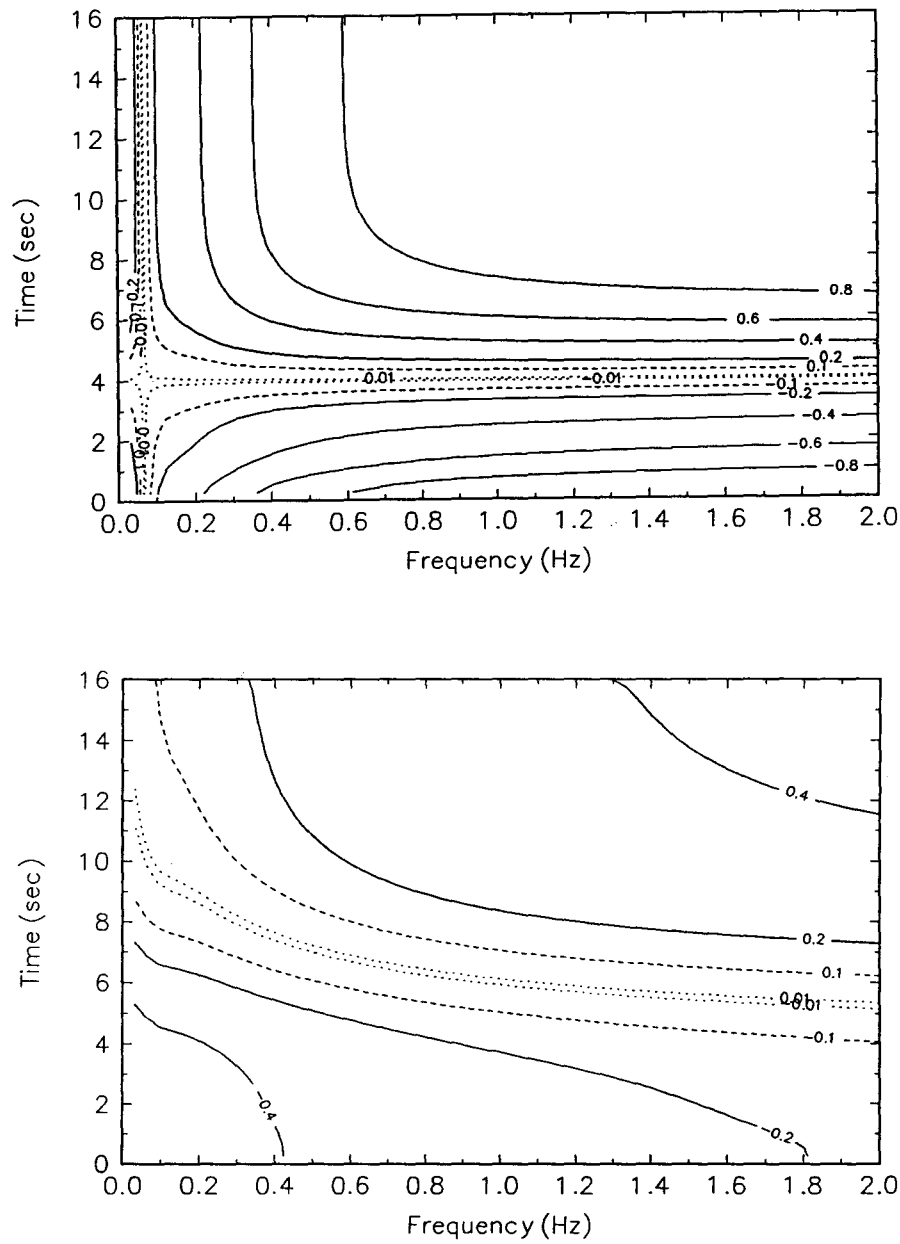

Figure 5.4: *Geometric figure of $\varphi_1(x,y)$ and $\varphi_3(x,y)$ for TS2.*

(a) Contour level plot of φ_1-function outside the main range of variation (0-8 s and 0 - 0.6Hz) shows that upper tails of both time and frequency cumulative distribution dominate the geometric figure of this kernel. There are a band of contour levels with an increasing rate of change. (b) Contour plot of φ_3 presents negative contour levels for frequency interval below 1 Hz and 8 s.

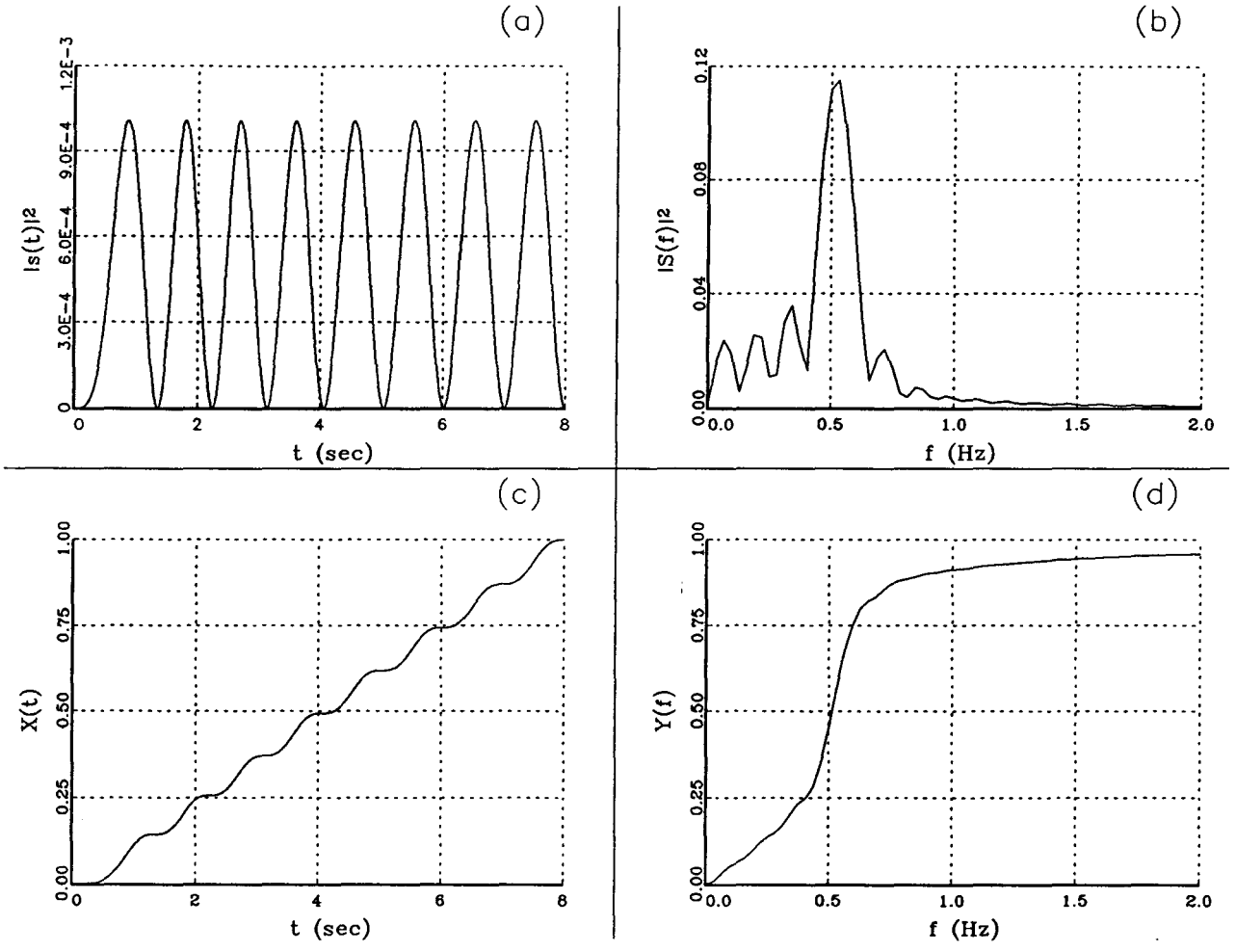

Figure 5.5: *The main components for calculating the PTFD of TS3*

(a) represents the signal power, the time delay at the begining is little bit higher than during the rest until the signal reaches the main frequency; (b) the spectral energy density with frequencies centre around 0.5 Hz; (c) the cumulative distribution of the signal power with respect to time, it is almost a straight line with a unity slope; and (d) the cumulative distribution of the spectral energy with respect to frequency: the most important range of variations is around 0.5Hz.

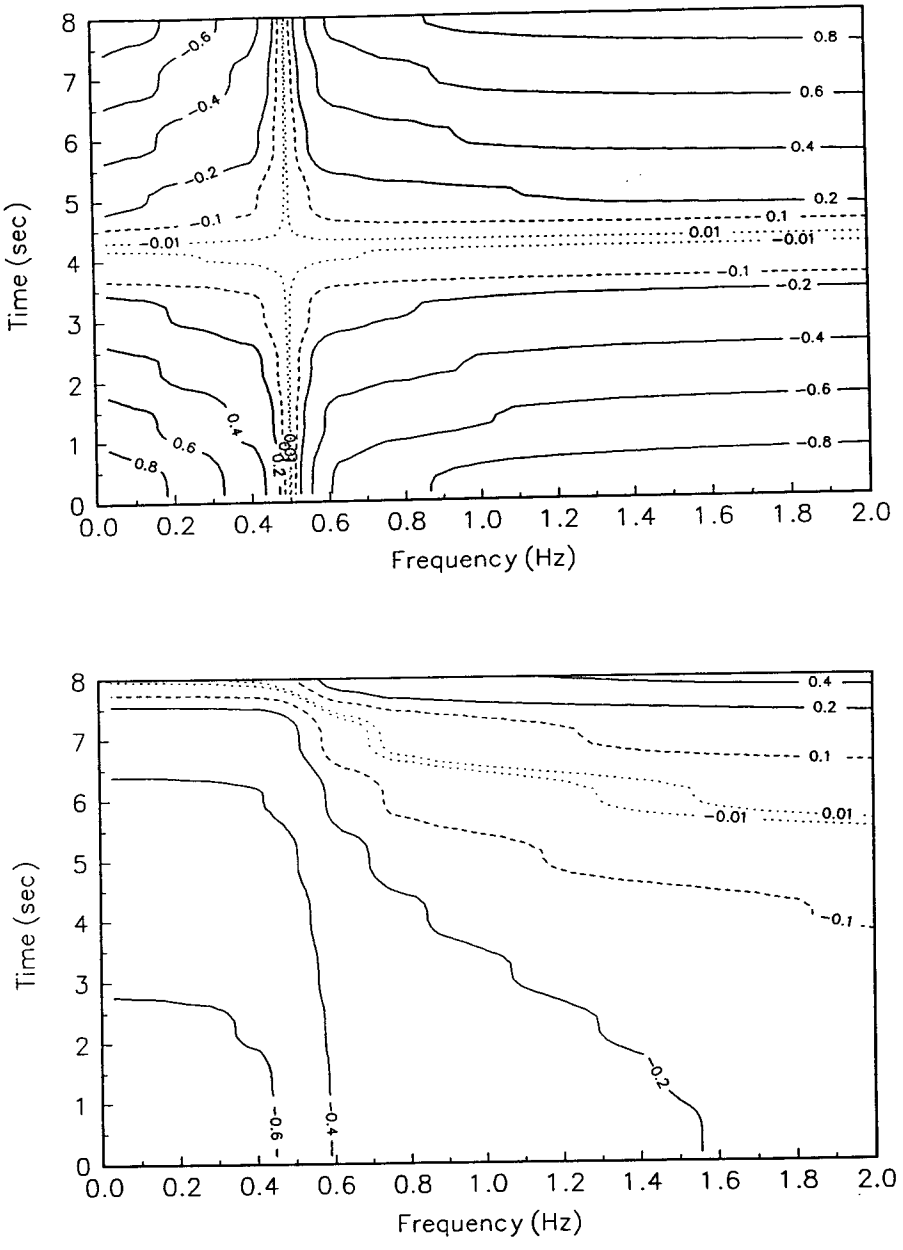

Figure 5.6: *Geometric figure of $\varphi_1(x,y)$ and $\varphi_3(x,y)$ for TS3.*

(a) Contour level plot of φ_1-function shows lines around 0.5Hz with small values. The plot shows a kind of center point at 0.5Hz and 4.2s. (b) φ_3 also presents parallel lines to time axis around 0.5Hz. There are contour lines with positive values in a small section at end of time interval.

Test signal 4 (TS4).

This test signal is an oscillatory burst model whose $f(t)$ is defined by a sinusoidal model (5.30). The frequency change for each burst is controlled by τ. For illustrative purpose, τ is set equal to 2.5. The signal power reaches its 50% with respect to total power at 7.8s. The cumulative signal power mantains a linear increase during the whole time segment. The power spectrum shows the importance of frequencies below 9 Hz. The cumulative power spectrum presents a rapid increase before 6Hz (Figure 5.7). This figure gives a brief description of the main signal characteristics in both domains. The kernel function combines both cumulative signal power and cumulative power spectrum and describes the interaction of the two domains. The contour plot of φ_1 (Figure 5.8) exhibits a section of low interaction delimited by contour lines around 3.2Hz and 7.8s. Most of the contour lines of φ_3 exhibit negative values. There is a section with low interaction at the end of the time interval for frequencies below 6Hz. The contour lines with postive values are in a small section during the last time interval and above 9 Hz. The range of φ_3 is between -0.998 and 0.4902 with a mean value of -0.3958 (Table 5.2).

Test signal 5 (TS5).

The frequency of this test signal is determined by the sinusoidal model (5.31). TS5 exhibits similar characteristics to TS4. The frequency changes by bursts are faster for TS5 than TS4 using the same τ value ($\tau = 2.5$). The marginal components in time and frequency for calculating the PTFD gives us a first approach to the time-frequency analysis (Figure 5.9). The signal power during the first second reaches almost one-fifth of the total power. The power spectrum displays a broad range

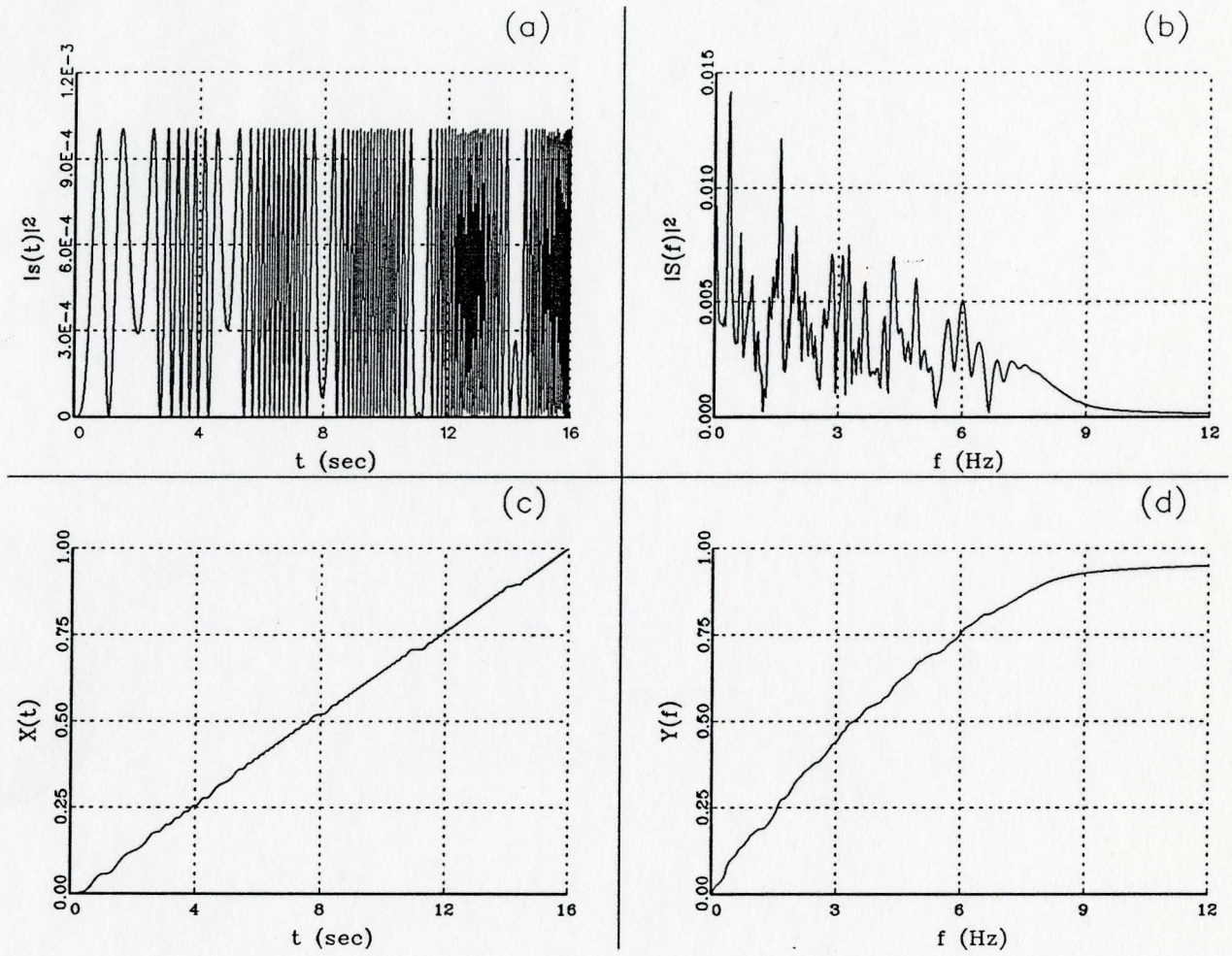

Figure 5.7: *The main components for calculating the PTFD of TS4*

(a) represents the signal power, it is clear the frequency increases by bursts; (b) the spectral energy presents a broad range of frequencies; (c) the cumulative distribution of the signal power looks like a straight line with small steps at the beginning; and (d) the cumulative distribution of the spectral energy presents small steps during the whole range.

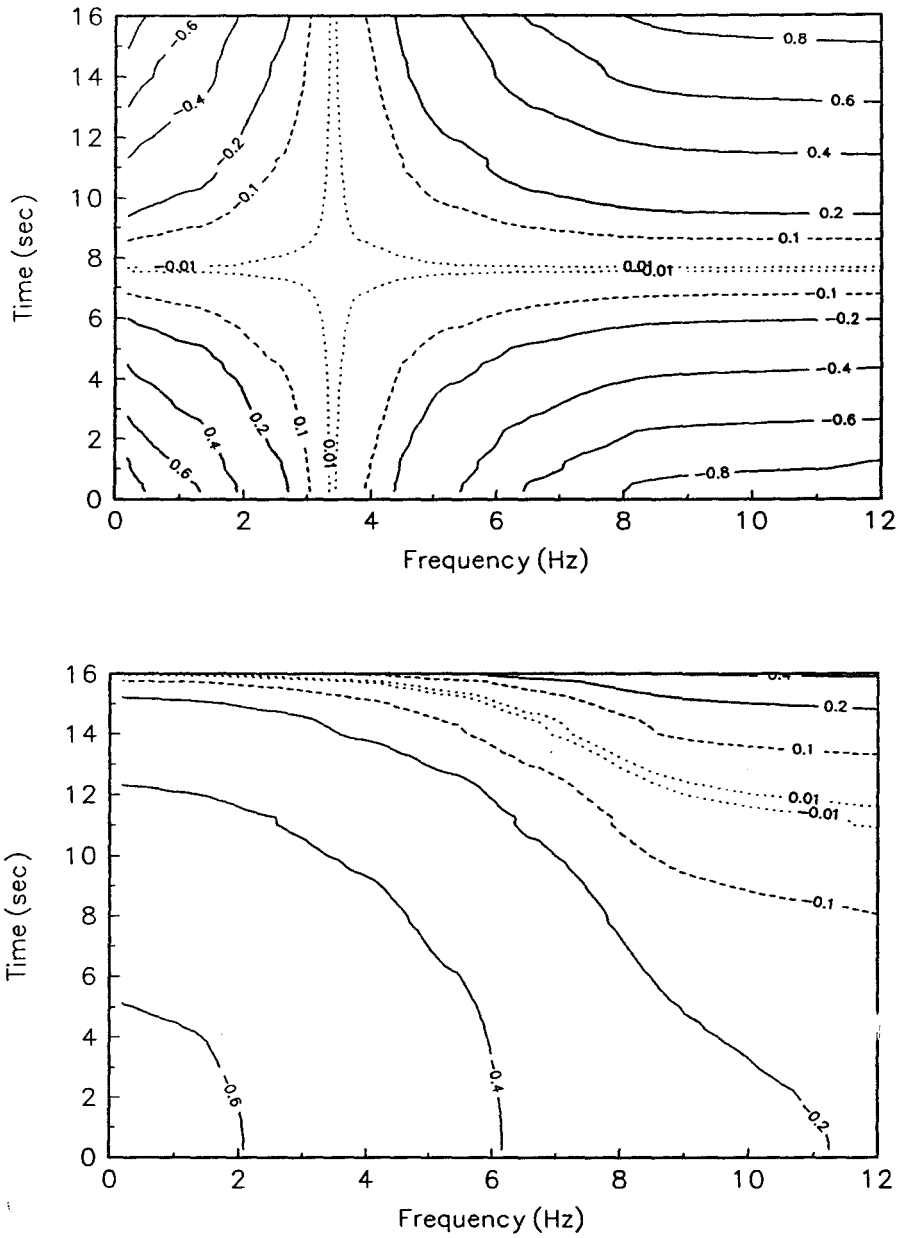

Figure 5.8: *Geometric figure of $\varphi_1(x,y)$ and $\varphi_3(x,y)$ for TS4.*

(a) Contour level plot of φ_1-function shows a surface with four sections: positive values (lower left and upper right section), otherwise negative values. Saddle point around 3.2Hz and 7.8s. (b) Contour plot of φ_3 exhibits a majority of negative levels except at end of time interval.

of frequencies whose influence in the signal is important. The geometric shape of the cumulative power spectrum presents small variations in between minimum and maximum significant frequency. The frequency content of this signal is quite similar to TS4. The contour lines of φ_1 exhibit a section with small values around 3.9Hz and 3.8s (Figure 5.10). The highest rate of change between contour lines is along the diagonal $x(t) = y(f)$ or $y(t) = -y(f)$. The section with small values in φ_3 is at end of time interval for frequencies below 6 Hz. This contour plot is dominated by lines with negative values.

Test signal 6 (TS6).

The frequency of this test signal is determined by the sinusoidal model (5.32) with $\tau = 2.5$. The marginal components in time and frequency for calculating the PTFD provide insight about this signal (Figure 5.11). The signal power reaches 25% of total power at 1s and mantains the same level until 1.5s. The cumulative signal power after this point shows a linear increase pattern. The power spectrum exhibits frequencies close to zero and in a range below 16 Hz. The main frequency is around 0.5Hz and it shows decreasing peaks for frequencies below 4Hz. There are another set of peaks between 4 and 8 Hz with almost the same power and another set of decreasing peaks below 12 Hz. The cumulative power spectrum presents almost a linear increase in the range between 0 and 12 Hz. It reaches 50% of power spectrum approximately at 6Hz. The kernel functions φ_1 and φ_3 applied to TS6 give more insights about the interaction between time and frequency components (Figure 5.12). The contour lines of φ_1 define a section with small values around 6Hz and 2.1s (centre point). φ_1 also shows lines in some frequencies that are parallel to the time axis during short periods

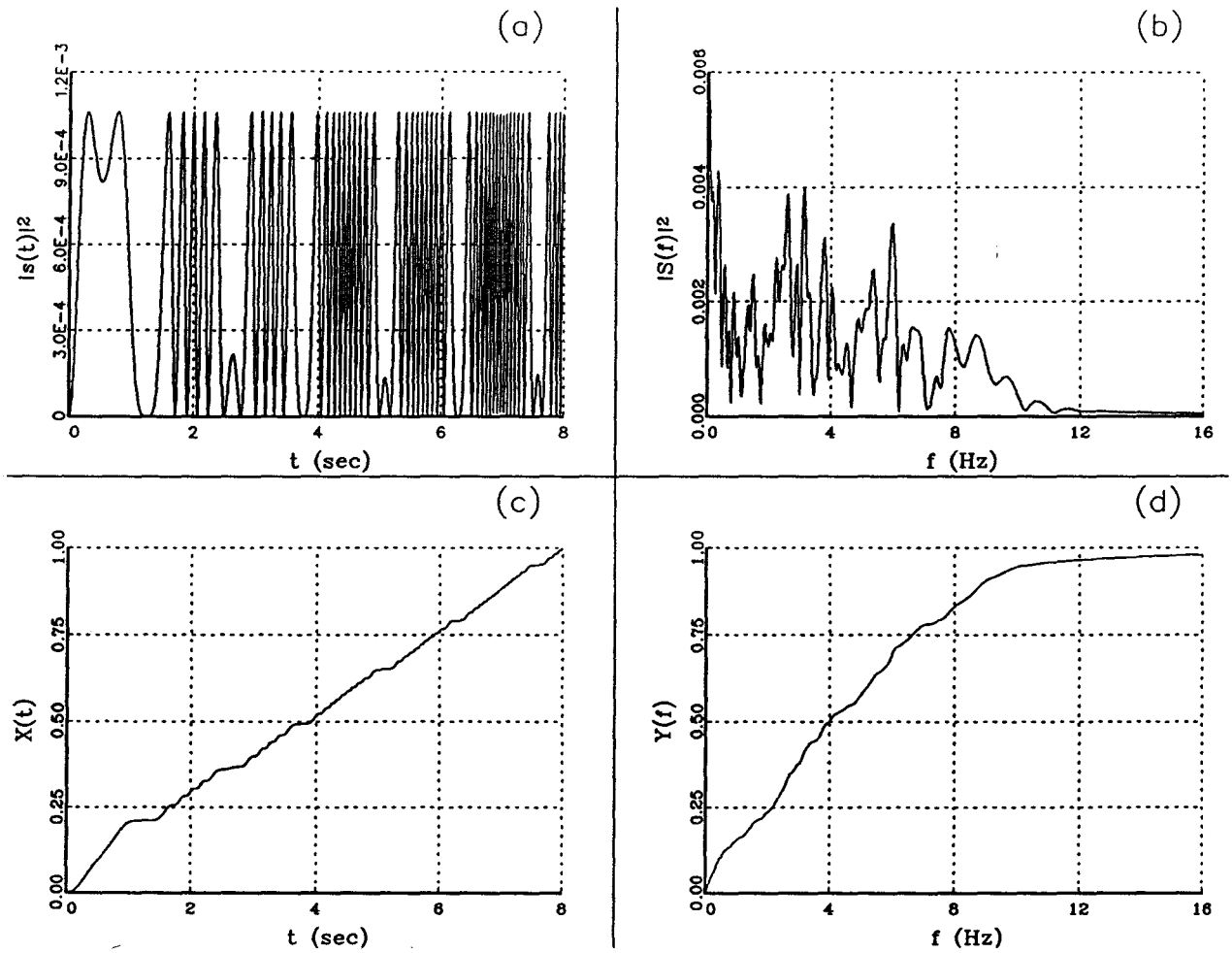

Figure 5.9: *The main components for calculating the PTFD of TS5*

(a) The signal power exhibits variations in amplitude and frequency; (b) the spectral energy exhibits a broad range of frequencies with the most important frequencies around zero; (c) the cumulative distribution of the signal power shows certain steps that corresponds to transitions between bursts (notice a big step at the beginning); and (d) the cumulative distribution of the spectral energy reaches its 50% at 4Hz. The variations in frequency are indicated with changes in the linear trend of $y(f)$.

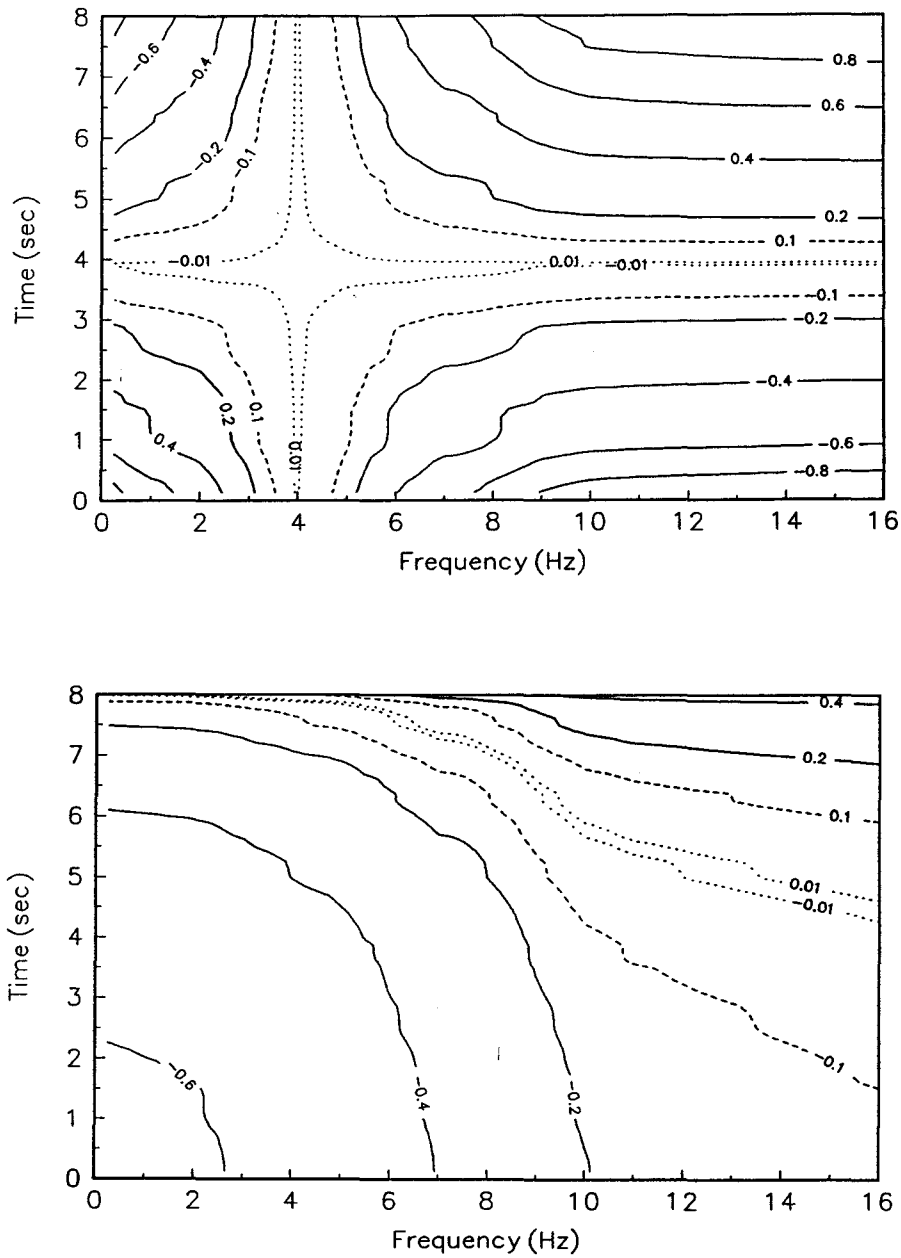

Figure 5.10: *Geometric figure of $\varphi_1(x,y)$ and $\varphi_3(x,y)$ for TS5.*

(a) Contour level plot of φ_1-function shows a centre point around 4Hz and 4s. where a section with small variation is located. (b) Contour lines of φ_3 exhibit a majority of negative values except at end of time interval.

of time. φ_1 decreases as you move from the origin toward the centre point. There are increasing values when the movement is away from the centre point to the points whose coordinates are 16Hz and 4s. Its range of values includes -0.8707 and 0.8698 with a mean value close to zero. φ_3 increases as you move from the origin toward the point at 16Hz and 4s in an upward shape. This kernel function presents parallel lines to the time axis for some frequencies during the time interval between 1 and 1.5 s. The values for this kernel are between -0.9979 and 0.3766 with a negative mean value away from zero.

5.6 PTFD of sinusoidal signals. Numerical Results and Discussion

We applied each kernel function to the complete set of sinusoidal signals and used a range of constant values. This range included minimum and maximum value of the associated kernel function. The final results are presented with a brief discussion.

The PTFD of TS1 is a correlationless case and it can be represented as a product of marginal distributions: $P(t,f) = |s(t)|^2 \cdot |S(f)|^2$. The interaction element disappears, the PTFD only depends on the intensity per unit time and frequency. This is consistent with the ideal signal characteristics and it is a trivial case. Any segment that we take produces the same spectrum, we do not have any variation between time and frequency, therefore the time-frequency distribution is constant and the kernel function is any constant value. The entropy and uncertainty coefficient can be improved with respect to the marginal product ($H = 4.1584$ and $U = 2.7e-5$) with any of the three kernel functions and c- value around zero (interval of ± 0.0125). The

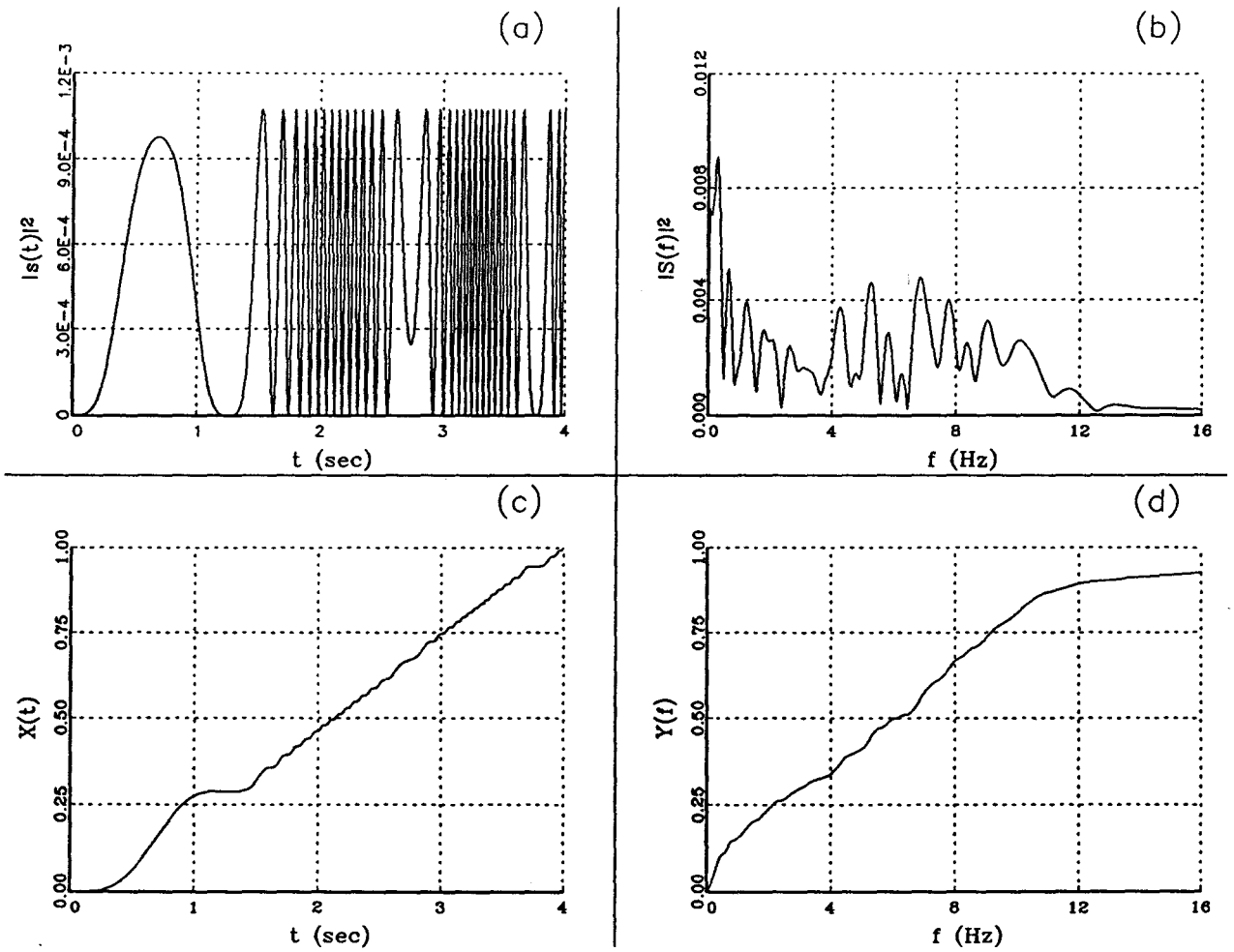

Figure 5.11: *The main components for calculating the PTFD of TS6*

(a) the signal power exhibits a slow wave at the first part, then two consecutive bursts of high increasing frequency; (b) the spectral energy presents several peaks during the range between 0.5 and 12Hz.; (c) the cumulative distribution of the signal power displays a big step that corresponds to the slow wave, after that a linear increasing frequency; and (d) the cumulative distribution of the power spectrum shows three general behaviours, one between zero and 6 Hz, another after 6 and below 12Hz and the last after 12Hz with an almost horizontal line.

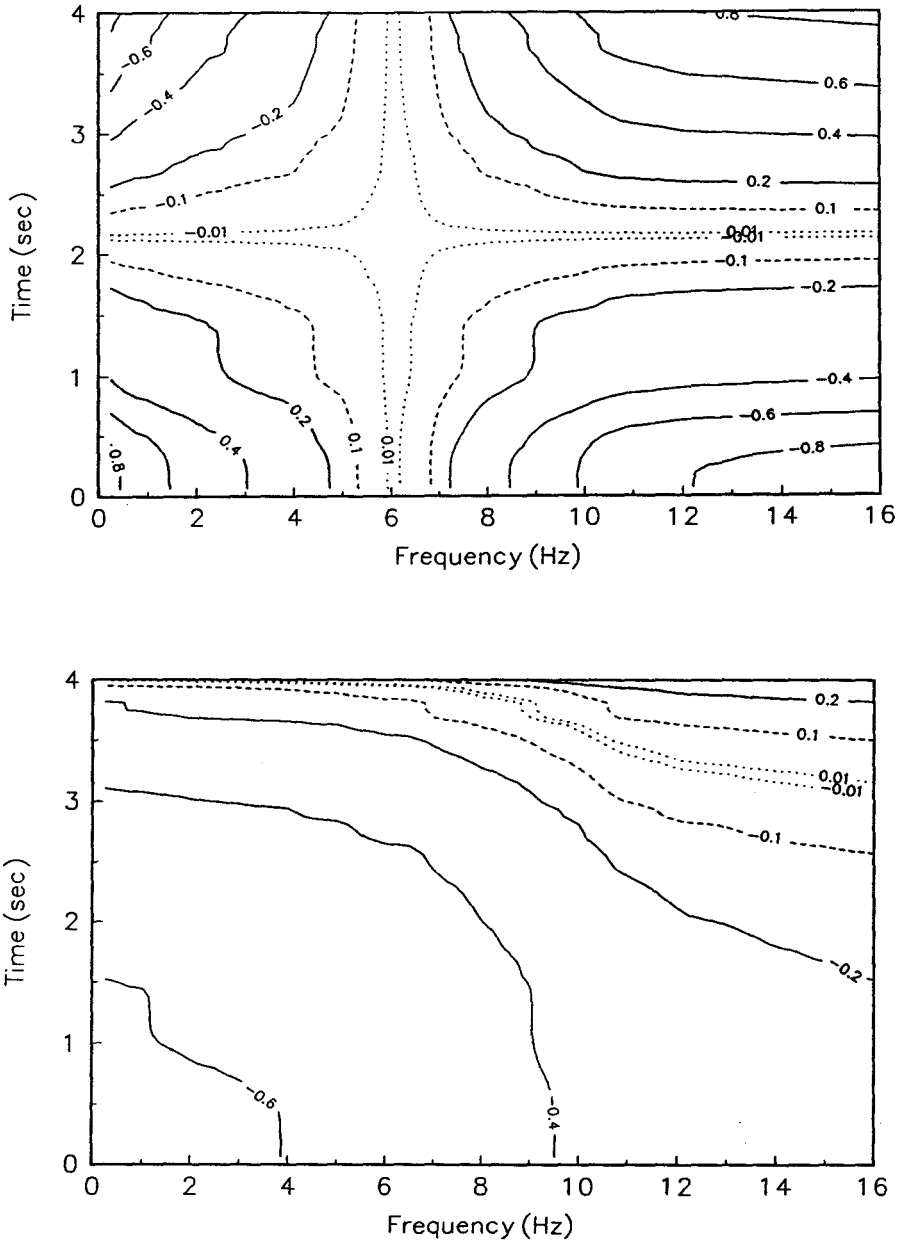

Figure 5.12: *Geometric figure of $\varphi_1(x,y)$ and $\varphi_3(x,y)$ for TS6.*

(a) Contour level plot of φ_1 shows a centre point around 6Hz and 2.1s and increasing or decreasing directions for positive and negative levels. (b) Contour plot of φ_3 exhibits an upward increasing direction with a majority of negative levels except at end of time interval.

Table 5.3: Entropy and uncertainty coefficients of each sinusoidal signal by marginal product and PTFD using a φ function.

	$\Gamma(t,f)$		$P(t,f)$		
Signal	$H(t,f)$	$U(t,f)$	$\varphi - function$	$H(t,f)$	$U(t,f)$
TS1	4.1584	2.7e-5	φ_3	4.1638	0.0026
TS2	5.9816	0.0528	φ_1	5.9663	0.0578
TS3	6.8026	0.0427	φ_1	6.7568	0.0559
TS4	7.7506	0.02	φ_1	7.7073	0.031
TS5	7.5903	0.0171	φ_1	7.5472	0.0284
TS6	7.3111	0.0734	φ_1	7.261	0.0866

PTFD of TS1 was calculated using φ_3 and c=0.125 (Figure 5.13). The entropy and uncertainty coefficient for this case were $H = 4.1638$ and $U = 0.0026$, respectively (Table 5.3). The distribution is concentrated along the main frequency.

The PTFD for TS2 using φ_1 with $c = -0.25$ improved the uncertainty coefficient and satisfied marginal conditions (Table 5.3). The energy for TS2 is clearly concentrated in a very small frequency interval close to zero with variations in time. The average of frequency-conditional PTFD as well as the average of time-conditional PTFD was practically the same as the respective marginal distribution (Figure 5.14). The PTFD was concentrated around frequency zero and decreased quickly to reach zero amplitude after the frequency 0.5 Hz (Figure 5.15). The conditional average frequency for a given time and the mean duration for a given frequency presented two important aspects: first, the average frequency ($< f >_t$) keeps on decreasing until time equals 8s and after that is constant; second, the average duration ($< t >_f$)

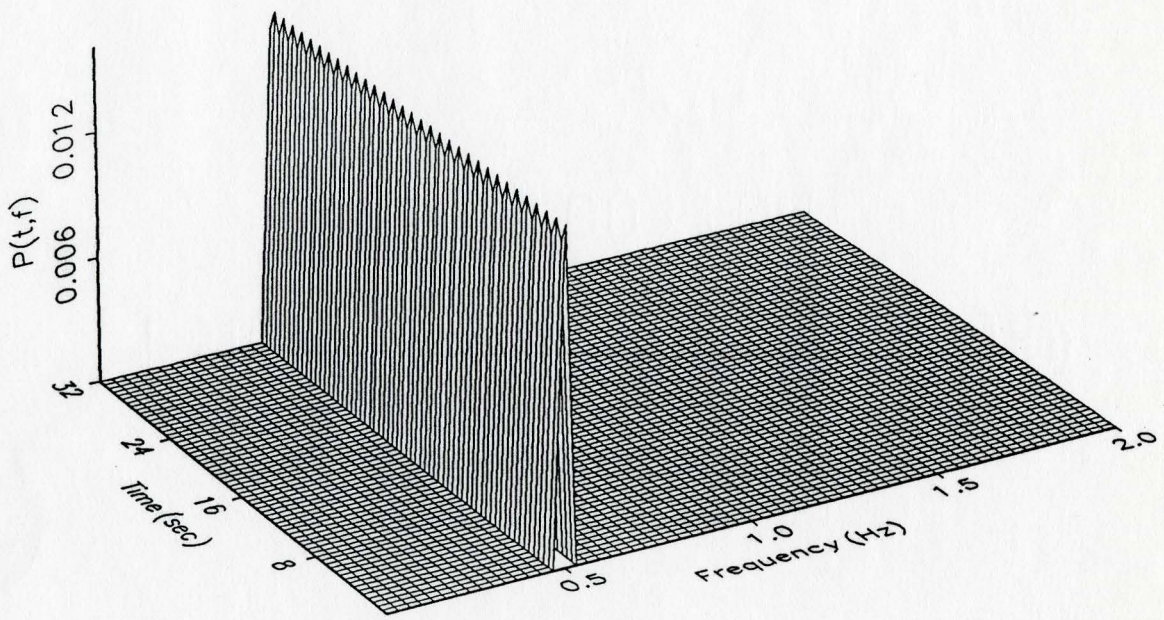

Figure 5.13: *PTFD of TS1.*

The PTFD plot of TS1 was calculated using φ_3 with $c = 0.0125$. The distribution has a constant shape for all time.

decreases faster during frequencies below 0.1Hz and then decreases more slowly (Figure 5.16). The former outlines frequency variations for the first part of the signal. The latter is consistent with the description of the power spectrum for TS2.

The φ_1 kernel function with $c = 0.9639$ for TS3 showed both a good approximation to the marginals in time and frequency and an improved uncertainty coefficient (Table 5.3). However, the average of time-dependent PTFD increased linearly over time unlike the signal power (Figure 5.17). This behaviour was consistent with φ_1 kernel function whose positive levels were given along the diagonal of time-frequency surface. The average of frequency-dependent PTFD was a very good estimation of the marginal distribution. The PTFD of TS3 was concentrated around frequency 0.5 Hz (Figure 5.18). The amplitude of PTFD increased with time for frequencies around 0.5Hz and decreased for frequencies below 0.4Hz. The conditional average frequency ($< f >_t$) was an increasing curve with a small range of variation (Figure 5.19). The conditional average duration ($< t >_f$) slowly increased during frequencies below 0.5 Hz, between 0.5 and 0.7Hz increased faster and during the last part it changed very little. $< f >_t$ and $< t >_f$ for a large c-value look like the cumulative marginal distributions.

The φ function that shows the best approximation to the marginals in time and frequency for TS4 is φ_1 and $c = 0.9618$. The PTFD satisfied the marginal distributions and the entropy condition. The average of the time-conditional PTFD presented a linear mismatch with only the midpoint matched (Figure 5.20). The frequency-conditional PTFD mantained a very good fit with respect to frequency marginal distribution. The PTFD of TS4 shows that main variations were presented below 7.5 Hz for the whole time interval (Figure 5.21). The conditional average frequency ($< f >_t$) kept increasing in value with some small steps which indicated

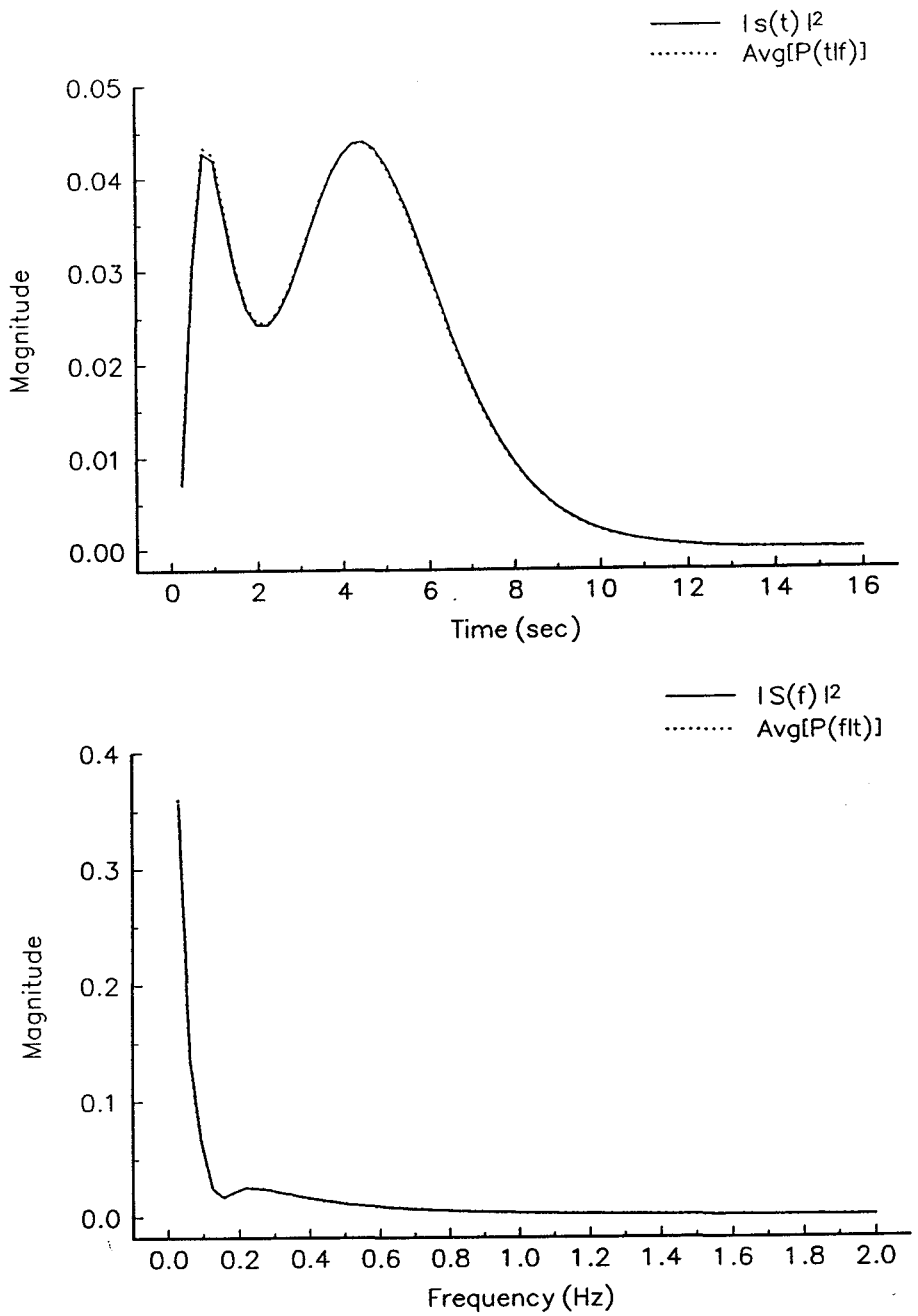

Figure 5.14: *Time and frequency marginal distributions and average of conditional PTFD in each case for TS2.*

Results for φ_1 and $c = -0.25$. (a) Time marginal distribution and average of time-conditional PTFD are practically the same. (b) Frequency marginal distribution and average of frequency-conditional PTFD are identical.

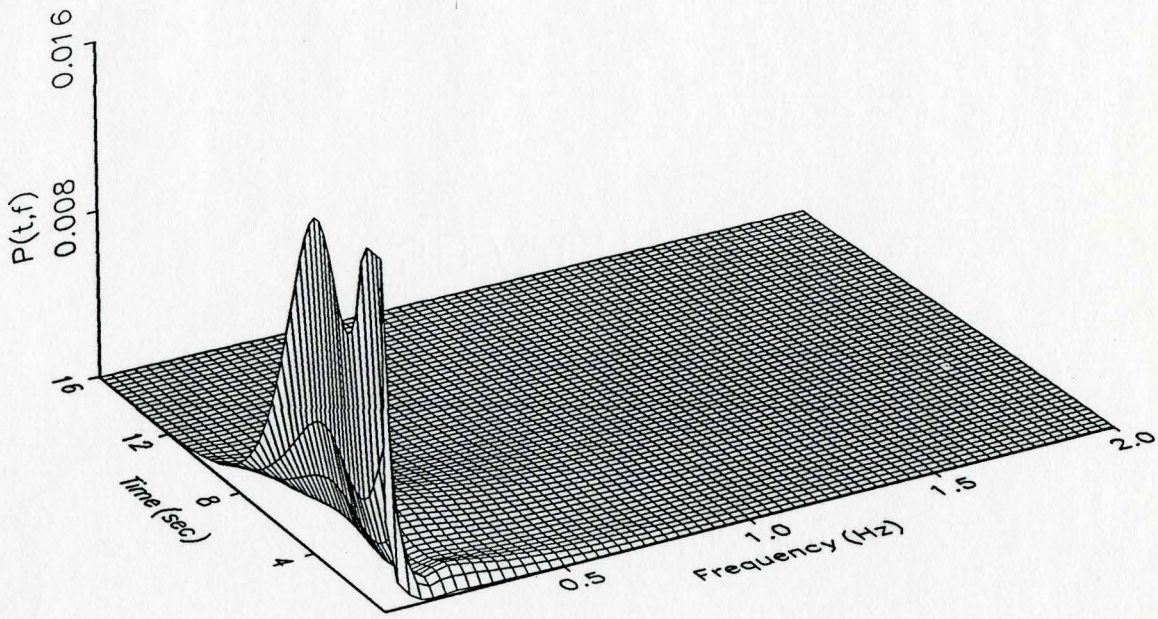

Figure 5.15: *PTFD of TS2 using* φ_1 *and* $c = -0.25$

PTFD exhibits a small correlation between time and frequency over a short frequency interval (0-0.2Hz).

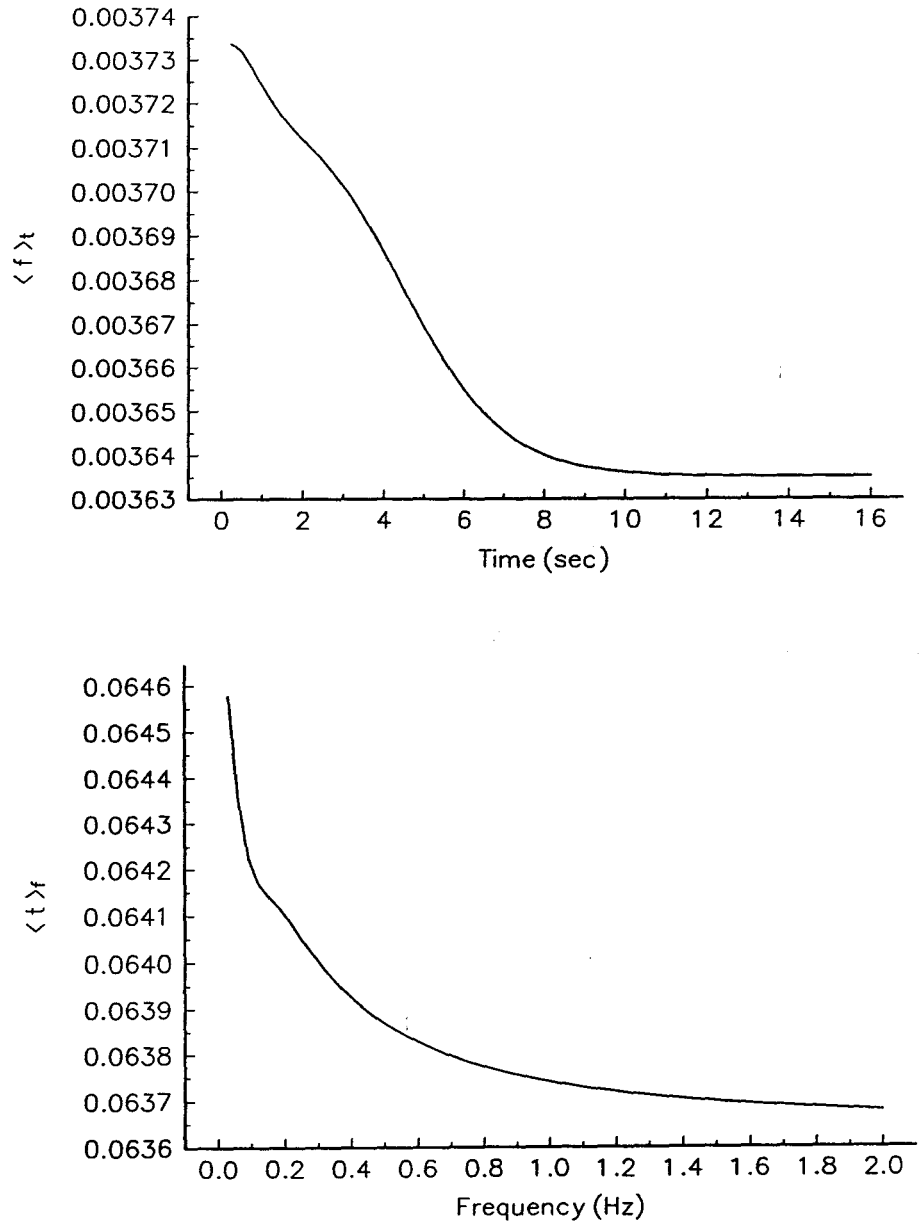

Figure 5.16: $< f >_t$ *and* $< t >_f$ *of TS2 using* φ_1 *and* $c = -0.25$

First moments of PTFD in terms of time and frequency. (a) The conditional average frequency for a given time. It has a small range of average frequency variations over the time signal duration. (b) The conditional average duration for a given frequency. It is a decreasing curve, fast below 0.1Hz and slow during the last frequencies.

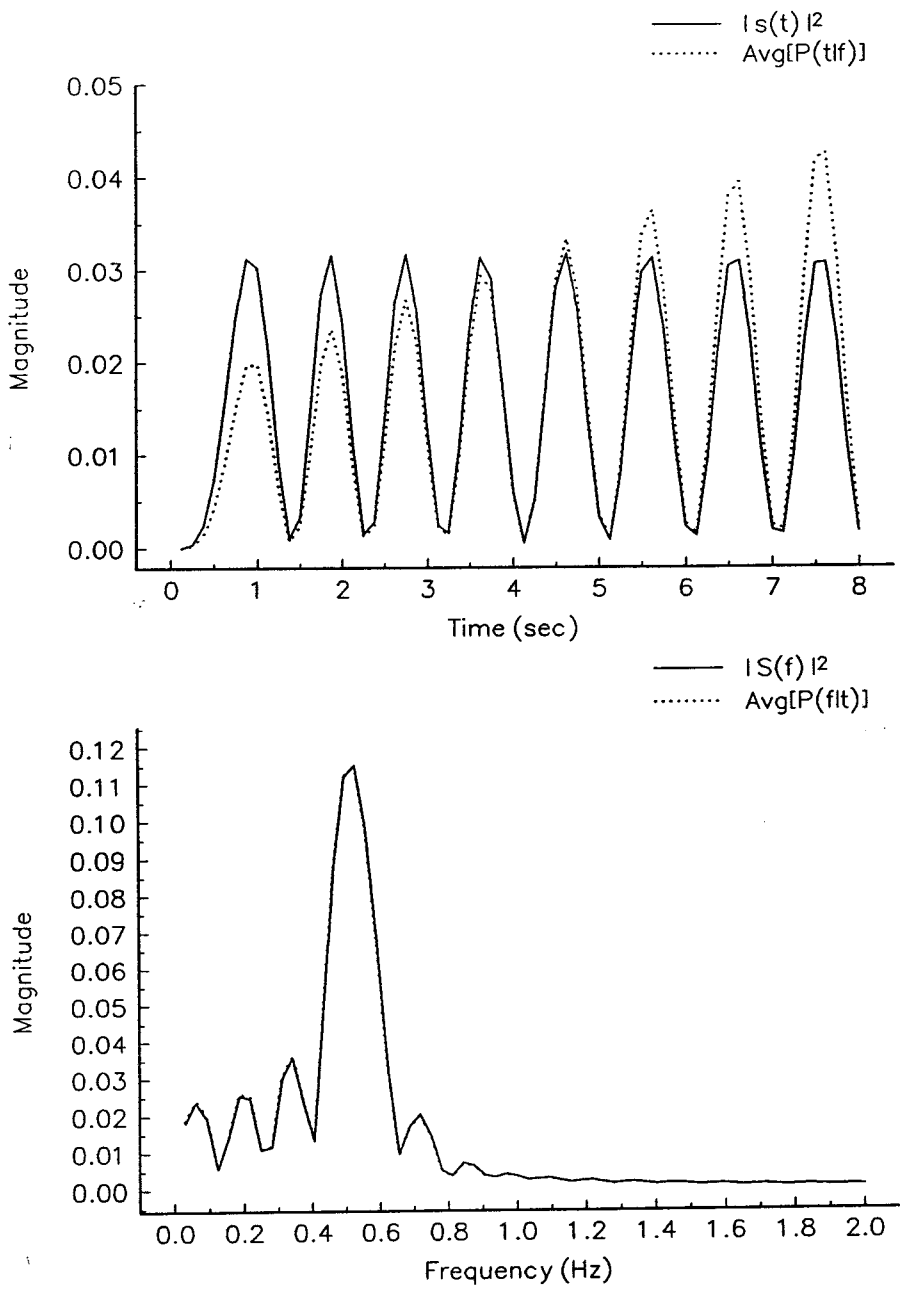

Figure 5.17: *Time and frequency marginal distributions and average of conditional PTFD in each case for TS3.*

Results for φ_1 and $c = 0.9639$. (a) Time marginal distribution and average of time-conditional PTFD. (b) Frequency marginal distribution and average of frequency conditional PTFD. The PTFD of TS3 gave more importance in terms of time to the last part than the first half of the signal. However, the frequency content was mantained uniform.

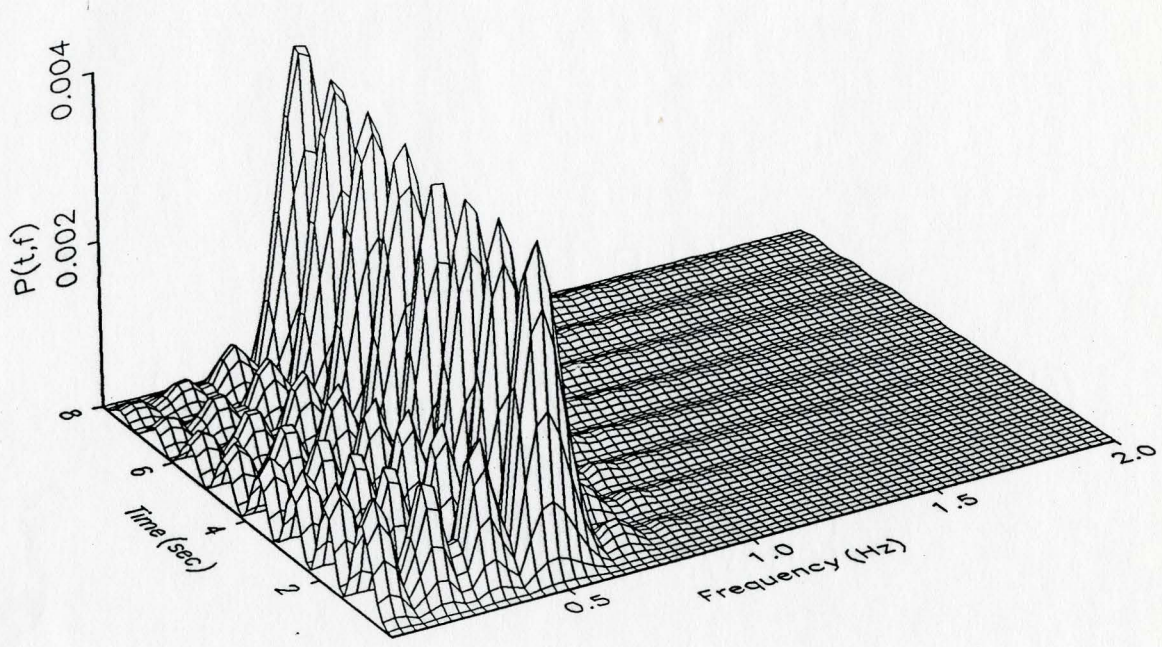

Figure 5.18: *PTFD of TS3 using* φ_1 *and* $c = 0.9639$

The basic principle of mantaining the same total energy under the PTFD was satisfied: when the surface pattern around 0.5Hz increases along time, the pattern for frequencies outside this range decreases.

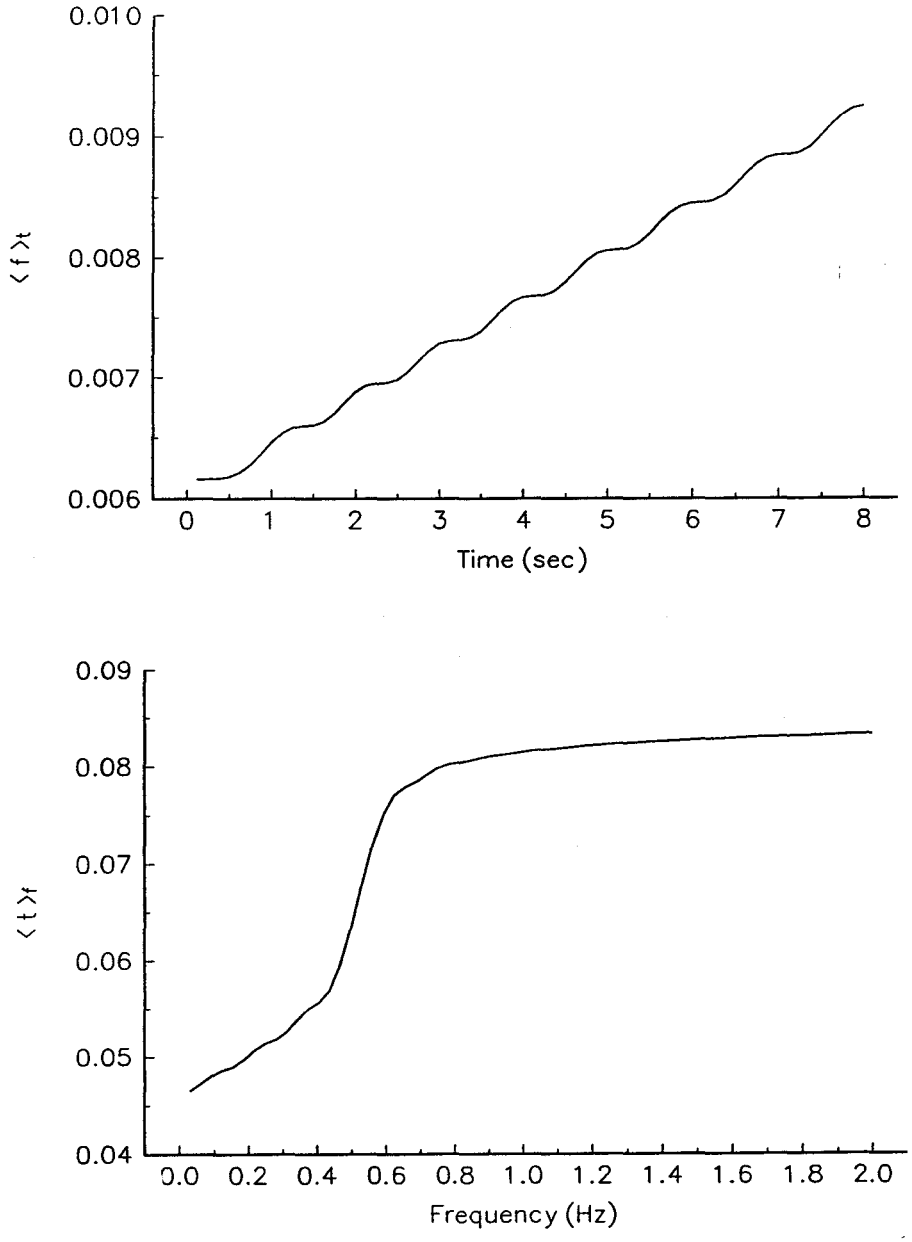

Figure 5.19: $< f >_t$ *and* $< t >_f$ *of TS3 using* φ_1 *and* $c = 0.9639$

First moments of PTFD in terms of time and frequency. (a) The conditional average frequency for a given time presents an increasng change; however, the range of variations is very small. (b) The conditional average duration for a given frequency exhibits the main variation for frequencies between 0.4 and 0.7 Hz.

the transition between bursts of different frequency (Figure 5.22). The conditional mean duration ($< t >_f$) increased slowly until it reached a frequency of 8 Hz and then mantained a constant behaviour.

φ_1 kernel function with $c = 0.9673$ showed the best approximation to the marginals in time and frequency for TS5 and improved the uncertainty coefficient with respect to the marginal product. The average of the time-conditional PTFD presented a linear mismatch with only the midpoint matched to the marginal distribution (Figure 5.23). However, the fit was very good for the frequency-conditional PTFD. The PTFD of TS5 showed that frequencies below 4 Hz were relatively important during the first 4s and decreased in importance over the last part of the signal (Figure 5.24). The relative importance of frequencies above 4Hz increased slowly over time. The conditional average frequency ($< f >_t$) kept on increasing with some steps which indicated the transition between bursts of different frequency (Figure 5.25). The conditional mean duration ($< t >_f$) increased slowly until it reached a frequency of 10 Hz and then it stayed constant.

φ_1 kernel function with $c = 1.0$ showed the best approximation to the marginals in time and frequency for TS6 and improved the uncertainty coefficient with respect to the marginal product. The average of the time-conditional PTFD presented a linear mismatch with only the midpoint matched to the time marginal distribution (Figure 5.26). However, the fit of the frequency-conditional PTFD was good with respect to the power spectrum. The PTFD of TS6 showed variations starting from the first section of 0-2Hz and 0-2s and it went into the section delimited by 12Hz and 4s. However, the band was not clearly defined (Figure 5.27). The conditional average frequency ($< f >_t$) presented a complex change during the first 1.5s, after that it increased linearly (Figure 5.28). The conditional mean duration ($< t >_f$) displayed

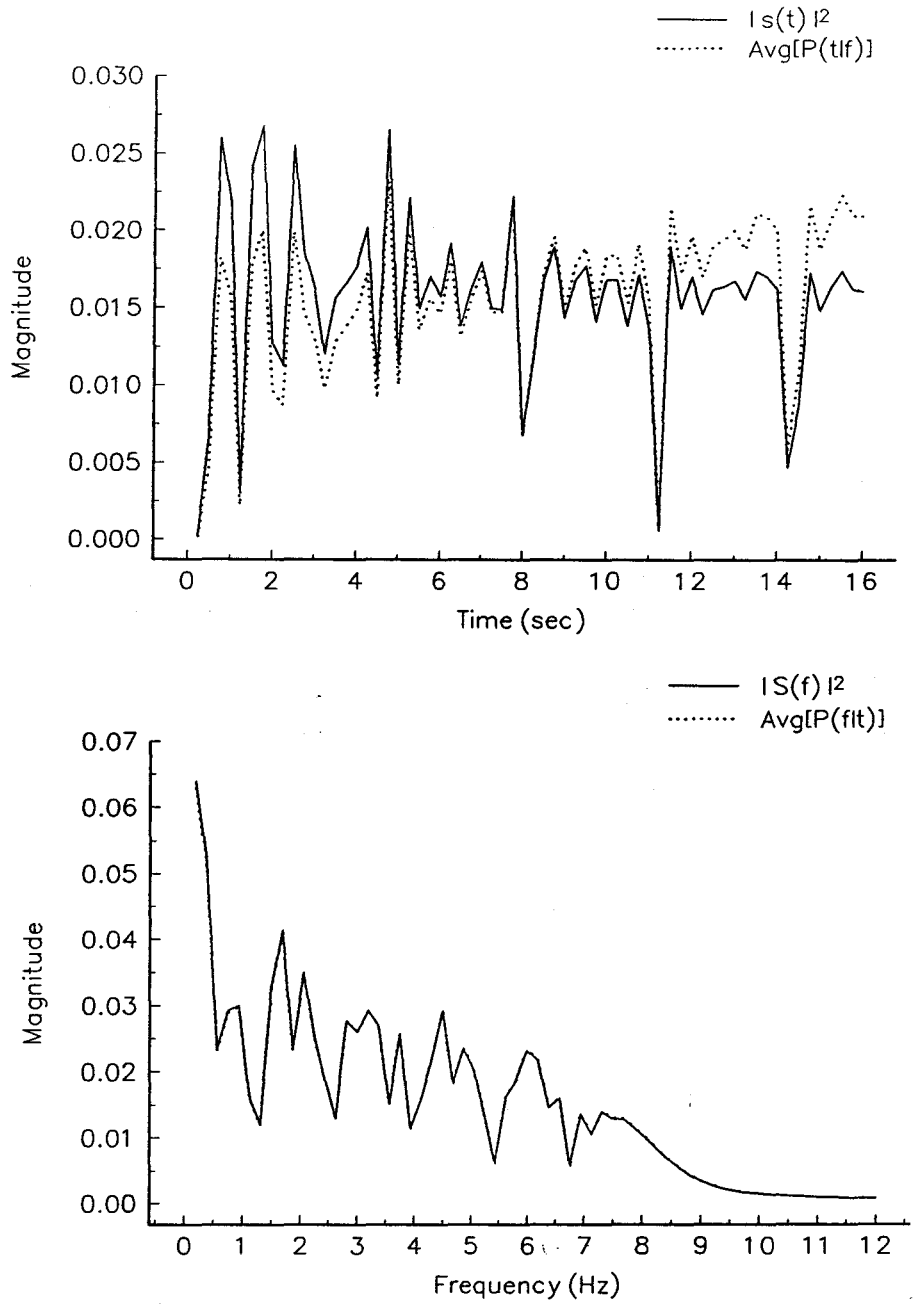

Figure 5.20: *Time and frequency marginal distributions and average of conditional PTFD in each case for TS4.*

Results for φ_1 and $c = 0.9618$. (a) Marginal time distribution and average of time-conditional PTFD. (b) Marginal frequency distribution and frequency- conditional PTFD. PTFD of TS4 is mismatched for time but matched for frequency.

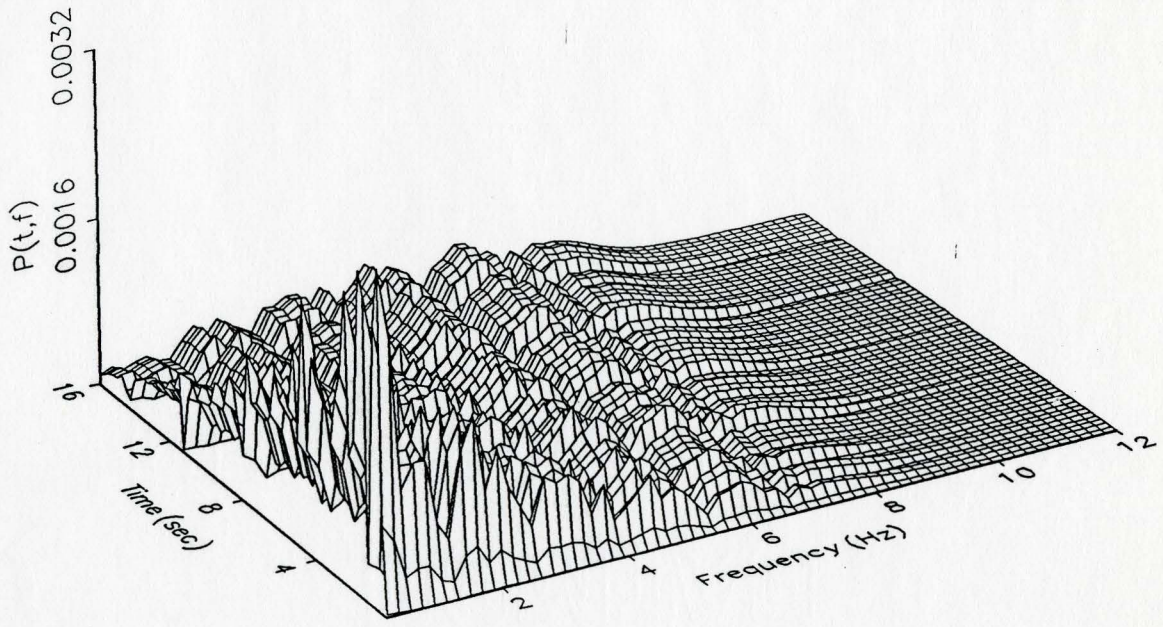

Figure 5.21: *PTFD of TS4 using* φ_1 *and* $c = 0.9618$

The PTFD variations were more important for the range of 0-2Hz and 0-8s because there were two important peaks in the power spectrum for this range.

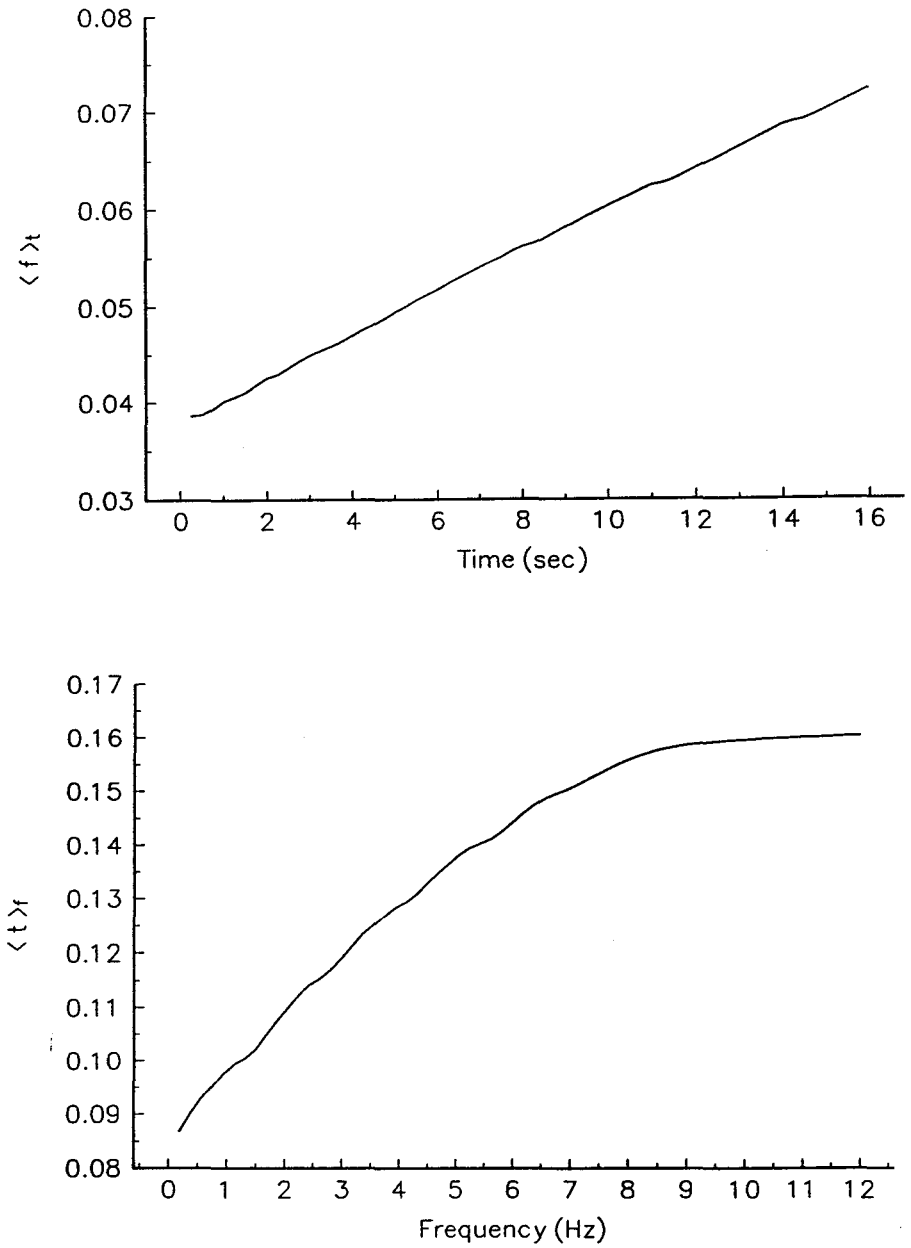

Figure 5.22: $< f >_t$ *and* $< t >_f$ *of TS4 using* φ_1 *and* $c = 0.9618$

First moments of the PTFD in terms of time and frequency. (a) The conditional average frequency for a given time. It is an increasing linear pattern with a small range of variation (b) The conditional average duration for a given frequency. The main range of variations ocurrs below 8Hz.

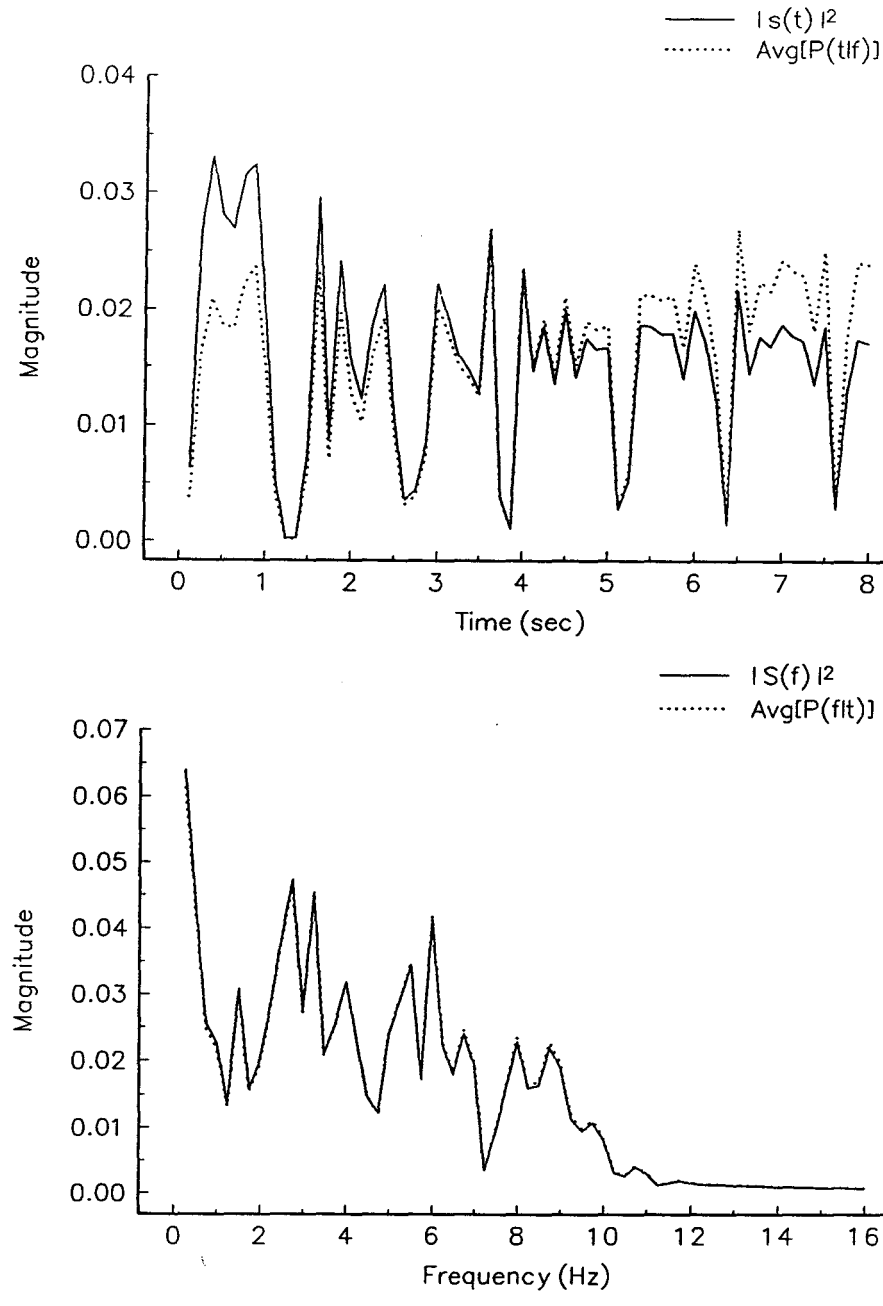

Figure 5.23: *Time and frequency marginal distributions and average of conditional PTFD in each case for TS5.*

Results for φ_1 and $c = 0.9618$. (a) Time marginal distribution and average of time-conditional PTFD. (b) Frequency marginal distribution and average of frequency-conditional PTFD. PTFD varies in amplitude along time due to kernel function influence. However, PTFD is practically like the frequency marginal distribution.

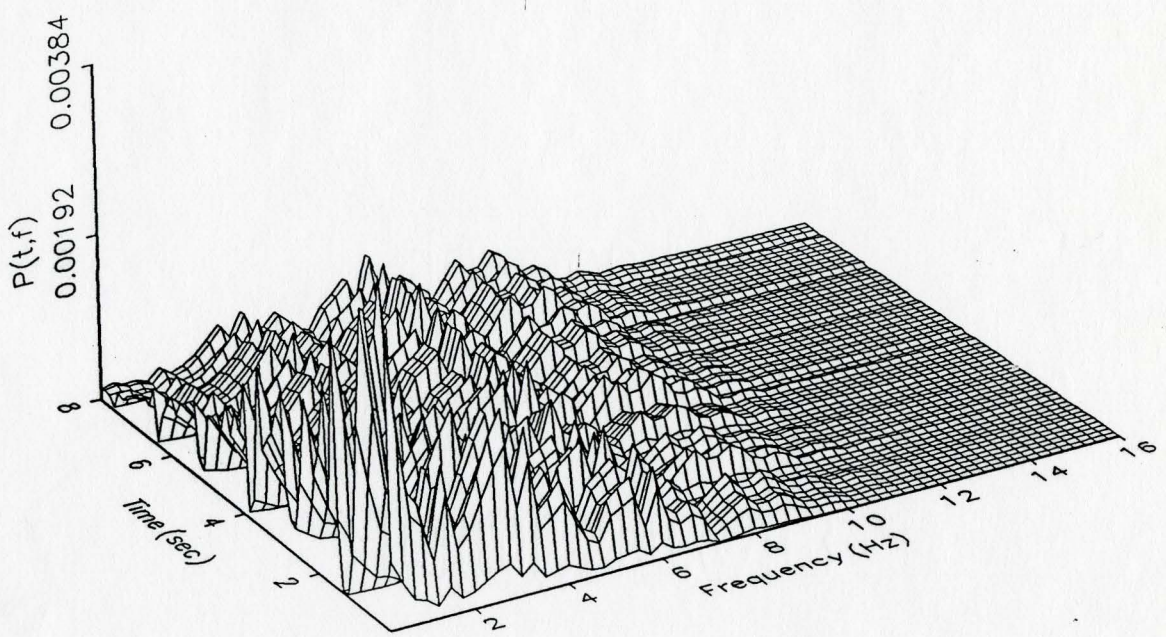

Figure 5.24: *PTFD of TS5 using* φ_1 *and* $c = 0.9618$

The PTFD variations are dominated by the first sector (0-4Hz and 0-4s). Some changes are also seen during the last part of time and between 6 and 10Hz.

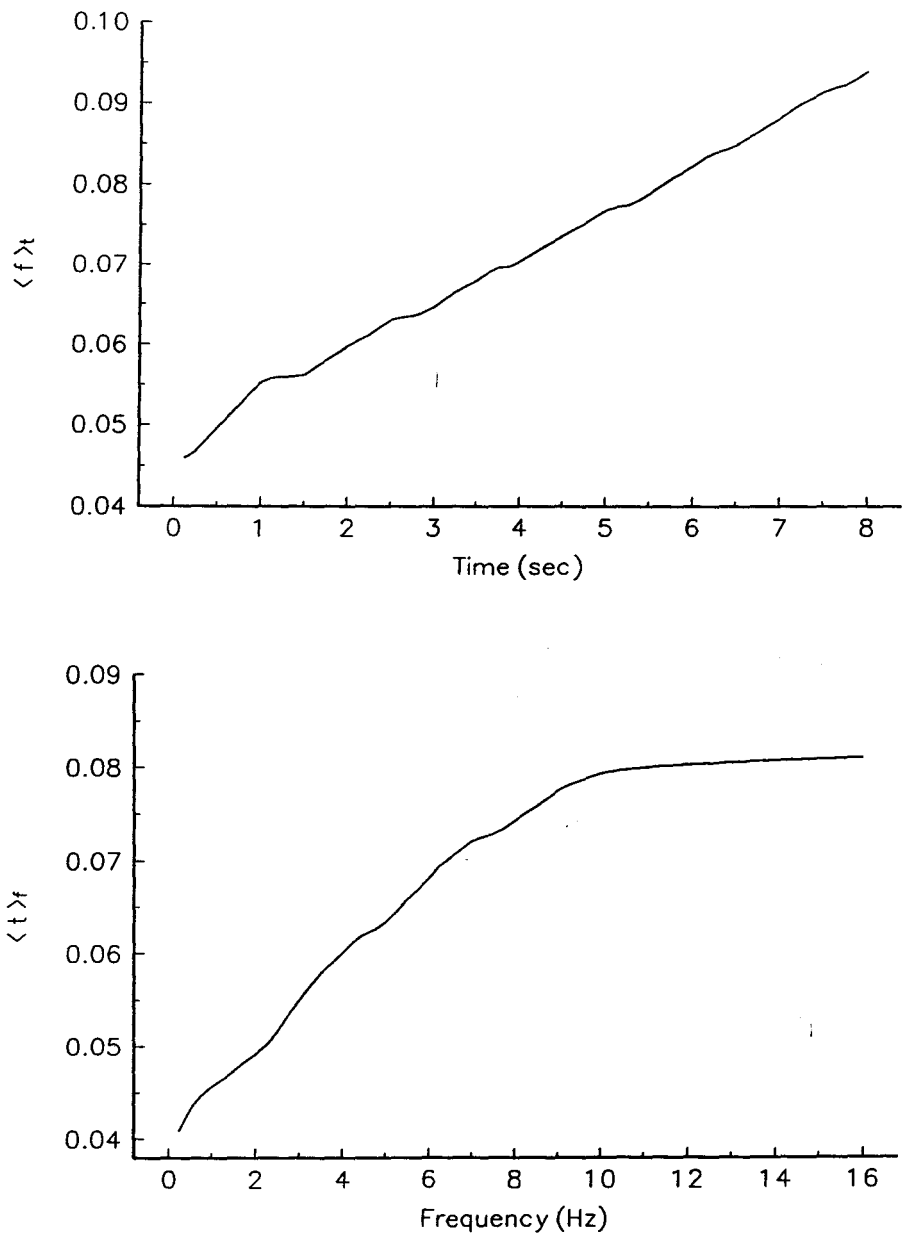

Figure 5.25: $< f >_t$ *and* $< t >_f$ *of TS5 using* φ_1 *and* $c = 0.9618$

First moments of PTFD in terms of time and frequency. (a) The conditional average frequency for a given time. (b) The conditional average duration for a given frequency.

almost a linear increase for frequencies below 11Hz.

5.7 Conclusions

The kernel function played an important role to define a PTFD. It described the relative importance of the correlation between the time and frequency marginal distributions. The mathematical expression of the kernel function can be signal dependent. Therefore, the number of kernel functions that we have to investigate can be very large and specific for each signal. We decided to start with a simple set of three known kernel functions and to calculate the PTFD of six sinusoidal signals. The variations of this group of sinusoidal signals were selected taking into account periodicity, frequency variation in a short interval and with abrupt changes along time and finite or infinite energy. These characteristics were not a complete expression of the main variations of the colonic electrical activity. However, they represented a first approximation to the PTFD analysis of this activity. These characteristics were delimited to a special type of time-varying signals so that we could focus our analysis on the kernel function and PTFD techniques. We used the PTFD as an exploratory technique of the time- frequency variations and we found that the kernel function was an important tool to understand these variations.

For the three kernel functions we found that φ_1 and φ_2 had similar characteristics except the scale was lower in φ_2. φ_1 defined a centre point in the coordinates associated with $x(t)$ and $y(f)$ equals to 50% and it maintained symmetry about this point to be consistent with total energy equal one. However, φ_3 did not satisfy symmetry and for different values of c, total energy could be different from one. We decided that one important criterion to select a kernel function and c-value was to

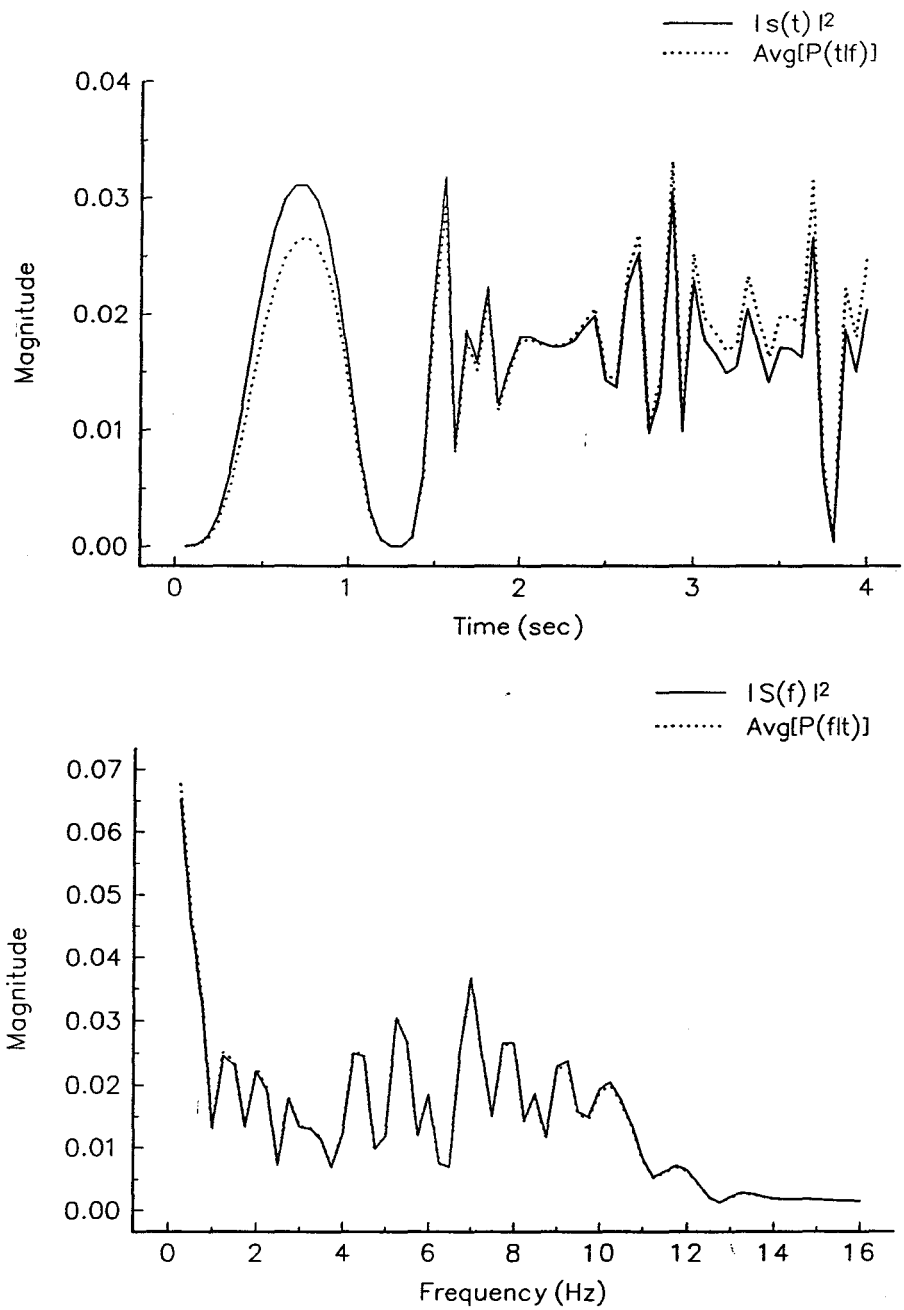

Figure 5.26: *Time and frequency marginal distributions and average of conditional PTFD in each case for TS6.*

Results for φ_1 and $c = 1.0$. (a) Time marginal distribution and average of time-conditional PTFD. (b) Frequency marginal distribution and average of frequency-conditional PTFD.

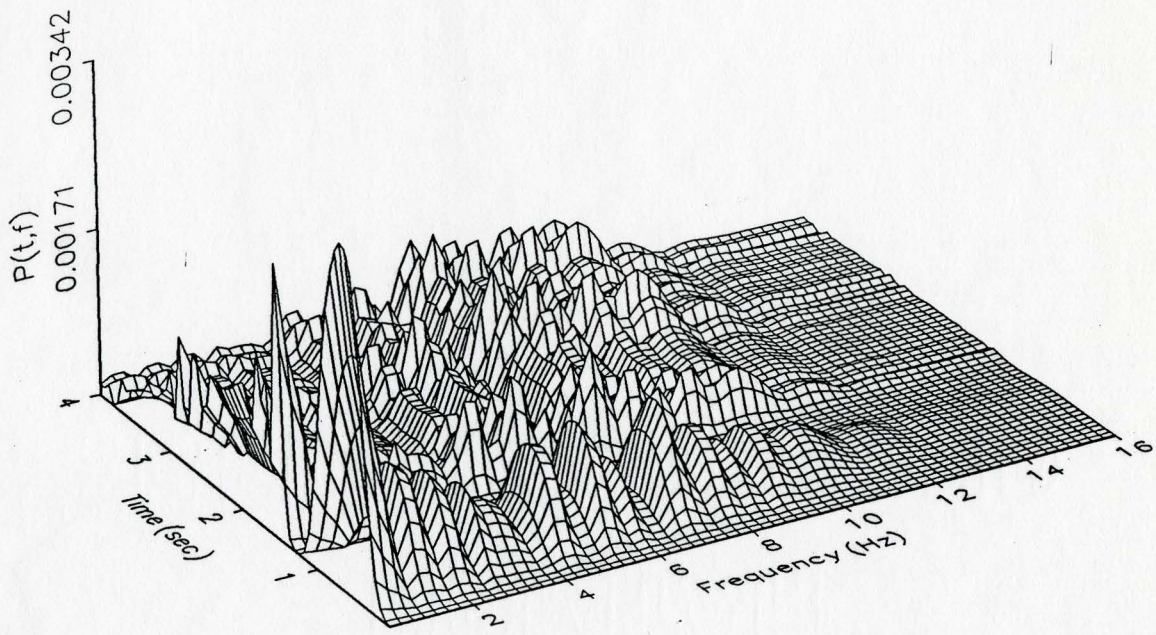

Figure 5.27: *PTFD of TS6 using* φ_1 *and* $c = 1.0$

PTFD variations are dominated by the first section (0-2Hz and 0- 4s). The variations of frequencies between 6 and 12Hz are mainly in the last section of time.

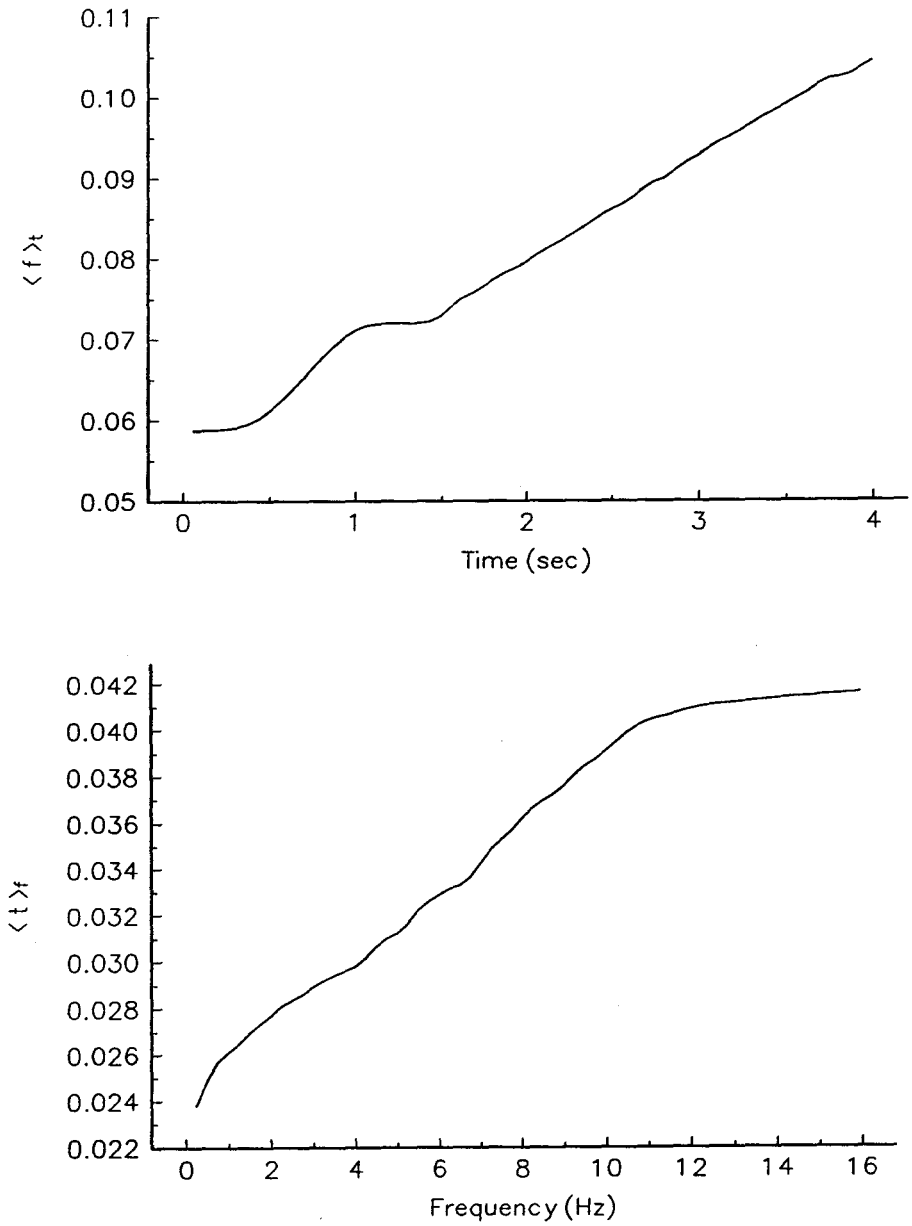

Figure 5.28: $< f >_t$ *and* $< t >_f$ *of TS6 using* φ_1 *and* $c = 1.0$

(a) The conditional average frequency for a given time shows complex variations in the first 1.5s and a linear increase during the last part. (b) The conditional average duration for a given frequency shows almost linear variations over the first 11Hz.

maintain total energy equal one, in order to be consistent with our interpretation of the PTFD between different signals.

In a practical setting, we do not know the characteristics of the PTFD associated with any particular signal. However, we can impose a set of constraints that the conditional PTFD in time and also in frequency must satisfy to decide which kernel function is appropriate for a signal. The uncertainty coefficient was another constraint that we applied to determine which kernel function and c-value can be used for calculating the PTFD of a sinusoidal signal. We found that those constraints were useful to select a kernel function and associated constant value for each sinusoidal signal.

In general, the kernel function φ_1 was useful to calculate the PTFD of a sinusoidal signal. The constant c-value varied, but in general always corresponded to the maximum value associated with the kernel function. φ_2 was always a conservative estimation of the PTFD (it had a stable uncertainty coefficient for different c-values). φ_3 showed more variability for its uncertainty coefficients and it was consistent only for the first sinusoidal signal. In particular, we found that a large deviation from the total energy equal to one was associated with large variations in the uncertainty coefficient. The uncertainty coefficient was an important criteria to select a c-value for the kernel function. The importance of the c-value was to amplify or reduce the influence of the kernel function over the product of both time and frequency marginal distributions. This value did not alter the interaction between time and frequency components.

PTFD analysis gave us the possibility to use same reference template (kernel function) to compare time-frequency variations between two or more different signals. Total energy equal one is an important concept to maintain in order to compare different signals. The product of marginal distributions satisfies the total energy equal one

criterion but it does not give us any information about the interaction between time and frequency components. The kernel function does carry this information. This statement implies that each signal is associated with a kernel function. Therefore, it is a difficult issue to find a specific kernel function. We proposed to use a simple kernel function as template and applied it to different signals. The PTFD of similar signals would be similar in some aspects. The kernel function defined a partition of the time- frequency plane, each section being associated with the same weights or absolute values depending on the interaction between the cumulative time and frequency marginal distributions. For example, the localization and size of sections where the interaction between time and frequency was practically nil can be compared among different signals. These sections were almost equivalent to the marginal product and delimited by the points where $x(t)$ and $y(f)$ reached 50% of the marginal distribution. The partition defined by the kernel function specified which sections can be contrasted among several signals.

We can establish comparisons between time-frequency variations of two different signals. TS1 and TS2 were completely different from the rest of the set of sinusoidal signals. The φ_1 function and PTFD were different between them and with respect to the other signals. The PTFD pattern in TS1 was completely characterized with φ_1 or φ_3 for c-values near to zero because the correlation information was practically nil. The time-frequency variations of TS2 were delimited to a short section due to signal characteristics: frequency decreased to zero (finite energy). The PTFD analysis of this signal was realized using φ_1 with a negative c-value quite close to zero. When the signal did not have finite energy, the c-value was close to one. The last concept was consistent with the PTFD results of TS3, TS4, TS5 and TS6 which were not finite energy signals. For all of them, the c-value was almost close to one.

The PTFD of TS3 showed that the main frequency components of the power spectrum matched with the contour plot section with the smallest variation; therefore, the importance of this section dominated the 3D plot. However, in the PTFD of TS4, TS5 and TS6 the main frequency components of their power spectrum fell outside the smallest variation section of their contour plot; then, the importance of this section was diminished by main frequency components with large weights.

PTFD techniques cannot track exactly frequency along time, it can give us an approximation to the frequency variations along time in order to compare between different signals. Because the kernel function is signal dependent, the PTFD can be used to explore which characteristics a kernel function must satisfy to analyze time-frequency variations in a specific signal. The potential application of PTFD to colonic signals is to compare time-frequency variations of the same signal for different experimental conditions like pre and postpandrial periods, under medication or pre and post-therapy. The possibility of using the same kernel function to establish comparisons among signals recorded in different sections of the human colon provides elements to investigate how those sections can be related. The results of this chapter were useful to determine a specific criterion which can be employed to analyze electrical activity recorded in the human colon.

Chapter 6

An analysis of the human colonic electrical activity using Positive Time-Frequency distribution techniques

6.1 Abstract

The human colonic electrical activity is a time-varying frequency process whose analysis requires the consideration of how the main frequency components change along time. An application of positive time-frequency distribution (PTFD) is described for analyzing the time-varying frequency components of the human colonic electrical activity. The kernel function is an important aspect of the PTFD. Three known kernel functions were applied and one of them was selected by using criteria based on the

uncertainty coefficient, marginal conditions and conditional PTFD given time or frequency. Three different segments of one signal recorded under different experimental conditions and frequency characteristics were analyzed. The PTFD analysis of each segment was realized using a low resolution lattice in time and frequency. The PTFD technique showed variations of main frequency components and changes in time-frequency patterns for different segments. Moreover, the PTFD analysis revealed some insights about the time-varying components of the human colonic electrical activity: the relative importance of the band of frequency 0-10 cpm was greater in some periods of time than the rest of the signal. As well a meal induced changes in the relative importance of frequencies below 10 cpm and in the band of 30-40 cpm.

6.2 Introduction

The electrical activity generated in the gastrointestinal smooth muscle cells is an important mechanism to control the spatial and temporal organization of contractions throughout the gastrointestinal tract. The recording of the electrical activity of the human colon is important to analyze who muscular contractions are initiated, controlled and propagated [28]. The diverse motor functions of the human colon are controlled by individual phasic contractions (short and long duration), organized groups of contractions (migrating and nonmigrating motor complexes) and ultrapropulsive contractions. The colon generates long duration contractions as the luminal contents become more viscous and may require stronger and longer duration contractions to mix and propel them. The slower propulsion rate in the colon is achieved largely by contractions that are highly uncoordinated in time and space. This lack of coordination is due to the highly irregular frequency patterns of electrical activity in the colon

[29]. Due to the dynamical behaviour of different influences (i.e. neural and hormonal stimuli), the colonic electrical activity apparently changes during a recording session [21]. The analysis of this pattern variability plays an important role in establishing a colonic activity profile. For some time, Fourier analysis has been used to describe the frequency components of this activity [30, 31]. The short-duration contractions are controlled by the omnipresent control activity with frequency range from 2 to 13 cpm. The long duration contractions are mainly controlled by intermittent burst of membrane potential oscillations whose frequency varies from 25 to 40 cpm. Sometimes, the individual contractions associated with each oscillation can be superimposed on the long duration contractions creating a complex oscillatory pattern. The complexity of muscular contractions as well as irregular oscillatory patterns of the electrical activity of the human colon have motivated the use of different analysis methods. Some of them correspond to time-frequency distribution techniques (TFD) like the spectrogram [14]. The basic idea of using TFD techniques is to analyze the frequency variations of the human colonic electrical activity over time.

The time-frequency analysis can be improved if a TFD is interpreted as an energy distribution. A TFD must be positive to obtain an energy distribution [23]. Cohen et.al. developed a model and properties of the positive time-frequency distributions (PTFD) that can be used in signal processing [22]. Because the PTFD describes the intensity per unit time and unit frequency that corresponds to each elementary cell, we decided to use this technique in the analysis of the human colonic electrical activity. The definition of a PTFD for any particular signal depends on a kernel function which describes main interactions in time and frequency. The set of kernel functions associated with a PTFD could be large and implicitly related to the original signal. We applied three known kernel functions [22] for analyzing the human

colonic electrical activity and one of them was selected by using criteria based on the uncertainty coefficient, marginal conditions and conditional time-frequency distributions. The main objective of this work was to show that the PTFD techniques can be used to compare the time-varying phenomena of the human colonic electrical activity under three different experimental conditions, before, during and after intake of a meal in one subject.

This chapter is organized as follows. In section 3, after a description of the experimental conditions, a brief review of PTFD and kernel functions is presented. The numerical results of PTFD for three different segments are examined and compared in section 4. Finally, section 5 is dedicated to identifying important aspects of applying PTFD techniques to the human colonic electrical activity.

6.3 Materials and Methods

6.3.1 Experimental method

Human colonic electrical activity was recorded from serosally implanted electrodes (temporary bipolar electrodes sutured to the transverse colon). The recordings were made on an 8-channel Beckman recorder (Beckman Instruments, Inc., Fullerton,Calif.) with the lower and upper cut-off frequencies at 0.16 and 30 Hz respectively and through it on an 8-channel Hewlett-Packard FM tape recorder (model 3968A). The FM recordings were later played back into a computer through an 8-channel AD converter by using CODAS (Dataq Instruments, Inc.) package software. The signal was first sampled at 200 samples/sec, then decimated (low pass filter and reducing sampling frequency) by using a MATLAB (The Mathworks, Inc.) function. The cutoff

frequency was set at 5 Hz and the final sampling frequency at 12.5 Hz. Three different sections (pre-, inter- and postprandial) from a continuous recording were selected. The discrete signal that corresponds to each section after decimation is represented by 2048 data points and lasts approximately 375s. These segments were selected mainly because they visually presented dissimilarities, so that comparative analysis could be done.

6.3.2 Positive time-frequency distribution technique

Each segment was analyzed using the positive time-frequency distribution technique (PTFD) to describe and to characterize its frequency fluctuations over time. PTFD indicates what fraction of the total energy or intensity corresponds to each frequency at any one time. A complete description of this method is presented in chapter 5. Therefore, only a brief summary of the method is given here.

A PTFD for any signal $s(t)$ is defined [9] by the following expression

$$P(t,f) = |s(t)|^2 \cdot |S(f)|^2\{1 + c \cdot \varphi(x(t), y(f))\}, \tag{6.1}$$

where $S(f)$ is the Fourier Transform

$$S(f) = \int s(t)e^{-j2\pi ft}dt,$$

$\varphi(x,y)$ is the kernel function associated with the PTFD and whose arguments $x(t)$ and $y(f)$ are the cumulative marginal distributions of time and frequency respectively. c is a numerical constant which must be in the range of the minimum and maximum value of $\varphi(x,y)$. The discrete representation of PTFD may be given by the following expression

$$P(t_k, f_n) \approx |s_k|^2 \cdot |S_n|^2\{1 + c \cdot \varphi(x_k, y_n)\}, \tag{6.2}$$

where s_k and x_k are discrete variables in time, as are S_n and y_n in frequency.

The PTFD must satisfy a set of conditions such that the total energy of the distribution should be the total energy of the signal, i.e.

$$E = \int P(t,f)dtdf = 1.$$

This implies the marginal conditions

$$\int P(t,f)dt = |S(f)|^2 \qquad \text{and} \qquad \int P(t,f)df = |s(t)|^2.$$

The description of any PTFD is determined both by the product of the marginal distributions and the kernel function with its c- value. When the PTFD represents a correlationless case the c- value is close to zero and the description only depends on the marginal product; otherwise, the kernel function plays an important role. The establishment of this role must be consistent with marginal constraints and additional conditions such as the uncertainty coefficient and the average of conditional PTFD in time ($P(f|t)$) or conditional PTFD in frequency ($P(t|f)$). A measure of the association between time and frequency is the uncertainty coefficient [32, 38] and it can be calculated in terms of the entropy as follows

$$U(t,f) = 2\left(\frac{H(t) + H(f) - H(t,f)}{H(t) + H(f)}\right). \tag{6.3}$$

where $H(t)$ and $H(f)$ are the entropy of the marginal time and frequency distributions respectively, and $H(t,f)$ the entropy of the joint PTFD. U is zero if time and frequency are completely independent ($H(t,f) = H(t) + H(f)$). U equals unity if time and frequency are completely dependent ($H(t,f) = H(t) = H(f)$). We have a lower bound of the uncertainty coefficient calculated from the marginal product ($\Gamma(t,f) = |S(f)|^2 \cdot |s(t)|^2$). We expect to improve this value and always satisfy the

marginal conditions. We will select the kernel function and c-value that satisfy both conditions: improve lower bound of $U(t,f)$ and satisfy marginal conditions. The additional restriction in terms of the conditional time- frequency distribution is that the average value of $P(f|t)$ for all values of t should be proportional to the power spectrum $|S(f)|^2$ of the signal for each value of f. Also, the average value of $P(t|f)$ for all values of t should be proportional to the signal power $|s(t)|^2$. These restrictions are important in order to determine if a kernel function can be used to estimate the PTFD of any particular signal. They can also be used to determine the constant value associated with the kernel function.

The following three φ functions [9] were used to analyze each segment

$$\varphi_1(x,y) = (2\cdot x - 1)(2\cdot y - 1), \tag{6.4}$$

whose constant value is given by $-1 \leq c \leq 1$;

$$\varphi_2(x,y) = \frac{6}{7}(2xy - x - y + \frac{1}{2}), \tag{6.5}$$

with constant value expressed by $\frac{-7}{2} \leq c \leq \frac{7}{4}$ and

$$\varphi_3(x,y) = \frac{2}{\pi}\cdot(1 - \sqrt{1-x^2} - \sqrt{1-y^2}), \tag{6.6}$$

whose constant value is $\frac{-\pi}{2} \leq c \leq \frac{\pi}{2}$.

The PTFD analysis of each experimental signal was displayed as follows: the marginal distribution with respect to time and frequency, the contour plot of the kernel function that satisfied the criteria and a 3D plot of the PTFD. A detailed analysis for a selected interval in time and frequency domain was also presented. Variations over time of the intensity of the signal for each band of frequency were obtained. The PTFD was calculated using the whole segment in time, and frequency

range between 0 and 70 cpm. The resolution in frequency for this computation was 1 cpm. For the comparison of relative importance of each band of frequency, the intensity levels were accumulated for each lattice and expressed in percentages with respect to the whole distribution.

6.4 Experimental results and discussion.

The experimental signal ES1 was a sample of the electrical activity recorded during the preprandial period (Figure 6.1). The amplitude varied along the whole segment with some slow oscillations which were clearly seen in the first and last minute. Several spikes were presented along the complete segment, some of them with high amplitude. There were two predominant bursts during the fourth and fifth minute. The electrical activity recorded during the ingestion process or ES2 presented variations in amplitude as well as in frequency over the recording time. The activity during the first minute looked completely dissimilar from the rest. The amplitude was small with some oscillations at the beginning. There was then an abrupt change where the activity was characterized by high amplitude with a range of frequencies. The signal presented several bursts of different duration and amplitude. For example, one burst lasted approximately 33 s with superimposed oscillations of 2.1 s or bursts of 5.5 s which include events of 0.8 s. The electrical activity registered during the postprandial period or ES3 showed very small amplitude except in some short intervals where the signal displayed spikes of high amplitude. The pattern of this segment was completely different from other segments (ES1 and ES2). The signal presented slow waves with durations 11, 17 and 20 s and high frequencies with small amplitude. Four spikes with high amplitude were present in this signal. After the second largest

spike, there were slow waves that lasted approximately 12 seconds and they included short spikes.

6.4.1 The main components for calculating the PTFD.

The description of ES1 in time and frequency domains respectively (figure 6.2) showed variations in amplitude and a broad frequency range. The marginal distribution in time was dominated by oscillations whose square value of amplitude was less than 0.002 units. These oscillations represented a small variation in the cumulative power signal distribution $x(t)$. The presence of bursts at 4 and 5 minutes determined large changes in the cumulative power signal distribution. The power signal reached 50% of the total power before t=4 min. The remaining component of the total power was over a relatively short time segment. The maximum amplitude of the power spectrum was obtained around 36 cpm and its effect can just be seen in the cumulative frequency distribution. The 50% of the total power spectrum was reached before f=90 cpm.

The description of ES2 in time and frequency domains respectively (figure 6.3) displayed its activity in terms of signal amplitude and history over time, as well as its frequency content. The marginal distribution in time showed that 40% of total power was present during the first half of the signal. The power spectrum showed the strongest peak around 33 cpm, the amplitude then decreased slowly except around 75 cpm.

The marginal description of ES3 in time and frequency domains respectively (figure 6.4) was completely dominated by the highest activity (largest amplitude and short duration). In this case, the cumulative power distribution in time showed that 50% of total power was present during the first half of the signal. The presence of the

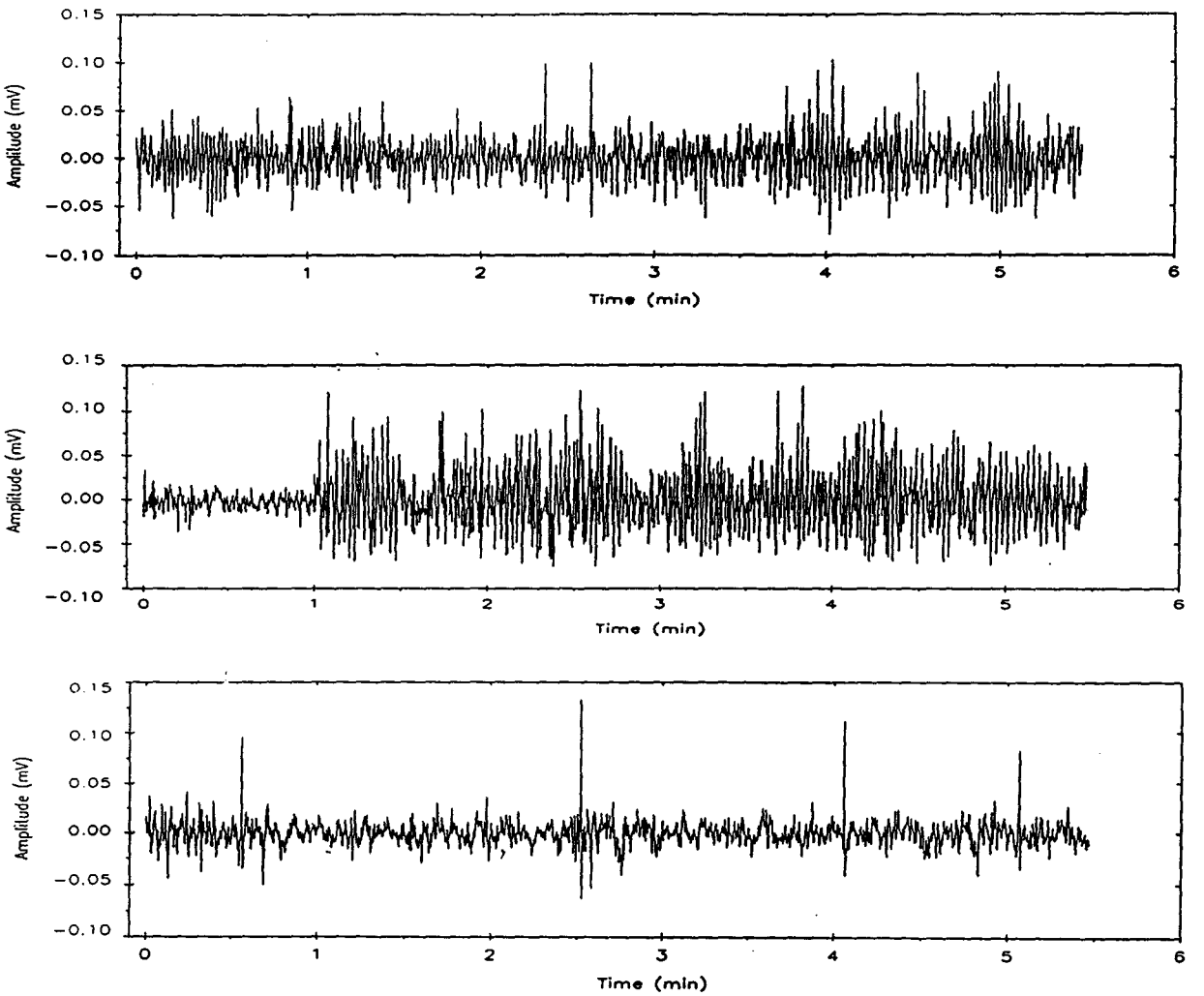

Figure 6.1: *Short recording segments of the human colonic electrical activity.*
The human colonic electrical activity recorded during three different experimental conditions: (a) prepandrial period or ES1, (b) food intake or ES2, and (c) postpandrial period or ES3. The three tracings corresponded to the same electrode position on the same subject.

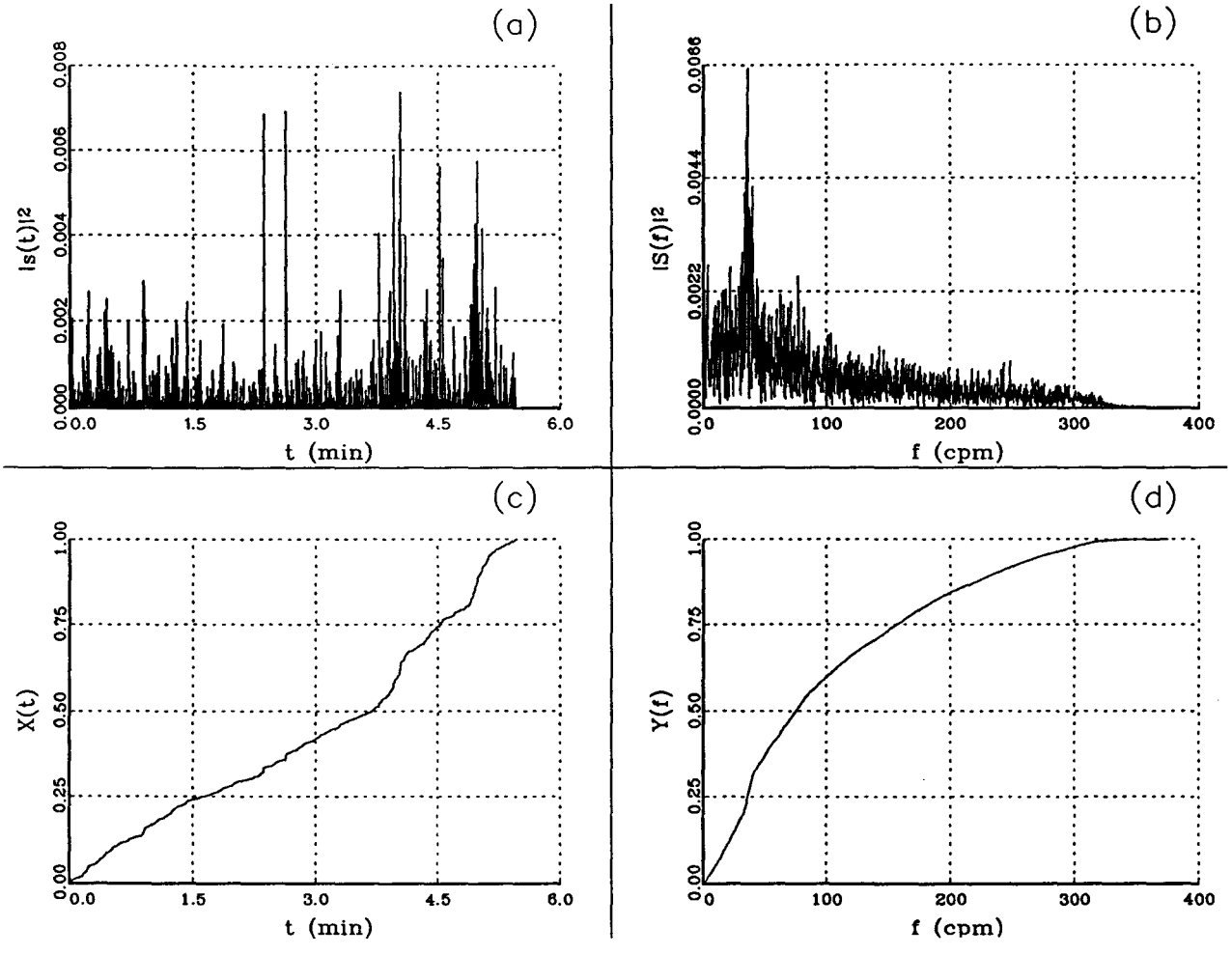

Figure 6.2: *The main components for calculating the PTFD of ES1*

(a) The largest spikes can be easily seen, during the first half the events were relatively smaller than in the second part. (b) The most important frequency component of the power spectrum was around 36 cpm. (c) The cumulative distribution of the signal power with respect to time presented a clear change in its pattern due to spikes with large amplitude. (d) The cumulative distribution of the spectral energy with respect to frequency exhibited a variation in pattern before the main frequency.

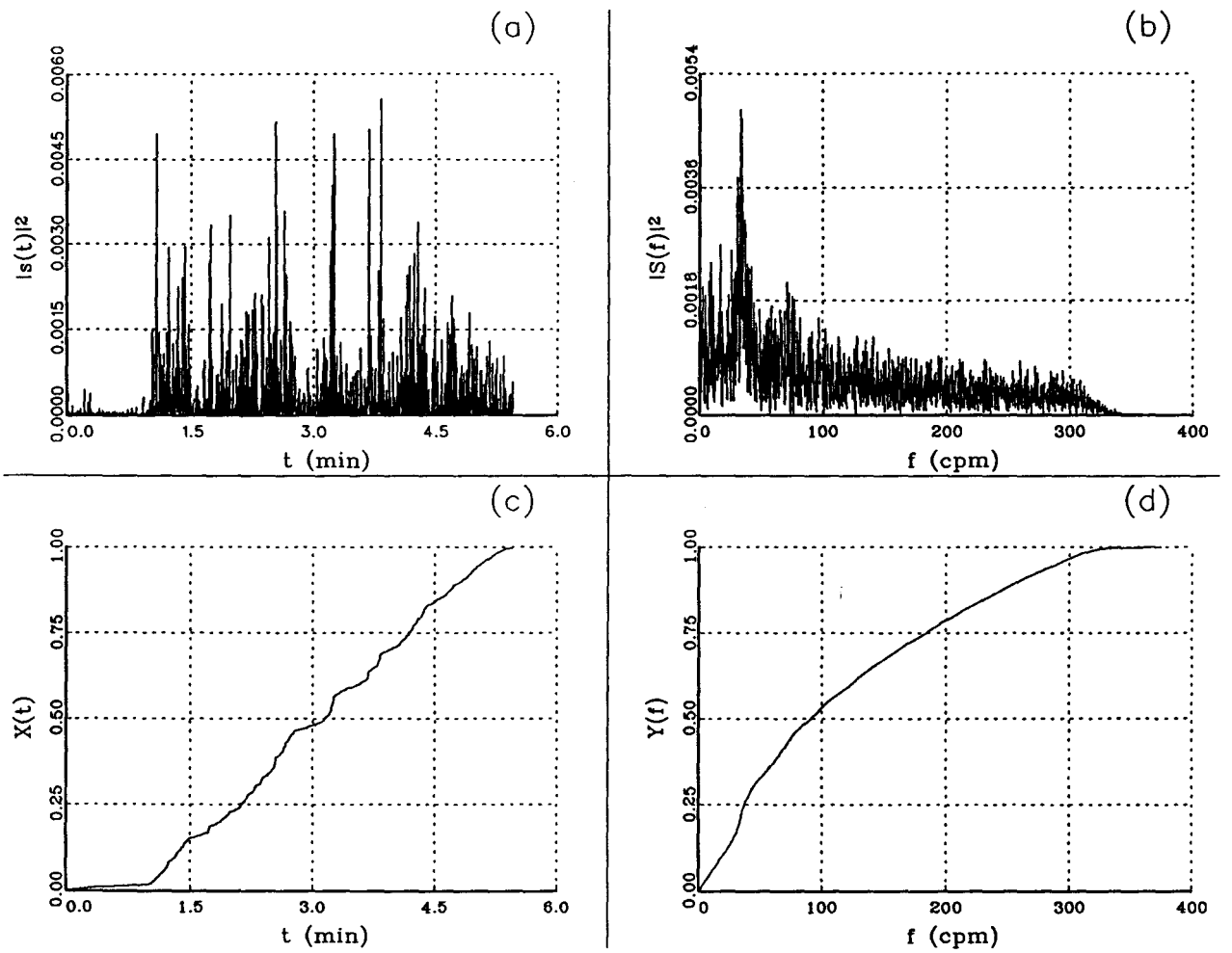

Figure 6.3: *The main components for calculating the PTFD of ES2*

(a) The signal power showed differences in amplitude. The events during the first minute were relatively smaller than for the remainder; some spikes with high amplitude could be seen. (b) The power spectrum showed important frequency components around 30, 33 and 35 cpm with another peak around 75 cpm. (c) The pattern of the cumulative distribution with respect to time presented a parallel line to the t-axis indicating a null activity; after that it increased linearly with some small variations. (d) The cumulative distribution with respect to frequency exhibited a variation in pattern before the main frequency.

Table 6.1: Entropy and uncertainty coefficients of each experimental signal by marginal product and PTFD using a φ function.

	$\Gamma(t,f)$		$P(t,f)$		
Signal	$H(t,f)$	$U(t,f)$	$\varphi - function$	$H(t,f)$	$U(t,f)$
ES1	7.7219	0.0002	φ_1	7.6712	0.0133
ES2	7.7688	0.0002	φ_1	7.7224	0.012
ES3	7.5307	0.0003	φ_1	7.454	0.0207

highest peak before the end of the half part resulted in the big step in the cumulative power distribution. The other steps can also be attributed to large spikes. The power spectrum showed the strong frequency component at 5.6 cpm, the amplitude then decreased until end of the frequency interval. The pattern of the cumulative power distribution was always increasing with small variations.

6.4.2 Kernel functions

The kernel function φ_1 improved the uncertainty coefficient and satisfied the marginal conditions in all experimental signals (Table 6.1). The constant value was $c = 1$ for both ES1 and ES2 and $c = -1$ for ES3. The kernel function allocated a weight to the time-frequency matrix cell using both time and frequency cumulative distributions.

To compare the three electrical signals in terms of the time- frequency variations, the contour plots of those signals using φ_1 were presented. The centre point of the entire plot for ES1 (Figure 6.5) was located around 75 cpm and 3.6 min. This defines where the PTFD was equivalent to the product of the individual marginal

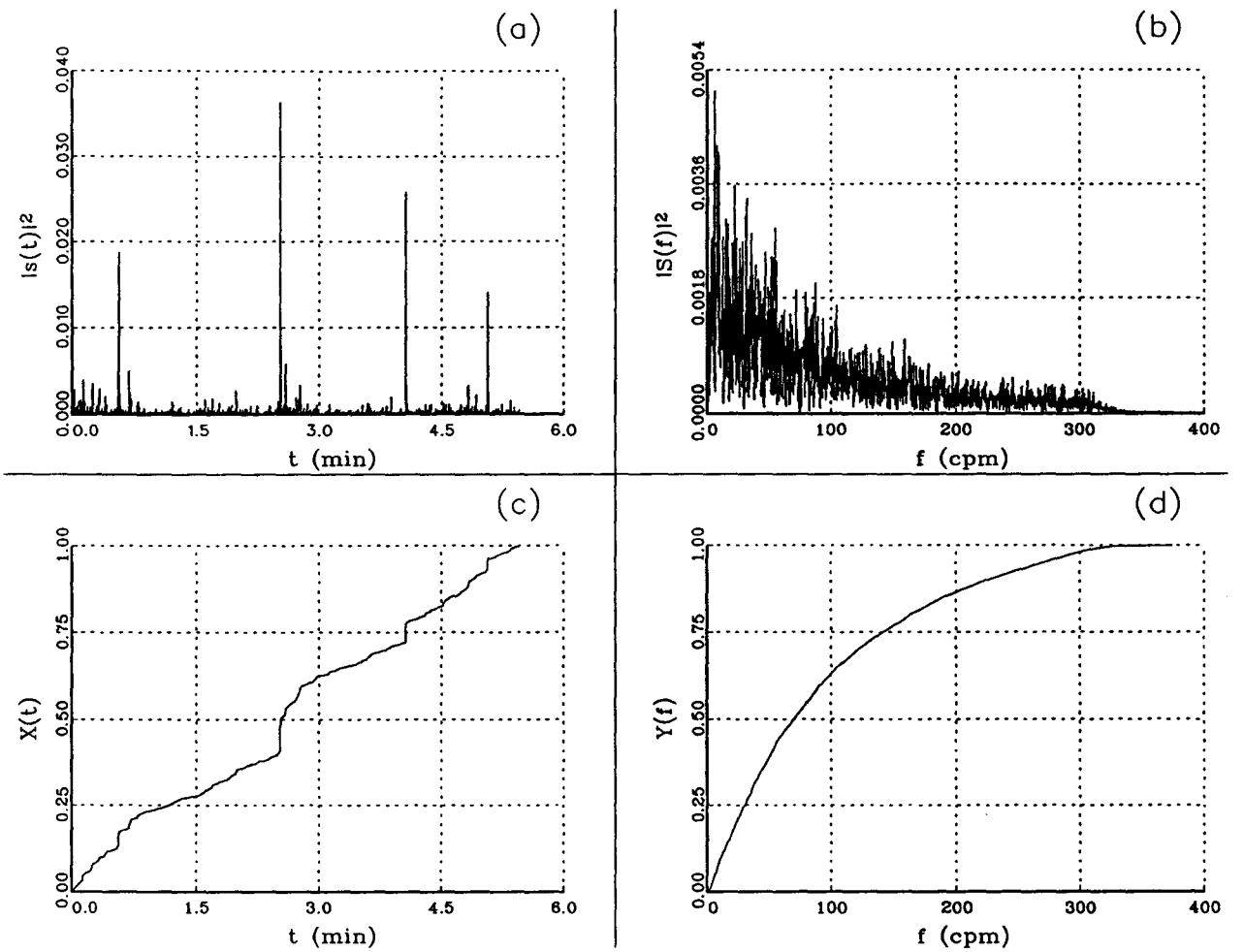

Figure 6.4: *The main components for calculating the PTFD of ES3*

(a) The signal power displayed a large difference in amplitude for the highest peaks with respect to the background activity. (b) The power spectrum did not exhibit dominant frequency components. (c) The pattern of the cumulative distribution of the signal power with respect to time showed abrupt steps corresponding to the large spikes. (d) The cumulative distribution of the spectral energy with respect to frequency exhibited a smooth shape along the whole frequency.

distributions. It was then located a section around this point showing very weak time-frequency interaction. The contour lines outside this area with positive and negative values represented the main time-frequency interactions especially below 75 cpm. The geometric pattern of φ_1 for ES2 (Figure 6.6) presented a section with small values along frequency 90 cpm and time 3.2 min. This was the characteristic section of φ_1 where the PTFD was almost equivalent to the marginal product. The contour lines with positive and negative values outside this range described the main time-frequency interactions especially below 90 cpm. The geometric pattern of thess lines were quite uniform in some frequencies along the first minute. The section with small variation in ES3 (Figure 6.7) was comparatively shorter than in ES2. This section was located around 70 cpm and 2.5 min. The contour lines outside this range indicated the main time-frequency changes. The kernel function always determined the time-frequency variations in the same way, but the difference was given by the geometric pattern of contour lines.

6.4.3 PTFD analysis of experimental signals

The PTFD analysis of ES1 showed an energy distribution pattern (Figure 6.8) with clear predominance of frequencies below 75 cpm. The maximum energy level was 4.24E-3 intensity units (using a scale between 0 and 1). The PTFD analysis of ES2 displayed an energy distribution pattern (Figure 6.9) with clear predominance of frequencies below 70 cpm. The maximum energy level was 3.56E-3 intensity units during the fourth minute and band of frequency 30-40 cpm. The PTFD analysis of ES3 displayed an energy distribution pattern (Figure 6.10) with predominance of frequencies below 120 cpm. The maximum energy during the first minute was

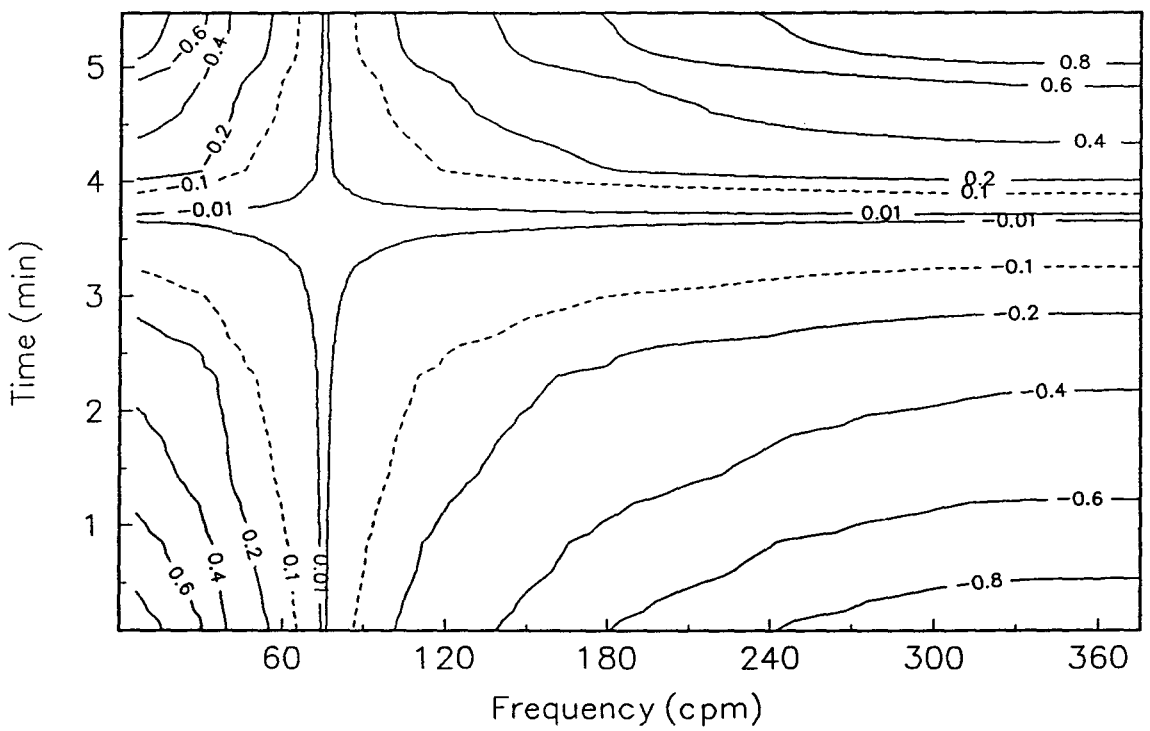

Figure 6.5: *Contour level plot of φ_1 for ES1.*

Different contour levels were represented in the frequency band below 75 cpm during total time interval. The low levels were in a section around 75 cpm and 3.75 min.

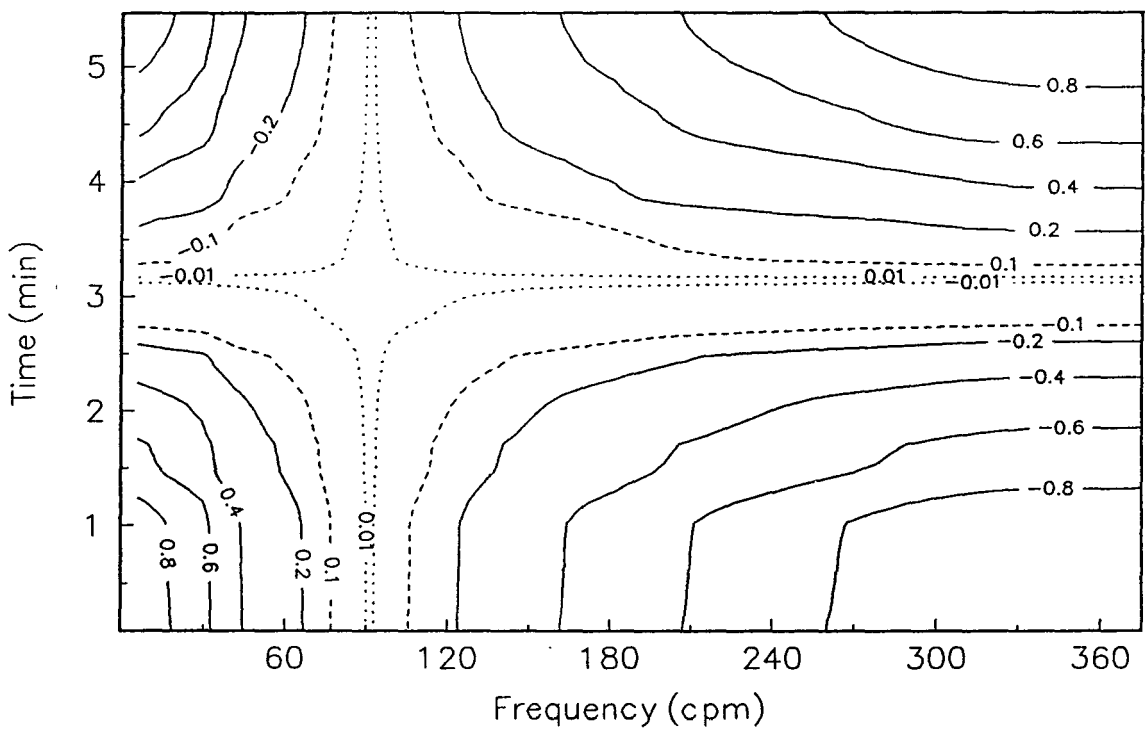

Figure 6.6: *Contour level plot of φ_1 for ES2.*

Different contour levels were represented in the frequency band below 100 cpm during total time interval. The low levels were in a section around 100 cpm and 3.2 min.

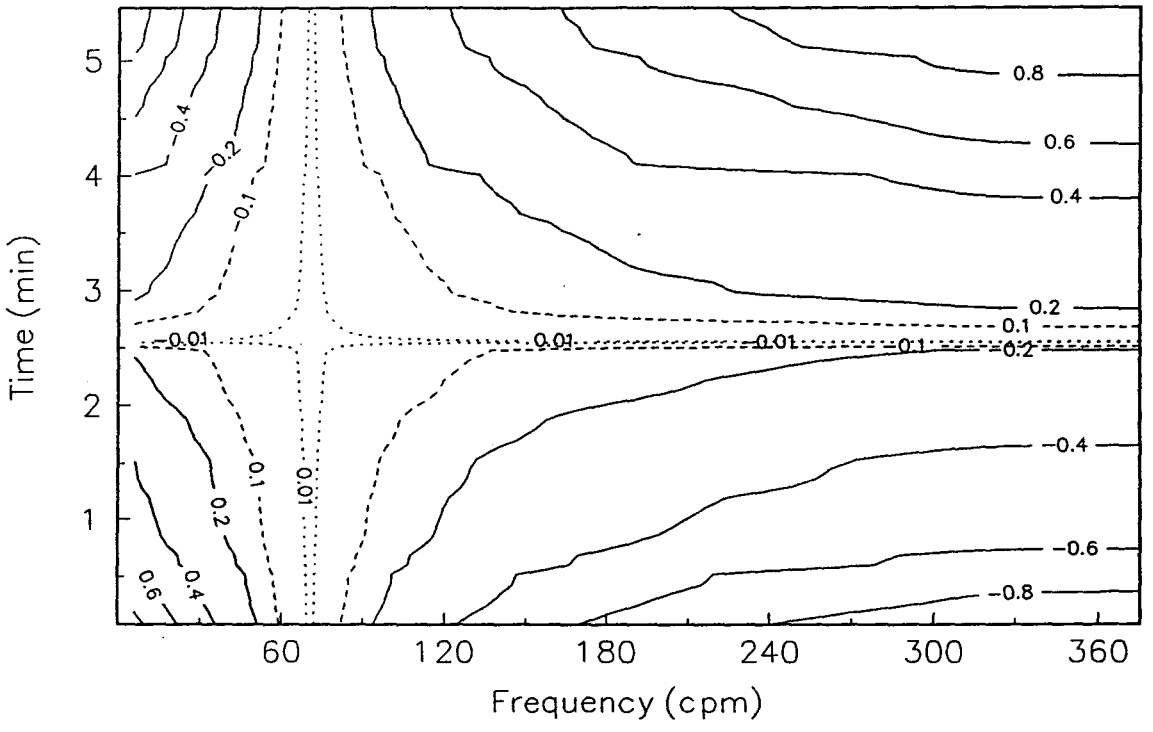

Figure 6.7: *Contour level plot of φ_1 for ES3.*

Section with small influence in the marginal product was delimited around 70 cpm and 2.5 min. This section was comparatively shorter than in ES1 and ES2.

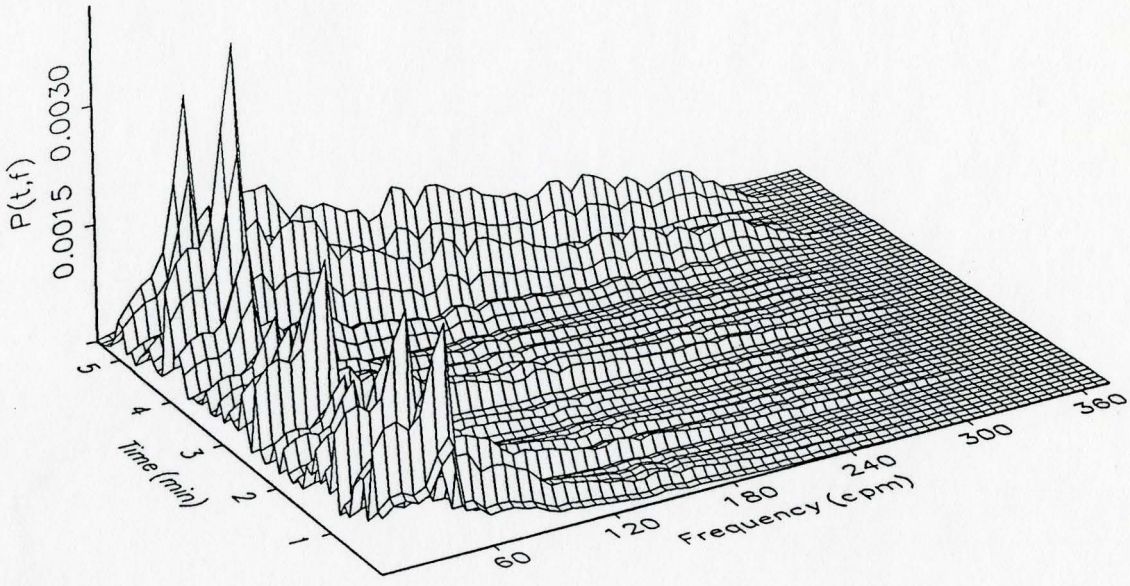

Figure 6.8: *PTFD analysis of ES1 using the whole segment in time and frequency range between 0 and 360 cpm.*

Lattice with an increment in time and frequency of 2.5 s and 3 cpm respectively. The most dominant frequencies are below 120 cpm with a relative shift to higher frequencies after the fourth minute.

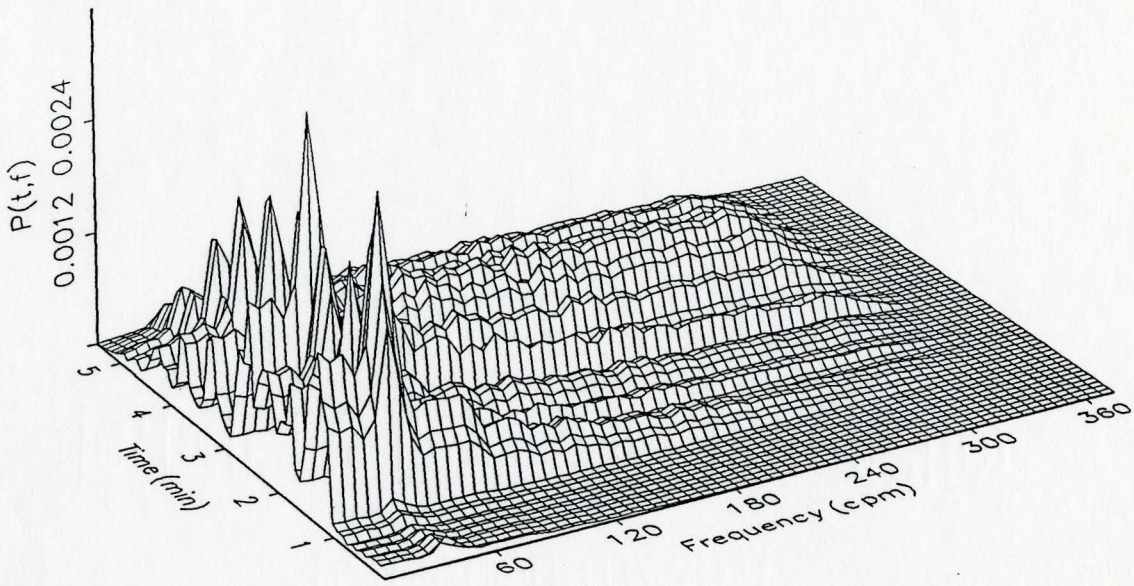

Figure 6.9: *PTFD of ES2 using the whole segment in time and frequency range 0 - 370 cpm.*

Dominant frequencies occur after the first minute and are below 60 cpm. Intensity levels during the first minute were practically zero for the whole frequency range

Table 6.2: *Comparison of relative contribution of bands of frequency for ES1 (percent).*

time	*frequency (cpm)*							
(min)	10	20	30	40	50	60	70	sum
0-1	0.19	0.32	0.50	1.24	0.74	0.67	0.82	4.48
1-2	0.32	0.42	0.55	1.14	0.61	0.53	0.62	4.19
2-3	0.50	0.61	0.75	1.41	0.71	0.59	0.68	5.25
3-4	0.98	1.13	1.31	2.30	1.09	0.87	0.97	8.65
4-5	2.34	2.60	2.87	4.69	2.06	1.57	1.67	17.80
sum	4.33	5.08	5.98	10.78	5.21	4.23	4.76	40.37

around 60 cpm and during the rest was localized near zero frequency. The main PTFD variations matched large amplitude variations of the original signal.

The total relative contribution of the ES1 segment below 5 minutes and between 0 and 70 cpm was 40.37% with respect to the complete PTFD. The comparison of relative contributions to ES1 (table 6.2) showed that during the first five minutes, the frequency range 30-40 cpm represented 10.78%, where the highest value (4.69%) occurred at the last minute. The next bands in importance were 60-70 cpm and 20-30 cpm during time intervals at 0 - 2 min and 2 - 5 min, respectively. There were also important bands of frequency around 40-50 cpm and 10-20 cpm that occurred at 0 - 3 min and 3 - 5 min, respectively. The PTFD of ES1 presented two frequencies with maximum energy: 37.8 cpm during time interval between 0 and 2 min and 35.7 cpm from 2 to 5 min.

The total relative contribution to ES2 during the first time of 5 minutes and

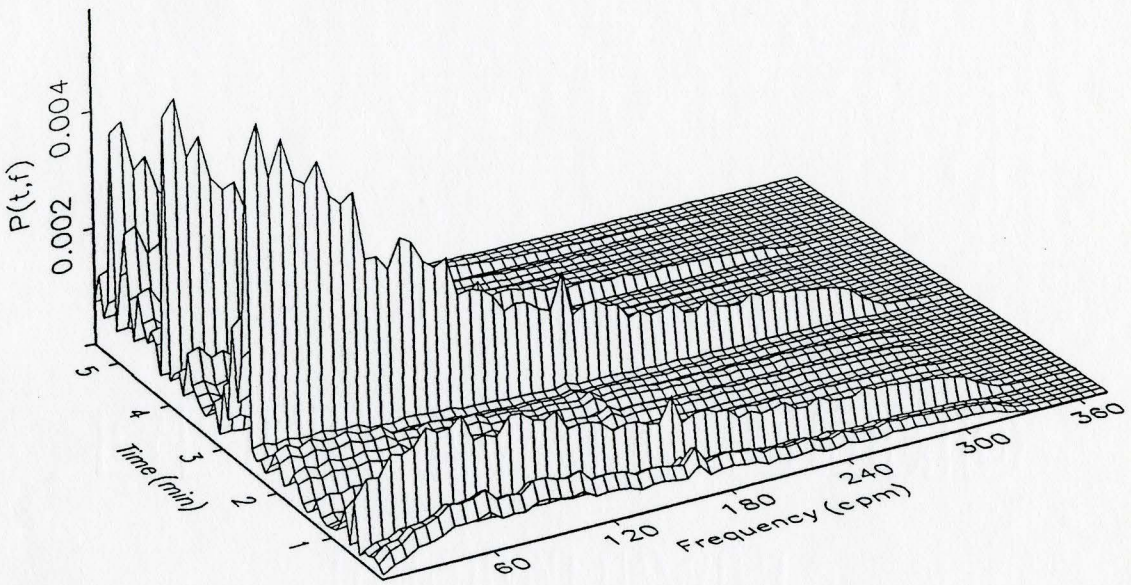

Figure 6.10: *PTFD of ES3 using the whole segment in time and frequency range between 0 and 370 cpm.*

The PTFD during the first minute showed a peak about 60 cpm. However, the peak of the PTFD between the third and fifth minute was below 10 cpm.

Table 6.3: *Comparison of relative contribution of bands of frequency for ES2 (percent).*

time	*frequency (cpm)*							
(min)	10	20	30	40	50	60	70	sum
0-1	0.17	0.16	0.18	0.27	0.12	0.10	0.10	1.10
1-2	1.94	1.85	2.09	3.22	1.37	1.16	1.20	12.83
2-3	1.70	1.66	1.94	3.11	1.39	1.21	1.30	12.31
3-4	1.01	1.04	1.27	2.21	1.07	0.97	1.08	8.65
4-5	0.48	0.56	0.78	1.58	0.85	0.82	0.97	6.04
sum	5.30	5.27	6.26	10.39	4.80	4.26	4.65	40.93

between 0 and 70 cpm was 40.93% with respect to the complete PTFD. The comparison of relative contribution of each band of frequency (table 6.3) showed that during the first five minutes, the frequency range 30-40 cpm represented 10.39%, where the highest value (3.22%) occurred during the second minute. The next band in importance during time interval between 0 and 4 min was 20-30 cpm with maximum value (2.09%) also at the second minute. The relative contribution of low frequencies during first three minutes was different from that in the last minute. The highest energy contribution was obtained at 34.7 cpm along time interval 4-5 min. The time intervals of the signal with the highest energy occurred during the second and third minute.

The total relative contribution to ES3 for the first 5 minutes and between 0 and 70 cpm was 44.56% with respect to the total PTFD. The comparison of relative contribution of each band of frequency (table 6.4) showed that during the first and

Table 6.4: *Comparison of relative contribution of bands of frequency for ES3 (percent).*

time	*frequency (cpm)*							
(min)	10	20	30	40	50	60	70	sum
0-1	0.67	0.84	1.02	1.22	1.23	1.32	1.01	7.31
1-2	0.71	0.68	0.71	0.76	0.71	0.72	0.53	4.82
2-3	2.49	2.17	2.07	2.06	1.79	1.71	1.21	13.50
3-4	1.14	0.94	0.86	0.81	0.67	0.62	0.42	5.46
4-5	3.00	2.42	2.15	1.97	1.59	1.41	0.93	13.47
sum	8.01	7.05	6.81	6.82	5.99	5.78	4.10	44.56

second minute the highest energy contributions were by frequencies between 30-60 cpm. The highest energy contribution during the last three minutes corresponded to frequencies 0-20 cpm. The pattern of energy levels over time went from high to low frequencies. The PTFD of ES3 presented that the highest energy levels occurred approximately at 56 cpm during 0 - 1.5 min, 32 cpm at 1.5 - 1.7 min and 8 cpm from 1.7 min until the end of time interval. The results of the conditional PTFD given time (percentage values) of two bands of frequency (0 -10 and 30 - 40 cpm) showed that in the same signal the band 0 - 10 cpm varied among different periods and the band 30-40 cpm was almost constant over time (Table 6.5). The last band was relatively important in ES1 and ES2 but less so ES3. The band of frequencies below 10 cpm showed an increasing relative importance in ES1 and ES3 and decreasing in ES2.

Table 6.5: *Conditional PTFD given time of two bands of frequency (percent).*

time	*0 - 10 cpm*			*30 - 40 cpm*		
(min)	ES1	ES2	ES3	ES1	ES2	ES3
0-1	4.24	15.45	9.17	27.68	24.55	16.69
1-2	7.64	15.12	14.73	27.21	25.10	15.77
2-3	9.52	13.81	18.44	26.86	25.26	15.26
3-4	11.33	11.68	20.88	26.59	25.55	14.84
4-5	13.15	7.95	22.27	26.35	26.16	14.63
sum	10.73	12.95	17.98	26.70	25.38	15.31

6.5 Conclusions

An important characteristic of the colonic musculature is that not only their spiking activity but also their slow wave or oscillatory activity changes with time. The time course and frequency content of colonic electrical activity may vary from one cycle to the next. This variation may be due to the inherent instability of electrical activity in colonic smooth muscle cells and the fact that extracellular electrodes in vivo record simultaneously from a large number of uncoordinated cells. This problem makes difficult the analysis of the colonic electrical activity and the comparative analysis among signals under different experimental conditions is still problematic. A PTFD with a fixed kernel function describes the interactions between time and frequency in terms of positive values. For the PTFD to track accurately time-frequency variations requires a better estimation of the kernel function. However, the PTFD analysis in

a first approach can be used to compare time-frequency changes among signals if the kernel function satisfies a basic set of constraints: marginal conditions, uncertainty coefficient and conditional PTFD given time or frequency.

The main work of this chapter was a comparative analysis of time- frequency variations among different signals. From a practical point of view, we used a set of criteria to select a kernel function and c-value. The kernel function showed a relation between time and frequency components. The pattern of contour plots between ES1 and ES3 was different around the section with small correlations. This section occurred at about the same frequency but its shape was larger in ES1 than ES3. It may be due to the fact that ES3 was dominated by several spikes with high amplitude. Another important difference was the c-value: it was the same value but opposite sign. Therefore, the contour lines indicated reverse geometric patterns in the same section. The power spectrum of ES1 presented a band of frequencies where the amplitude increased until it reached the maximum amplitude and then decreased. No band of frequencies with increasing amplitude existed in the power spectrum of ES3. The geometric pattern of the kernel function for ES2 was different from the other signals. The cumulative power spectra of both ES1 and ES2 were almost similar but the cumulative signal power differed for some time intervals. The cumulative distributions for ES2 and ES3 were dissimilar for several intervals. For ES2 and ES3 the c-values were the same and sections with increasing or decreasing contour lines were equivalent in terms of direction. The pattern of PTFD of ES3 was mainly affected by the section where the marginal product was not modified by the kernel function (around 2.5 min). The PTFD of this signal showed a relative difference during the first minute with respect to the rest of the time interval (main frequency around 60 cpm).

We divided the frequencies into bands thought to have functional significance based on in vivo and in vitro data. We chose a range of frequencies below 70 cpm, as this range was dominant in all signals. The frequency range was divided in sections of 10 cpm to do a detailed analysis and to compare the time-frequency variations. The comparison of relative importance between bands of frequency showed that in ES1 and ES2 the band with the highest values was 30-40 cpm. These frequencies during the preprandial and interprandial period may play a role in the generation of bursts that were predominantly in these signals. The frequency range 0- 10 cpm was dominant in ES3 unlike to ES1 and ES2. The analysis of the conditional PTFD given time could provide arguments that support the results of the visual analysis: the relative contribution of the band of frequency 0-10 cpm was larger in some periods of time (4-5 min in ES1, 0-2 min in ES2 and 3-5 min in ES3) than the rest of each signal. The numerical results suggested that a meal can induce changes in the relative importance of frequencies below 10 cpm (more important in ES3 than ES1) and the frequency difference was most marked in the band 30-40 cpm (its relative importance in ES1 was higher than ES3).

The frequency changes over time require a technique that simultaneously combines both time and frequency components. The development of time-frequency distribution techniques has created new alternatives of analysis for this type of process. PTFD techniques can be a standard method to establish comparisons between signals under different experimental conditions. It is possible with PTFD to compare the relative importance of certain bands of frequency among signals recorded under different experimental conditions and to obtain normalized results that can be used to differentiate patients from control subjects.

The PTFD analysis provides a comprehensive method to compare time-frequency

variations of different signals using the same template. To best track instantaneous frequency variations along time requires a better definition of the kernel function. However, the variability of certain bands of frequencies can be appreciated using the PTFD with a fixed kernel function that satisfies all requirements. The possibility of using positive values simplifies the comparative analysis of the time-frequency changes of two different signals. The analysis of the colonic signals in this chapter reflects the potential of comparing time-frequency changes using PTFD techniques. However, long time segments must be included to obtain a better comparative analysis.

Chapter 7

Conclusions and future developments

7.1 Conclusions

The analysis of temporal variations of colonic electrical activity is important in understanding functional and organizational characteristics of the human colon. Both visual and computer-based methods have been used to analyze this type of activity. Because of the complexity of colonic signals as frequency varying in time, its analysis requires a technique that combines both time and frequency components.

In this thesis, a methodology was presented whose main objective was to analyze time-frequency variations of the human colonic electrical activity. The methodology was implemented in a computer program system using a discrete representation of the positive time-frequency distribution (PTFD) technique. This computer implementation was used to analyze theoretical signals in order to characterize a kernel

function. Finally, a recording of the human colonic electrical activity was analyzed using the same technique.

A PTFD can be interpreted as the signal energy localized in both time and frequency domains. The numerical implementation of the PTFD depends on the evaluation of the Fourier transform of nonperiodic signals. A computer implementation of Chakravarti's method for calculating Fourier integrals was presented (chapter 3). It is based on the generalized Euler-Maclaurin formula with forward and backward differences. This implementation with only using rectangular windows improved the numerical approximation of the power spectrum when the truncation interval in a signal did not match with its fundamental period. The Chakravarti method can improve the numerical approximation of the Fourier integral of nonperiodic signals. The power spectrum calculated by using correction terms decreased faster to zero than TS results. The method can be used for non-smooth signals like the electrical activity recorded in the human colon. The implementation of this method was an important aspect for computing the PTFD of nonperiodic signals.

A PTFD representation depends on a kernel function which is related to the signal to be analyzed. For any particular signal, it is difficult to know its PTFD by only using time and frequency marginal distributions. We showed that the uncertainty coefficient based on the entropy principle and frequency-dependent PTFD (time-dependent PTFD) are good tools to decide which kernel function could be appropriate for analyzing a set of sinusoidal signals (chapter 5). Furthermore, a lower bound of the uncertainty coefficient was defined based on the marginal product (correlationless case of PTFD).

The PTFD technique was successfully implemented in a computer program system (chapter 4). This system prepares, processes and analyzes the time-varying

electrical signals recorded from the human colon using positive time-frequency distribution techniques. It contains three known kernel functions to calculate the PTFD. The selection of the kernel function is realized manually using the results provided by the program: uncertainty coefficient, conditional PTFD and marginal conditions. The analysis results are presented in terms of relative and absolute values by using tables and plots. The system can be useful for different types of signals especially for those representing the electrical activity recorded in the human colon. It was an important tool for going from theoretical signals to actual experimental signals. It was useful for determining appropriate criteria in the analysis of PTFD results. The computerized data analysis system provides a ready-to-use software package for investigators who compare signal recordings under different experimental conditions. The computer system was used to decide whether or not a kernel function was appropriate for a time-frequency varying signal and to determine which known kernel functions were useful in the analysis of time- frequency variations in a set of sinusoidal signals.

The kernel function described the relative importance of the correlation between time and frequency marginal distributions. The mathematical expression of the kernel function can be signal dependent. Therefore, the number of kernel functions that we have to investigate can be very large and specific for each signal. We decided to start with a simple set of three known kernel functions and to calculate the PTFD of six sinusoidal signals (chapter 5). This group of sinusoidal signals were selected taking into account periodicity, frequency variation over a short interval, abrupt changes along time and finite or infinite energy. These characteristics were not a complete expression of the main variations of the colonic electrical activity. However, they represented a first approximation to the PTFD analysis of this activity, so that we could focus our analysis on the kernel function and PTFD techniques. We used the PTFD

as an exploratory technique of the time- frequency variations and we found that the kernel function was an important tool to understand these variations. We decided that one important criterion to select a kernel function and c-value was to maintain total energy equal one, in order to be consistent with our interpretation of the PTFD between different signals. The uncertainty coefficient was another constraint that we applied to determine which kernel function and c-value can be used for calculating the PTFD of a sinusoidal signal. We found that these constraints were useful in selecting a kernel function and associated constant value for each sinusoidal signal. In particular, we found that a large deviation from one of the total energy was associated with large variations in the uncertainty coefficient. The uncertainty coefficient was an important criterion to select a c-value for the kernel function. The importance of the c-value was to amplify or to reduce the influence of the kernel function over the product of both time and frequency marginal distributions. This value did not alter the interaction between time and frequency components.

PTFD analysis gave us the possibility of using the same reference template to compare time-frequency variations among two or more different signals. Total energy equal one is an important concept to maintain in order to compare different signals. The product of marginal distributions satisfies the total energy equal one but does not give us any information about the interaction between time and frequency components. The kernel function does carry this information. It is a difficult issue to find a specific kernel function. We proposed to use a simple kernel function as template and applied it to different signals. The kernel function defined a partition of the time-frequency plane, each section being associated with similar weights or absolute values depending on the interaction given by the cumulative time and frequency marginal distribution. For example, we could obtain sections where the interaction between

time and frequency was practically null; that section among signals could be different in localization (time and frequency position), size or energy levels. This section was almost equivalent to the marginal product or without any correlation at all. This section was delimited by the point where $X(t)$ and $Y(f)$ reached 50% of the marginal distribution. Those sections helped to compare among different signals using the same pattern or template (it defined equivalent partitions). The PTFD technique by using φ_1 forces zero correlation between time and frequency at that point.

PTFD techniques cannot exactly track a particular frequency along time, they can give us an approximation to the frequency variations along time in order to compare between different signals. Because the kernel function is signal dependent, the PTFD can be used to explore which characteristics a kernel function must satisfy to analyze time-frequency variations in a specific signal. The potential application of PTFD to colonic signals is to compare time-frequency variations of a signal recorded for different experimental conditions like pre and postprandial periods, under medication or pre and post-therapy. The possibility of using the same kernel function to establish comparisons among signals recorded in different sections of the human colon provides a mechanism to investigate how those sections can be related. The results presented in this thesis were useful to determine specific criteria which can be employed to analyze electrical activity recorded in the human colon. We have criteria to decide which kernel function and c-value can be used to calculate the PTFD of any of the signals associated with human colonic electrical activity.

An approach to time-frequency analysis of the human colonic electrical activity was presented: to analyze the time-varying frequency components of the human colonic electrical activity using PTFD and to compare the time-frequency results between three different segments of a recording obtained before, during and after intake

meal in one subject (chapter 6). This was a comparative analysis of time-frequency variations among different signals. The PTFD technique showed variations of main frequency components and changes in time-frequency patterns for different segments. Moreover, the PTFD analysis revealed some insights about the time-varying components of the human colonic electrical activity: the relative importance of the band of frequency 0-10 cpm was larger in some periods of time than the rest of the signal, meal induced changes in the relative importance of frequencies below 10 cpm and in the band of 30-40 cpm.

7.2 Future developments

The work of this thesis started from the concept that the human colon can be considered as a "black box". The functions of the colon are well known but how they are organized, synchronized or changed under different experimental conditions is not completely clear. The inputs to this system can be of several types such as neural and chemical control mechanisms. The output is represented by with the activity of the system such as mechanical activity or contractions and electrical activity. Since studies have been conducted in vitro, in vivo and using animal models, there is some knowledge about the interplay between input and output. The concept of "black box" slowly changes to a "grey box". The analyses in the time or frequency domains realized separately have been important factors in this process. The PTFD analysis by using simultaneously both components has tried to provide more insights about the "grey box". The importance of this thesis is given in that direction and it is only a first approach to providing a comparative analysis of the electrical activity under different experimental conditions. This process needs to be improved in computa-

tional and methodological aspects. The following recommendations are considered from the computational point of view :

- An improved algorithmic implementation of Chakravarti's method is required to reduce numeric computations.

- An algorithm that determines automatically the best kernel function and its constant value must be developed.

- To improve the PTFD definition of any signal using optimization techniques. The cumulative marginal distribution in time and frequency provides valuable information for using as input to optimization techniques and supplies a better criteria to weight a marginal product.

From the methodological point of view, there is an important area for future development in terms of combining the formulation of mathematical models for biomedical systems and its application to clinical or experimental environments. These aspects must go together and be mutually supportive. The topological analysis of time series data can be a good link for those aspects. A geometric structure can be associated with a colonic signal and establish a qualitative model that is susceptible to testing with other types of colonic signals. A set of criteria must be defined to test a qualitative model. Topology aims to define these criteria and establish a good support to modify the qualitative model and go to the clinical or experimental environment to verify the new modifications. The development of new methods of signal analysis based on the dynamical systems viewpoint is one of the most significant achievements of nonlinear systems theory. A suitable kernel function for tracking frequency variations of the human colonic electrical activity requires a major development in terms of nonlinear dynamic problems.

From a practical approach longer recording times and more specific segments

of human colonic electrical activity must be included to obtain a better comparative analysis.

Bibliography

[1] B.C. Arnold, E. Castillo and J.M. Sarabia. *Conditionally Specified Distributions.* Springer-Verlag, USA, 1992.

[2] B.L. Bardkjian and S.K. Sarna. A computer model of human colonic electrical control activity (eca). *Transactions on Biomedical Engineering*, 27(4):193–202, 1980.

[3] J.V. Candy. *Signal Processing, The modern approach.* McGraw-Hill, 1988.

[4] P.C. Chakravarti. *Integrals and Sums.* The Athlone Press, London, 1970.

[5] J. Christensen. Motility of the colon. In L.R. Johnson, editor, *Physiology of the Gastrointestinal tract*, chapter 21, pages 665–693. Raven Press, second edition, 1987.

[6] C.J. Stoddard, H.L. Duthie, R.H. Smallwood and D.A. Linkens. Colonic myoelectrical activity in man: Comparison of recording techniqes and methods of analysis. *Gut*, 20:476–483, 1979.

[7] L. Cohen. Generalized phase-space distribution functions. *J. Math. Phys.*, 7:781–786, 1966.

[8] L. Cohen. A critical review of the fundamental ideas of joint time-frequency distributions. In *Proceedings IEEE Int. Conf. Circuits and Systems*, volume 1, pages 28–33, 1986.

[9] L. Cohen. Positive and negative joint quantum distributions. In G. Moore and M. O. Scully, editors, *Non-Equilibrium Quantum Statistical Physics.* Plenum Publishing Co., 1989.

[10] L. Cohen. Time-frequency distributions- a review. *Proceedings of the IEEE*, 77(7):941–981, July 1989.

[11] L. Cohen. Time-frequency distributions- a review. *Proceedings of the IEEE*, 77:941–981, 1989.

[12] L. Cohen. Introduction: A primer on time-frequency analysis. In B. Boashash, editor, *Time-frequency signal analysis.* John Wiley and Sons, Inc., 1992.

[13] L. Cohen. Introduction: A primer on time-frequency analysis. In B. Boashash, editor, *Time-Frequency signal analysis. Methods and applications.* Longman Cheshire, 1992.

[14] E.J. van der Schee and J.L. Grashuis. Running spectrum analysis as an aid in the representation and interpretation of electrogastrographic signals. *Medical, Biological Engineering and Computing*, 25:57–62, 1987.

[15] F. Pezzolla, G.Riezzo, M.A. Maselli and I. Giorgio. Electrical activity recorded from abdominal surface after gastrectomy or colectomy in humans. *Gastreoenterology*, 97:313–320, 1989.

[16] G. Tijskens, J. Janssens, G. Vantrappen, F. de Bondt and J. Vandewalle. Algorithm for data reduction and automatic analysis of intestinal motility tracings and other smooth biological signals. *Medical, Biological Engineering and Computing*, 27:27–56, 1989.

[17] G.C. Goodwin and K.S. Sin. *Adaptive filtering, prediction and control.* Prentice-Hall, 1984.

[18] H. Choi and W.J. Williams. Improved time-frequency representation of multi-component signals using exponential kernels. *IEEE Transactions on Acoustics, Speech, and Signal Processing*, 37(6):862–871, June 1989.

[19] J.D. Huizinga. Electrophysiology of human colon motility in health and disease. *Clinics in Gastroenterology*, 15:879–901, 1986.

[20] J. Chen, J. Vandewalle, and W. Sansen. Adaptive spectral analysis of cutaneous electrogastric signals using autoregresive moving average modelling. *Medical, Biological Enginnering and Computing*, Nov. 1990.

[21] J.D. Huizinga,H.S. Stern,E. Chow,N.E. Diamant and T.Y. El-Sharkawy. Electrical basis of excitation and inhibition of human colonic smooth muscle. *Gastroenterology*, 90:1197–1204, 1986.

[22] L. Cohen and T.E. Posch. Positive time-frequency distribution functions. *IEEE Transactions on Acoustics, Speech, and Signal Processing*, 33(1):31–37, February 1985.

[23] L. Cohen and Y.I. Zaparovanny. Positive quantum joint distributions. *J. Math. Phys.*, 21:794–796, 1980.

[24] L. Ljung. *System identification - Theory for the user.* Prentice-Hall, 1987.

[25] W. Mecklenbrauker. A tutorial on non-parametric bilinear time-frequency signal representations. In G. Longo and B. Picinbono, editors, *Time and Frequency Rperesentation of signals and systems*, pages 11–68. Springer-Verlag, 1989.

[26] P.D. Finch and R. Groblicki. Bivariate probability densities with given margins. *Found. Phys.*, 14:549–552, 1984.

[27] P.J. Davis and P. Rabinowitz. *Methods of numerical integration.* Academic Press, New York, 1984.

[28] S.K. Sarna. In vivo myoelectric activity: methods, analysis, and interpretation. In J.D. Wood, editor, *Handbook of Physiology. The gastrointestinal system. Motility and circulation*, chapter 21, pages 817–864. American Physiological Society, 1989.

[29] S.K. Sarna and M.F. Otterson. Myoelectric and contractile activities. In M.M. Schuster, editor, *Atlas of Gastrointestinal motility in Health and Disease*, chapter 1, pages 3–42. Williams and Wilkins, first edition, 1993.

[30] S.K. Sarna, B.L. Bardakjian, W.E. Watrefall and J.F. Lind. Human colonic electrical control activity (eca). *Gastreoenterology*, 78:1526–1536, 1980.

[31] S.K. Sarna, W.E. Waterfall, B.L. Bardakjian and J.F. Lind. Types of human colonic electrical activities recorded postoperatively. *Gastroenterology*, 81(1):61–70, 1981.

[32] J. Skilling. Fundamentals of maxent in data analysis. In B. Buck and V. A. Macaulay, editors, *Maximum Entropy in action.* Oxford University Press, 1991.

[33] J.H. Szurzewski. Electrical basis for gastrointestinal motility. In L.R. Johnson, editor, *Physiology of the Gastrointestinal tract*, chapter 12, pages 383–422. Raven Press, second edition, 1987.

[34] T.A.C.M. Classen and W.F.G. Mecklenbrauker. The wigner distribution - a tool for time-frequency signal analysis. part i. *Philips J.Res.*, 35(3):217–250, 1980.

[35] T.A.C.M. Classen and W.F.G. Mecklenbrauker. The wigner distribution - a tool for time-frequency signal analysis. part ii. *Philips J.Res.*, 35(4/5):276–300, 1980.

[36] T.A.C.M. Classen and W.F.G. Mecklenbrauker. The wigner distribution - a tool for time-frequency signal analysis. part iii. *Philips J.Res.*, 35(6):372–389, 1980.

[37] W. Martin and P. Flandrin. Wigner-ville spectral analysis of nostationary process. *IEEE Transactions on Acoustics, Speech, and Signal Processing*, 33(6):1461–1470, December 1985.

[38] W.H. Press, S.A. Teukolsky, W.T. Vetterling and B.P. Flannery. *Numerical recipes in C. The art of scientific computing.* Cambridge University Press, USA, 1992.

[39] E. Wigner. On the quantum correction for thermodynamic equilibrium. *Phys. Rev.*, 40:749–759, 1932.

[40] K.B. Wolf. *Integral Transforms in Science and Enginnering.* Plenum Press, New York, 1979.